Review

Tools and Tactics for the Optical Detection of Mercuric Ion

Elizabeth M. Nolan, and Stephen J. Lippard

Chem. Rev., **2008**, 108 (9), 3443-3480 • DOI: 10.1021/cr068000q • Publication Date (Web): 25 July 2008

Tools and Tactics for the Optical Detection of Mercuric Ion

Elizabeth M. Nolan and Stephen J. Lippard*

Department of Chemistry, Massachusetts Institute of Technology, Cambridge Massachusetts 02139

Received November 9, 2007

Contents

* To whom correspondence should be addressed. E-mail: lippard@mit.edu.

1. Introductory Remarks

Because of continuing concern over mercury in the environment and its deleterious effects on human health, obtaining new mercury detection methods that are cost-effective, rapid, facile and applicable to the environmental and biological milieus is an important goal. This objective has recently emerged as a focal point in the chemistry and, more broadly, sensing communities. The purpose of the present review is to provide a comprehensive account of recent progress in the design and application of optical sensors for mercury. A significant body of literature, guided by seminal work on cation sensing,[1–6] describes the preparation of small molecule Hg(II) detectors, and we highlight these strategies. We also cover complementary approaches that incorporate similar design principles and provide optical feedback, including Hg(II)-responsive biomolecules and materials. Potentiometric[7] and ampometric/conductometric/electrochemical[8–14] approaches to Hg(II) analysis are not discussed. Traditional analytical techniques for Hg(II) quantification, including atomic absorption spectroscopy,[15] cold vapor atomic fluorescence spectrometry,[16,17] and gas chromatography,[18] are also outside the scope of this review.

To put the need for new mercury detection methods into perspective, we begin in Section 2 with a discussion of the causes and consequences of mercury pollution, the latter of which impact human and environmental health on a global scale. In Section 3, we describe several instrumental approaches that employ chromophores for mercury detection. Our discussions of Hg(II) probes begin with Section 4, which highlights design considerations and the challenges in small-molecule optical sensor development. Many of the topics addressed in this section also pertain to biomolecule- and materials-based sensors. Sections 5–7 focus on fluorescent small-molecule Hg(II) detectors, with "turn-off" detection covered in Section 5, "turn-on" in Section 6, and ratiometric in Section 7. We subdivide Sections 5–7 according to the solvent system(s) employed for characterization: (i) organic, (ii) aqueous/organic, or (iii) aqueous. We define aqueous/organic mixtures as those in which the organic component comprises $\geq 5\%$ of the mixture. This subdivision emphasizes that achieving water-solubility or -compatibility is an important goal, and significant progress has been made to extend water-insoluble sensors to aqueous media. Colorimetric Hg(II) detection is a focus for a number of research laboratories, and we outline progress in this area in Section 8. In some cases, a probe has been characterized in the literature as both fluorometric and colorimetric. In these instances, we place the sensor into the category where it displays superior behavior or is better characterized. Sections 9 and 10 address approaches to Hg(II) detection that rely on biomolecules and

10.1021/cr068000q CCC: $71.00
Published on Web 07/25/2008

Elizabeth M. Nolan was born in Albany, New York, and graduated magna cum laude from Smith College in 2000 with highest honors in chemistry. As an undergraduate, she conducted computational research with Professor R. G. Linck, which addressed long-range stereoelectronic effects in substituted alkanes. She was named Beckman Scholar, elected into Phi Beta Kappa, and received a Fulbright Scholarship. She conducted her graduate studies in inorganic chemistry at the Massachusetts Institute of Technology, where she joined the laboratory of Professor Stephen J. Lippard. Her doctoral research focused on the synthesis, characterization, and application of small-molecule fluorescent sensors for detecting zinc in biological samples and mercury in aqueous solution. She was a recipient of a NDSEG graduate fellowship and a National Young Investigator Award from the ACS Division of Inorganic Chemistry. Liz is currently a NIH postdoctoral fellow in the laboratory of Professor Christopher T. Walsh at Harvard Medical School. She is studying several proteins involved in the assembly of an antibiotic "Trojan horse" peptide that targets Gram-negative bacteria expressing siderophore uptake pumps.

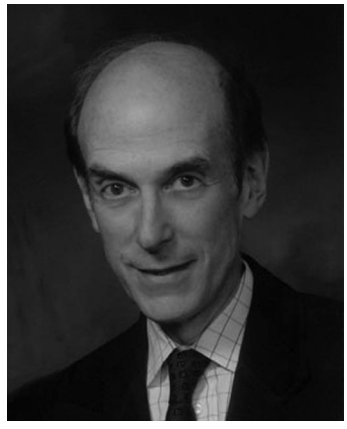

Stephen J. Lippard is the Arthur Amos Noyes Professor of Chemistry at the Massachusetts Institute of Technology. He was born in Pittsburgh, Pennsylvania, and attended Haverford College and MIT before assuming a faculty position at Columbia University in 1966. He returned to MIT in 1983 and was Head of the Chemistry Department there from 1995 to 2005. His research spans chemistry, biochemistry, and neuroscience. Specific areas of interest are platinum anticancer drugs, biological and chemical studies of carboxylate-bridged diiron centers for hydrocarbon oxidation, including methane and arene monooxygenases, and metalloneurochemistry. The last topic includes probing and understanding mobile zinc and nitric oxide as signaling agents and elucidating the fundamental reactions of NO with metal, especially iron, thiolates. Interest in the subject of this review grew out of work pioneered by coauthor Liz Nolan to devise fluorescent sensors for Hg^{2+} ion in the environment.

materials, respectively. We close in Section 11 with future directions. We cover work published through July 2007.

2. Mercury in the Environment

The biogeochemical cycling of mercury is complex and influenced by many factors that include human activities, climate fluctuations, geology, and natural disasters. Our knowledge of mercury toxicity is mainly derived from epidemiological studies of accidentally exposed populations, complemented by in vitro and in vivo toxicological investigations. In the following sections, we provide a brief account of the sources and repositories of mercury in the environment and their effects on public health.

2.1. Sources of Mercury Contamination and Bioaccumulation

Mercury pollution is a global problem and a major source of human exposure stems from contaminated natural waters.[19–21] Inorganic mercury, Hg(0) and Hg(II), is released into the environment through a variety of anthropogenic and natural sources. Industrial sources of mercury include coal and gold mining, solid waste incineration, wood pulping, fossil fuel combustion, and chemical manufacturing.[22–25] Greater than 80% of mercury emissions in the United States result from fossil fuel combustion and solid waste incineration. Nonanthropogenic sources of inorganic mercury include volcanic and oceanic emissions as well as forest fires. The United States Environmental Protection Agency (EPA) has mandated an upper limit of 2 ppb (10 nM) for Hg(II) in drinking water.[23]

Emitted elementary mercury vapors are easily transported in the atmosphere, often across continents and oceans, and are eventually oxidized to Hg(II). Atmospheric deposition of Hg(II) results in its accumulation on plants, in topsoil, and in waters. Irrespective of the source and initial site of deposition, Hg(II) ultimately enters freshwater and marine ecosystems. A fraction of this Hg(II) is reduced to Hg(0) by microorganisms, including algae and cyanobacteria, and is subsequently released back to the atmosphere.[26] Another portion of the Hg(II) accumulates in underwater sediments. Some prokaryotes that live in these sediments convert this inorganic mercury to methylmercury, which we define as any CH_3HgX species, as do bacteria that reside in fish gills and gut. In addition to this acknowledged source, some ecological studies point to the occurrence of abiotic mercury methylation under certain environmental conditions, but more work is needed to evaluate this hypothesis.[27] Because methylmercury is lipophilic, readily absorbed, and poorly excreted, it enters the food chain and biomagnifies in higher organisms, especially in the muscles of large predatory fish, including tuna, swordfish, and whales, and is subsequently ingested by humans.[19,20,28–32]

Although often overlooked, at least in the chemical literature, mercury bioaccumulation also occurs in plants, which provides additional routes of entry into the food web.[21,33] Mosses take up Hg(II) from atmospheric deposition and tree leaves are another Hg(II) repository. Mercury reduces photosynthesis and transpiration in plants, the former of which may impact the global carbon cycle. The bioaccumulated mercury reenters soils and natural waters following plant decay or is consumed by birds and mammals, and thereby further enters the food chain.

Additional sources of human exposure to mercury include the household[34] and workplace,[35] religious practices,[34,36] dental amalgams,[37–39] and vaccines.[40,41]

2.2. Consequences for Human Health

The biological targets and toxicity profile of mercury depend on its chemical composition.[42–44] Methylmercurials, the species of greatest concern, are readily absorbed by the

human GI tract, cross the blood-brain barrier, and target the central nervous system. In the absence of accidental poisoning, the only known source of human exposure to methylmercury is through seafood consumption. Many acute poisonings occurred in Minamata, Japan (1950–1960s) following the release of mercury into the Agano River; the subsequent case studies provided a significant portion of our knowledge about methylmercury intoxication.[45–48] Another noteworthy epidemic occurred in Iraq after methylmercury-tainted seed grain was used for bread.[49,50] Neurological problems associated with methylmercury intoxication are manifold and include prenatal brain damage, cognitive and motion disorders, vision and hearing loss, and death. The ramifications of long-term and low-level exposure to methylmercury are less clear and warrant thorough toxicological investigations. This mode of exposure is currently of particular concern for human embryos, the developing fetus, and children.[51–55] At the molecular and cellular levels, methylmercury causes oxidative stress[56] and lipid peroxidation,[57] and it inhibits the division and migration of neurons. It accumulates in astrocytes, preventing glutamate uptake, and thereby causes excitotoxic injury to neurons.[42,58] Inorganic mercury targets the renal epithelial cells of the kidney, causing tubular necrosis and proteinuria.[59,60] It is also a neurotoxin and causes immune system dysfunction.[35]

The global cycling of mercury and consequential human health risks present the scientific community with some important tasks, which include the development of safer manufacturing practices, performance of more detailed toxicological studies, and implementation of environmental remediation. Efforts directed toward the design and implementation of new mercury detection tools will ultimately aid these endeavors.

3. Instrumental Approaches to Mercury Detection Employing Chromophores

Traditional quantitative approaches to Hg(II) analysis in water samples employ a number of analytical techniques that include atomic absorption spectroscopy, cold vapor atomic fluorescence spectrometry, and gas chromatography. Many of these methods require complicated, multistep sample preparation and/or sophisticated instrumentation. More recently, to avoid tedious sample preparation and enhance detection limits, small-molecule chromophores have been combined with liquid chromatography and capillary electrophoresis as alternative approaches for monitoring both inorganic mercury and organomercurials.

3.1. Liquid Chromatography

High performance liquid chromatography (HPLC) facilitates the separation and identification of analytes in complicated mixtures and has been used in conjunction with organic chromophores to detect Hg(II). In one study, various metal complexes of *N*-methyl-*N*-9-(methylanthracene)-*N*′-benzoylthiourea, **1** (MABT, Figure 1), were extracted into chloroform and separated by HPLC, which afforded detection limits in the ng range.[61] A linear response from 2 – 200 ng of Hg(II) was obtained.

Three approaches to chromatographic Hg(II) detection have been described that utilize chemical reactions to form Hg(II)-chromophore complexes (Figure 2).[62–64] These methods rely on the known reactions of monosubstituted terminal alkynes with organic or inorganic Hg(II) species, which

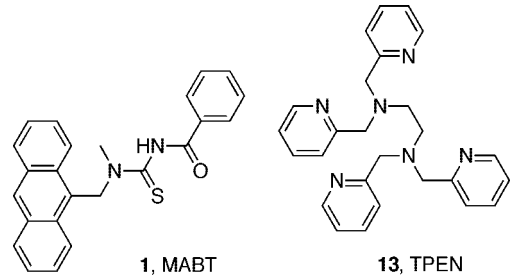

1, MABT **13**, TPEN

Figure 1. MABT, **1**, and TPEN, **13**, are compounds employed for fluorescent and UV detection of Hg(II) following separation of the complexes by HPLC or capillary electrophoresis, respectively.

afford Hg(II) acetylides in high yields. Incorporating a chromophore into the alkyne provides efficient and selective labeling of dissolved Hg(II), which can be analyzed by HPLC with UV or fluorescence detection. In one demonstration of this approach, the acridinone-appended silyated alkyne **2** was allowed to react with CH_3HgX (X = Cl, Br) in dichloromethane and in the presence of TBAF, and the resulting methylmercury acetylide **3** was detected by HPLC/UV (Figure 2a).[62] When excess **2** is employed, >85% formation of **3** occurs in 20 min at 20 °C. The sensitivity of this method is high; concentrations as low as 6 nM methylmercury were detected. Because the reaction is run in the organic phase, competition from metal ions that might interfere with mercury binding to the alkyne triple bond is unlikely. This procedure was used to analyze CH_3HgX in samples of tuna fish muscle with a certified CH_3HgX content of 5.12 μg/g. The fish samples were treated with aqueous $KBr/H_2SO_4/CuSO_4$ to dissolve CH_3HgX, which was then extracted into dichloromethane and analyzed by both cold vapor atomic fluorescence spectrometry and HPLC/UV following treatment with **2.** The latter approach detected 88 ± 5% of the extracted Hg(II). Further studies with samples from fish gills and clams gave similar agreement between the two analytical techniques, establishing the utility of this approach for methylmercury analysis.

In subsequent work, a luminescent bithiazole was derivatized with a terminal alkyne and employed for both methylmercury and inorganic Hg(II) detection by HPLC/UV spectroscopy (Figure 2b).[63] Ethynylbithiazole **4** reacts with Hg(II) and CH_3HgCl in mixed dichloromethane/water solvents containing NaOH and NaCl to form mercury acetylides **5** and **6**, respectively, in almost quantitative yield after 2 h at 20 °C. The acetylide products can be separated from **4** by reverse phase HPLC/UV with a THF/water mixture as the mobile phase. Linear correlations between the actual and determined mercury concentrations were obtained, >0.99 for both inorganic Hg(II) and methylmercury, with detection limits of ~0.5 and ~0.3 ng, respectively.

An analogous method employs fluorene-appended alkynes for Hg(II) detection (Figure 2c).[64] Essentially quantitative conversion of **7/8** to **9/10** occurs in 2 h (T = 20–25 °C) following addition of Hg(II) when a dichloromethane/water biphasic system containing NaOH and NaCl is employed. Acetylides **9/10** can be separated from **7/8** on a C8 reverse phase column with a THF/water gradient and detected by UV–vis spectroscopy. This system provides a linear response to Hg(II) and its sensitivity is comparable to that of the thiazole-based approach (Figure 2b) with >90% recovery possible (2.5 ppm mercury, 2 h reaction time) and a lower detection limit of ~0.5 ng Hg(II). Although **11** and **12** were

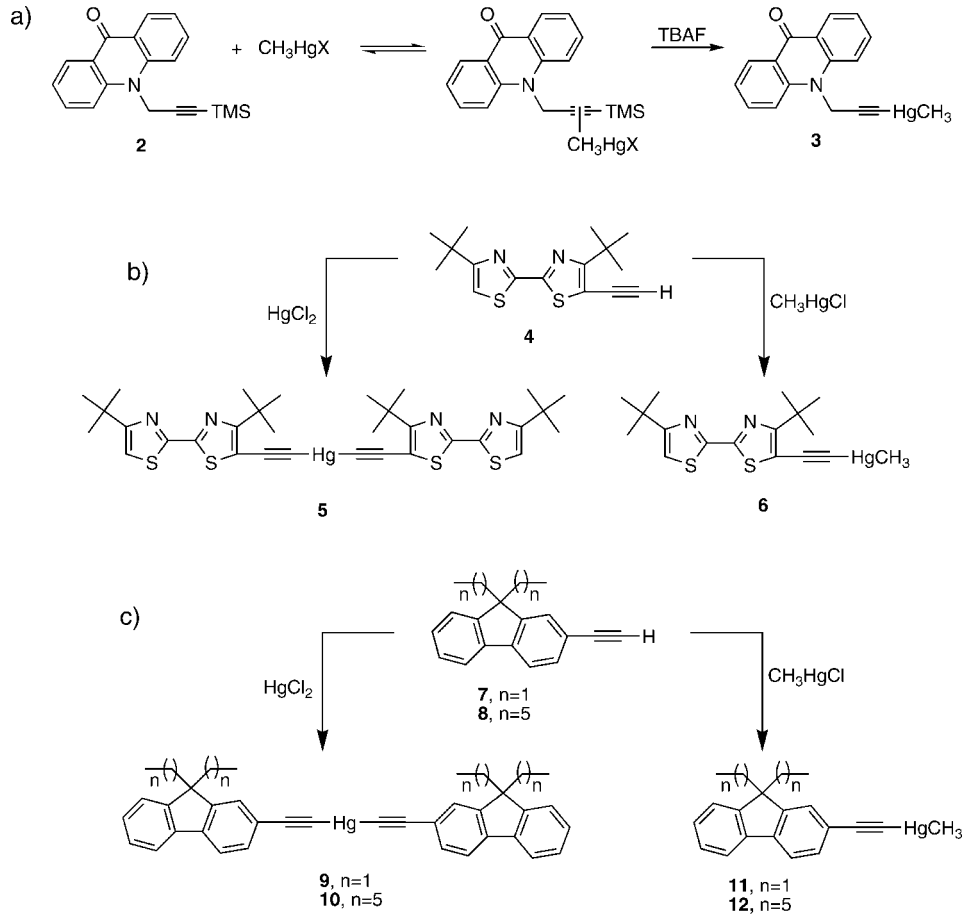

Figure 2. Chromophore-functionalized alkynes employed for Hg(II) detection by HPLC following chemical reactions. (a) Acridinone-functionalized alkyne, (b) bithiazole-functionalized alkyne, (c) fluorene-appended alkynes.

prepared and isolated on a preparative scale, the details of their HPLC/UV detection following treatment of **7/8** with CH_3HgX were not reported. This method was applied to seawater samples spiked with $HgCl_2$. Less Hg(II) (~44% at 2.5 ppm) was recovered from the seawater samples than from samples where deionized water was employed in the derivatization reactions, a result attributed to interference by other metal ions and/or soluble organic material.

3.2. Capillary Electrophoresis

Capillary electrophoresis has been employed to quantitate CH_3HgX extracted from fish samples. In early work, cysteine was employed in the final step of a Hg(II) extraction procedure,[65] which provides a Hg(II) complex well-suited for electrophoretic migration.[66] Because this approach requires UV detection at 200 nm, a wavelength where many other species absorb, the method is susceptible to false positives and unstable baseline readings. In subsequent work, the cysteine was substituted by dithizone sulfonate, which provides a Hg(II) complex stable to electrophoretic migration and UV detection at 480 nm.[67,68] The Hg(II) recovery following derivatization was 82.5 ± 1.98%. This method was applied to determine methylmercury content in a variety of fish and crab samples. For instance, analysis of a certified sample of dogfish muscle afforded a methylmercury value of 714 ± 12 μg/kg, in good agreement with the certified value of 731 ± 60 μg/kg.

More recently, the heavy metal-ion chelator *N*,*N*,*N*′,*N*′-tetrakis(2-pyridylmethyl)ethylenediamine, **13**, (TPEN, Figure 1) was used in conjunction with capillary electrophoresis to separate and quantify metal ions in a mixture.[69] A detection limit of 1.1 μM and a linear response up to 100 μM Hg(II) were obtained. The detection limit is higher than those obtained for other metal ions, including Zn(II), Cd(II) and Pb(II) (390 – 520 nM). Given the lipophilicity of the TPEN ligand, this approach or modifications thereof could prove useful in determining metal ion concentrations in tissues following digestion and extraction or in cells following lysis.

4. Considerations for Small-Molecule Mercury Sensor Design

The instrumental techniques discussed above often provide direct and quantitative information about Hg(II) concentrations, but are not well-suited for quick detection of Hg(II) in the field or for in vivo studies of Hg(II) biology and toxicology. The use of mercury-responsive small-molecule ligands that provide immediate optical feedback can overcome such limitations because their use does not require sophisticated instrumentation or sample preparation. In this section, we focus on the design of such small-molecule-based Hg(II) sensors. Many of the principles and attributes discussed here are also relevant to the development of detectors based on biomolecules and materials, which we discuss later in Sections 9 and 10, respectively.

Mercury(II) ion has no optical spectroscopic signature because of its closed-shell d^{10} configuration, which limits the kinds of methods that can be applied to its study. Optical detection, following changes in solution fluorescence or UV–vis spectroscopy resulting from a Hg(II)-induced per-

turbation of a chromophore, is arguably best suited for monitoring Hg(II) in either environmental or biological contexts. Small-molecule ligands designed to give optical read-outs of Hg(II) upon complexation can ultimately be engineered into assay kits, portable fiber optic devices, and commercial indicators, facilitating rapid Hg(II) detection in the laboratory, field, and even household.

A number of considerations influence the design of small molecule ligands for sensing Hg(II). First and foremost, the probe should be highly selective for Hg(II) over all other components in the environmental or biological sample, including thiols, organic acids, alkali and alkaline earth metal ions, and various transition metal ions. Probe affinity, defined by the K_d value for Hg(II), is also an important consideration. This value should approach the median concentration of Hg(II) in the sample to allow the detection of both increases and decreases in analyte concentration. If the concentration of Hg(II) is unknown, then a suite of sensors with varying affinity may be required. Given the EPA mandated limit of 2 ppb (10 nM) for inorganic Hg(II) in United States drinking water,[23] high affinity probes with detection limits in the ppt to low-ppb range are required to analyze natural water samples. This value range differs from that for fish, where mercury bioaccumulates and can reach ppm levels, for which lower affinity probes may be more appropriate. A fast and readily detectable response to Hg(II) is also important. For household use, visual detection is a paramount goal. For fluorescence detection of Hg(II), enhancement ("turn-on") is preferable to fluorescence quenching ("turn-off") because it lessens the chance of false positives and is more amenable to multiplexing, the simultaneous use of several detectors that uniquely respond to different analytes. Because Hg(II) is a heavy metal ion that can quench fluorescence by several mechanisms,[70–75] achieving turn-on detection can be a significant challenge. Ratiometric sensing offers several additional advantages.[76] In this approach, a change in absorption or emission with analyte binding is monitored at two wavelengths. Ratiometric sensing is less prone to artifacts and is superior for studies of inhomogeneous samples. It can also facilitate analyte quantification.

Reversibility may be important for attributing a signal to Hg(II), rather than some other phenomenon, and for recycling of the indicator. Strictly speaking, a "sensor" or "chemosensor" must respond to its analyte reversibly. Many of the systems described here respond to Hg(II) irreversibly and are therefore more appropriately designated as Hg(II)-responsive probes or detectors. If the probe relies on an irreversible chemical reaction it is classified as a dosimeter. In some cases, reversibility has not been proved, but can be anticipated based on the principles of coordination chemistry. Depending on the application, other features that may warrant consideration are water solubility, pH sensitivity, cell permeability, and toxicity. For work in live cells or tissues, all of these parameters are important because a nontoxic and water-soluble probe that functions at physiological pH is required. This need contrasts with the potential requirements for ecological studies where, for instance, sample pH can vary dramatically. Water-soluble probes that operate under acidic or basic conditions are therefore necessary.

Some of these desired attributes are easy to address in the design of a sensor. The affinity and selectivity can both be tuned through modifications of the Hg(II) binding unit. In this regard, principles of Hg(II) coordination chemistry should be considered in selecting a Hg(II)-responsive moiety for incorporation into the probe. Because of its $5d^{10}6s^2$ electronic configuration and lack of ligand field stabilization energy, Hg(II) can accommodate a range of coordination numbers and geometries. Two-coordinate linear and four-coordinate tetrahedral species are common. Hg(II) is a soft acid and the use of soft donor atoms, including thiols and thioethers, in a chelating unit will generally increase its affinity and selectivity for Hg(II). Other donor atoms well-suited for Hg(II) coordination include nitrogen and phosphorus, as well as halides. Hg(II) has a propensity to form Hg—Cl bonds, which can affect the speciation and optical readout of a Hg(II)-sensor complex in environmental and biological samples.

The Hg(II) ion detection limit can be tuned by both the choice of chelate and chromophore. These two variables also control the water-solubility of a probe. For fluorescent indicators, the excitation and emission wavelengths are dictated by the choice of fluorophore, and the brightness is defined as the product of the quantum yield and extinction coefficient ($\Phi \times \epsilon$). Similarly, the choice of chromophore will determine the absorption profile of a colorimetric sensor. Other factors are less readily predictable, especially for fluorimetric probes. Anticipating the Hg(II) response (turn-off vs turn-on) of an intensity-based fluorogenic probe is often not straightforward. For in vivo work, predictions of cell permeability can be made by comparisons with known biological reagents, but may vary with cell type and incubation conditions. The toxicity profile of a given sensor may also fluctuate with cell type or the organism under study and therefore must be evaluated in control studies.

A detailed account of the various mechanisms used to rationalize the behavior of small-molecule chromogenic Hg(II) probes is beyond the scope of this review. These topics are covered in detail elsewhere.[2] In brief, mechanisms commonly invoked to explain the response of optical sensors to Hg(II) are electron transfer (ET) and charge transfer (CT). These general categories include photoinduced electron transfer (PET), internal charge transfer (ICT), and photoinduced charge transfer (PCT). Fluorescence quenching by Hg(II) is often attributed to electron transfer and, more generally, the heavy atom effect. In most cases, the mechanistic details of the Hg(II)-induced response are unclear, which provides an open and important area for exploration. Such detailed photophysical studies will be invaluable for future work.

5. Intensity-Based "Turn-Off" Small-Molecule Fluorescent Hg(II) Detectors

In this section we describe fluorescent probes that provide turn-off detection of Hg(II). Fluorescence quenching by heavy metal ions is a well-documented phenomenon and occurs by a number of pathways that include spin–orbit coupling, energy transfer, and electron transfer.[70–75] Because Hg(II) has a propensity to quench fluorophore emission, turn-off detection is a facile approach for monitoring this metal ion.

5.1. Turn-Off in Organic Solution

Relatively few examples of Hg(II) detectors that display fluorescence quenching in organic solution have been documented.[77–79] These compounds are illustrated in Figure 3. Several azacrown ethers linked to 4,4′-bis(dimethylamino)biphenyl reporters, **14–16**, provide fluorescence turn-off

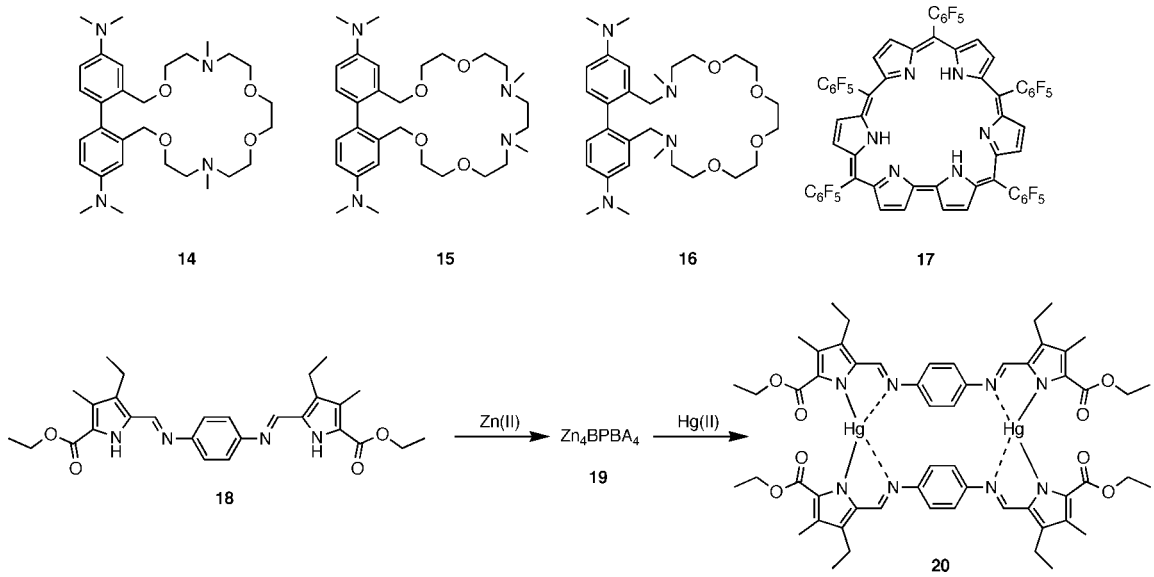

Figure 3. Sensors that give fluorescence turn-off following Hg(II) coordination (top) and metal-ion replacement (bottom) in organic solvents.

following Hg(II) addition in MeCN (λ_{ex} = 270 nm; λ_{em} = 370 nm).[77] These probes have low selectivity for Hg(II) because other divalent metal ions, including Ni(II), Zn(II) and Cd(II), also cause fluorescence turn-off. Furthermore, fluorescence enhancement is observed for **14** in the presence of Pb(II) ($\lambda_{em} \sim$ 420 nm) and **16** provides turn-on Cu(II) detection in MeCN (λ_{em} = 525 nm). As a result of their cross-reactivity, these macrocycles are not well-suited for Hg(II) detection in any complicated mixture.

A near-IR emitting probe, **17**, based on an expanded porphyrin containing six pyrrole rings (Figure 3), affords turn-off Hg(II) detection in MeOH.[78] The emission spectrum of apo **17** has two local maxima at 959 and 1085 nm (λ_{ex} = 514 nm). Addition of Hg(II) to **17** causes the solution color to change from bright red to blue with a shift in maximum absorption from 543 to 568 nm. An ~40-fold reduction in NIR emission intensity is also observed. Of the seventeen metal ions screened, only Hg(II) promotes significant fluorescence quenching, making this compound significantly more Hg(II)-selective than macrocycles **14**–**16**. Sensor **17** responds to Hg(II) in the presence of 40 equiv of Li(I), Na(I), K(I), Rb(I), Mg(II), Ca(II), Sr(II), Ba(II), Cr(III), Ag(I), Co(II), Pd(II), Ni(II), Zn(II), Cd(II), and Pb(II), which suggests that it can detect Hg(II) in a complicated matrix; however, the effect of Cu(II) on the fluorescence and Hg(II)-response of **17** was not reported. Metal-binding titrations indicate a 2:1 Hg:**17** stoichiometry, and **17** has a lower detection limit of 100 nM Hg(II).

Metal ion replacement is a strategy that has recently been employed for turn-off detection of Hg(II) in MeCN (Figure 3).[79] This approach takes advantage of the ability of various metal ions to differentially modulate the emission of a single ionophore. Addition of one equiv of Zn(II) to the nonfluorescent phenylene-bridged bis(pyrrol-2-ylmethyleneamine) ligand (**18**, BPBA) in MeCN affords a tetranuclear square complex, **19**, and fluorescence turn-on.[80] The BPBA:Zn(II) complex exhibits visible emission (λ_{ex}= 451 nm, λ_{em} = 534 nm), a quantum yield of 0.18, and a high extinction coefficient ($\varepsilon_{451} = 2.6 \times 10^5$ $M^{-1}cm^{-1}$). Introduction of Hg(II) to a solution of **19** causes its decomposition and formation of the nonemissive dinuclear complex **20**. Approximately 2.5-fold fluorescence quenching is observed following Hg(II) addition in MeCN and the wavelength of maximum absorption undergoes a hypsochromic shift from 451 to 422 nm ($\varepsilon_{422} = 1.2 \times 10^5$ $M^{-1}cm^{-1}$). Other cations, including Mn(II), Fe(II), Co(II), Ni(II), Fe(III), Al(III), Pb(II), Cd(II), and various alkali and alkaline earth metals, have negligible effect on the emission of **19**, which renders the turn-off response relatively selective for Hg(II). Copper(II) causes ~1.6-fold fluorescence quenching following its addition to **19**.

5.2. Turn-Off in Mixed Aqueous/Organic Solution

A diversity of platforms have been employed for turn-off Hg(II) detection in aqueous/organic solvent mixtures with varying degrees of success. Figure 4 depicts several calixarene-based fluoroionophores with dansyl or pyrene reporting groups that afford Hg(II)-induced fluorescence quenching. Sensor Calix-DANS2, **21**, has two dansyl groups appended to *p-tert*-butylcalix[4]arene through amide linkages.[81] In 60:40 MeCN/H_2O (pH 4), **21** exhibits its maximum emission at 575 nm (λ_{ex} = 350 nm). Addition of Hg(II) causes ~97% fluorescence quenching and an ~20 nm blue-shift in the wavelength of maximum emission. Based on electrochemical potentials and spectrofluorimetric experiments on frozen solutions (EtOH/MeOH, 100 K), the quenching was attributed to a nonradiative energy transfer process consisting of (i) reduction of Hg(II) by the excited dansyl chromophore and (ii) subsequent back electron transfer, which returns Hg(II) to its ground state. Titrations of **21** with Hg(II) reveal 1:1 binding stoichiometry, a K_d value of 67 nM for Hg(II), and a linear response range from 0 to 12 μM. The detection limit of **21** for Hg(II) is 300 nM. Metal-ion selectivity experiments indicate that the emission from **21** is unaffected by K(I), Ca(II), Cu(II), Zn(II), or Cd(II). Na(I) or Pb(II) addition causes modest, 2.1- or 2.9-fold, fluorescence enhancement and the presence of Pb(II) slightly diminishes the quenching of **21** by Hg(II).

Compound **22** has a dansyl group linked to a calix[4]-aza-crown base and provides turn-off Hg(II) detection in 4:1 MeCN/H_2O (λ_{ex} = 338 nm, λ_{em} = 520 nm).[82] Solution studies reveal 1:1 Hg(II)-binding stoichiometry and a K_d value of 7.6 μM. Up to >80% fluorescence quenching occurs

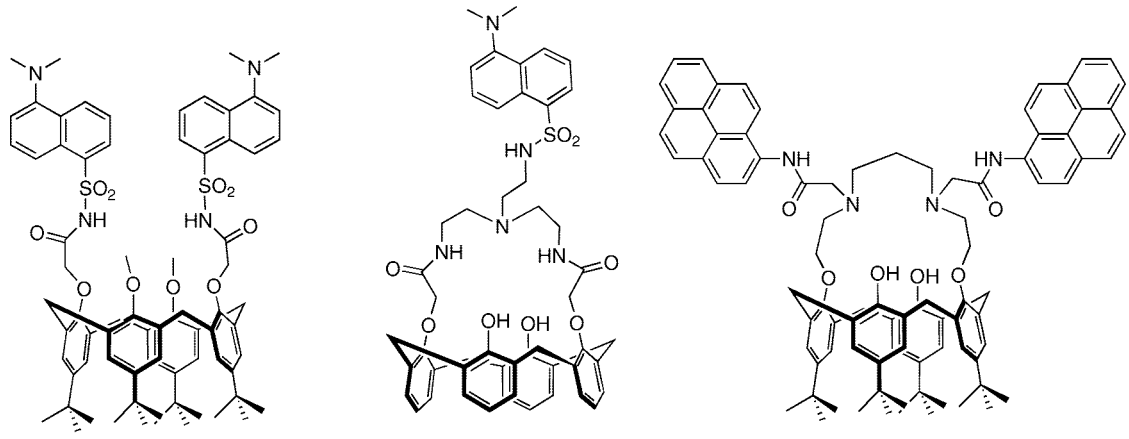

21 22 23

Figure 4. Calixarene-based compounds that give turn-off Hg(II) detection in mixed aqueous/organic solvents.

following Hg(II) addition and the detection limit is in the low μM range. The selectivity of **22** for Hg(II) is relatively poor. Other metal ions, including Pb(II), Cu(II), Cd(II), and Zn(II), interfere with the generation of the Hg(II)-induced fluorescence turn-off. In total, **22** is a poor candidate for a practical Hg(II) sensor.

A *p-tert*-butylcalix[4]arene appended with a dipyrene-linked diaza-crown ether, **23**, that operates in MeOH and mixed MeOH/H_2O has also been described (Figure 4).[83] Fluorescence turn-off occurs with Hg(II) addition in both solvent systems, but the pyrene monomer/eximer emission ratio strongly depends on the solvent composition. In pure MeOH, monomer emission (λ_{em} = 384, 404 nm) predominates, with only a small contribution from the eximer (λ_{em} = 475 nm), whereas in 1:1 MeOH/H_2O mostly eximer emission occurs. Introduction of 100 equiv of Hg(II) to a solution of **23** in MeOH results in a 96% decrease in emission at 384 nm, attributed to the heavy atom effect. Essentially complete disappearance of eximer emission occurs following Hg(II) addition in 1:1 MeOH/H_2O. The decrease in eximer emission is attributed to separation of the π-stacked pyrene moieties following Hg(II) coordination. The affinity of **23** for Hg(II) shows some dependence on solvent composition with K_d values of 22 and 83 μM in MeOH and 1:1 MeOH/H_2O, respectively. Although the affinity of **23** for Hg(II) is relatively low, the quenching effect is highly Hg(II)-specific. Of thirteen other metal ions tested, Cu(II) was the only other cation to generate a modest response in either solvent system.

The pyrene reporter has been linked to other recognition elements, macrocycles in particular, for turn-off Hg(II) detection in mixed solvent systems. These sensors are shown in Figure 5.[84–86] The bis(pyrene) diazatetrathia-crown ether, **24**, exhibits both monomer (370–440 nm) and eximer (~480 nm) emission from pyrene in 90:10 MeCN/H_2O.[84] Decreases in the intensity of both emission bands occur following Hg(II) addition (9.7-fold, monomer; 38-fold, eximer). As suggested for **23**, the diminished eximer emission probably stems from rearrangement and increased distance between the pyrenes following Hg(II) coordination. A 1:1 Hg(II):**24** complex was identified by MALDI-TOF and 95% of the total fluorescence change occurs in the presence of one equiv of Hg(II). IR studies reveal a shift of the amide carbonyl peak from 1668 to 1638 cm^{-1} following Hg(II) addition, which suggests amide involvement in Hg(II) binding. The detection limit of **24** for Hg(II) is 1.6 μM. This sensor maintains a linear fluorescence response to Hg(II) in the presence of millimolar concentrations of alkali and alkaline earth metals and micromolar concentrations of Zn(II) and Cu(II). Some fluorescence quenching occurs following addition of Cu(II) (5.1-fold, monomer; 6.4-fold, eximer).

Three Hg(II)-responsive cyclam receptors diametrically substituted with two pyrene groups have also been reported (Figure 5). In 9:1 H_2O/dioxane (pH 4.8, 10 mM acetate buffer), the fluorescence profile of sensor **25** is dominated by emission from the pyrene eximer (λ_{em} = 490 nm) with some contribution from the monomer (λ_{em} < 400 nm).[85] Addition of one equiv of Hg(II) causes an ~69-fold reduction in eximer fluorescence with little effect on monomer emission. Like the examples described above, it is proposed that Hg(II) binding to the cyclam receptor induces a conformational change that disrupts intermolecular eximer formation. Job plots reveal 1:1 binding stoichiometry. The fluorescence turn-off behavior is Hg(II)-specific and the detection limit of **25** is 1.3 μM, comparable to that of **24**. More recently, dipyrenyl cyclams **26** and **27** were described.[86] In 30:70 MeOH/H_2O (pH 4.9, 10 mM acetate buffer), the emission spectrum of **26** is dominated by the pyrene monomer and its fluorescence is quenched substantially following addition of Hg(II) or Cu(II). Because the dissociation constant for Hg(II) of **26**, ~44 μM, is relatively high, cyclam **27**, which contains two amide groups, was prepared for enhanced chelation. This modification lowers the K_d value for Hg(II) to 145 nM. Like **26**, the emission of **27** is predominantly from the pyrene monomer and sensitive to water content. The brightest fluorescence from **27** occurs in 1:1 MeCN/H_2O (pH 4.9, 10 mM acetate buffer). Addition of Cu(II) or Hg(II) to **27** in this solvent mixture results in substantial fluorescence quenching whereas addition of Ni(II), Cd(II), Zn(II) or Pb(II) affords significantly less fluorescence change. The quantum efficiency values for the Hg(II) complexes of **26** and **27** were not reported, but they are essentially nonfluorescent because the corresponding apo sensors have low quantum yields of 0.049 (**26**, 30:70 MeOH/H_2O) and 0.15 (**27**, 1:1 MeCN/H_2O). These low values are attributed to quenching of pyrene emission (Φ = 0.66 in cyclohexane) by the cyclam nitrogen atoms. The fluorescence decrease observed upon Hg(II) binding is insensitive to the presence of 10 equiv of Ca(II), Mg(II), Ni(II), Zn(II), Cd(II) or Pb(II). Interference by Cu(II) occurs.

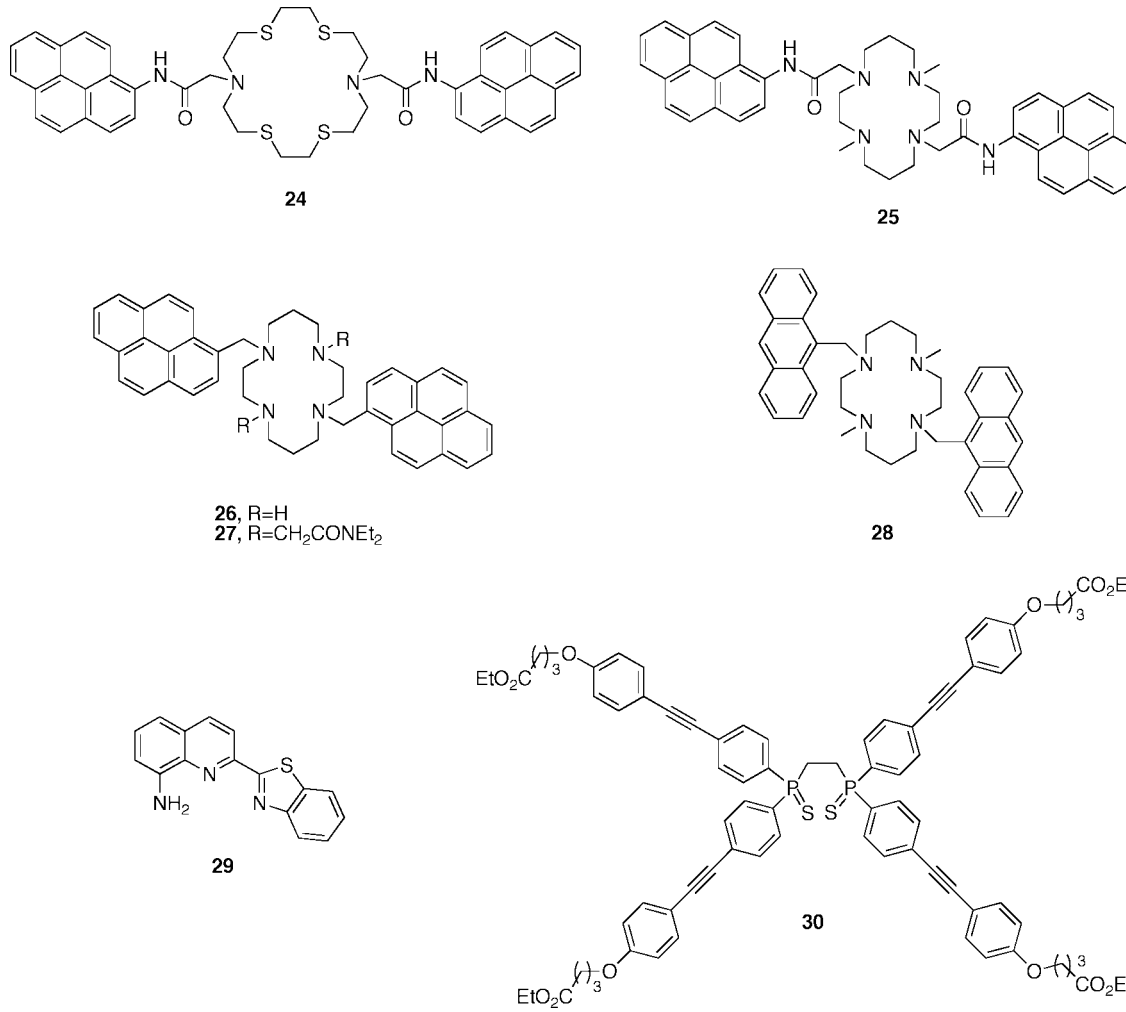

Figure 5. Additional small molecules that afford turn-off Hg(II) detection in mixed aqueous/organic solvents.

Dianthryl cyclam **28** serves as a turn-off Hg(II) detector in 1:1 MeCN/H_2O (10 mM acetate buffer, pH 5).[87] The emission spectrum of **28** is dominated by the anthracene chromophore and addition of 100 equiv of Hg(II) causes quenching with a 97% decrease in the 417 nm emission band. Introduction of other metal ions, including Pb(II), Cu(II), Zn(II) or Cd(II), evokes less than 15% turn-off and has only negligible effect on the Hg(II)-induced response when the metals are present in 10-fold excess over probe concentration. Titrations of **28** with Hg(II) reveal 1:1 binding stoichiometry, a dissociation constant for Hg(II) of 11.5 μM (1:1 MeCN/H_2O, 10 mM acetate buffer, pH 5), and a detection limit of 3.8 μM. Reduction of the water content in the MeCN/H_2O mixtures causes the mode of Hg(II) detection for **28** to switch from turn-off to turn-on. For instance, when only 10% water is employed, 5.8-fold enhancement of the 417 nm emission band occurs following addition of Hg(II). This turn-on, however, is not specific for Hg(II) because Cd(II) causes a 4.9-fold fluorescence enhancement in a 9:1 MeCN/H_2O mixture.

Two additional small molecule Hg(II) detectors that give turn-off in aqueous/organic solvent mixtures are depicted in Figure 5. The benzothiazole-derivatized 8-aminoquinoline, **29**, provides up to 98% fluorescence quenching following addition of excess Hg(II) in 9:1 dioxane/H_2O (λ_{ex} = 340 nm, λ_{em} = 580 nm).[88] NMR spectroscopy, mass spectrometry, and Job plots indicate 1:2 Hg(II):**29** binding stoichiometry. The turn-off effect is relatively Hg(II)-specific. With the exception of Cu(II), which provides up to 41% fluorescence quenching, less than 5% fluorescence change occurs following addition of Ca(II), Ni(II), Zn(II), Cd(II), or Pb(II). The detection limit of **29** for Hg(II) is 30 μM.

Lastly, phosphane sulfide **30** was recently reported to give fluorescence quenching following Hg(II) coordination at pH 4 in 80:20 MeCN/H_2O (Figure 5).[89] Based on electrochemical potentials, the fluorescence decrease is attributed to electron transfer from the excited fluorophore to Hg(II). Free **30** exhibits a large extinction coefficient in the UV region of the electromagnetic spectrum (150,000 $M^{-1}cm^{-1}$ in MeCN) and a quantum yield of 0.1 (80:20 MeCN/H_2O, pH 4). The quantum efficiency of the reaction mixture following addition of Hg(II) and the magnitude of fluorescence quenching were not reported. Mercury-binding titrations monitored by absorption spectroscopy reveal formation of 1:2, 1:1, and 2:1 Hg(II):**30** complexes. Linear coordination of Hg(II) to each sulfur atom is proposed for the 2:1 complex. The sensor has a detection limit of 3.8 nM for Hg(II), which is lower than the EPA mandate of 2 ppb (10 nM) for Hg(II) in drinking water. Other cations, including Na(I), K(I), Ca(II), Mg(II), Cu(II), Zn(II), Cd(II), Pb(II), and Ag(I) provide no fluorescence change and do not interfere with Hg(II) coordination. The insensitivity of **30** to Cu(II) is a significant advantage over many probes described in this section. Addition of 2,3-dimercapto-1-propanol to solutions of **30** and Hg(II) provides reversibility and causes the emission to return to baseline levels. Given its brightness ($\Phi \times \epsilon$), Hg(II)

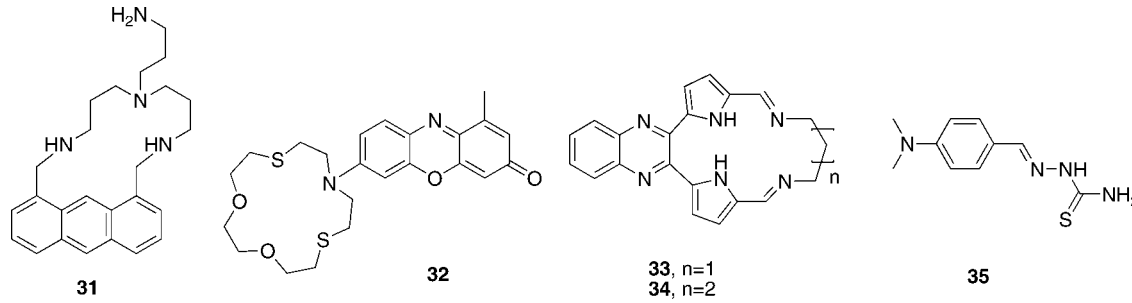

Figure 6. Small-molecule turn-off detectors for Hg(II) that operate in aqueous solution.

specificity, reversibility, and excellent detection limit, modification of **30** to make it water-soluble or further alteration to switch its detection mode from turn-off to turn-on would be worthwhile.

5.3. Turn-Off in Aqueous Solution

There are relatively few examples of Hg(II)-responsive probes that give fluorescence quenching in pure aqueous solution. This fact may stem, in part, from the difficulties associated with the low water solubility of many fluorophores that are either commercially available or easily accessible synthetically. These water-compatible turn-off Hg(II) sensors are shown in Figure 6.[90–94]

One early example of a Hg(II)-sensitive probe is the anthracene-derivatized polyamine **31**, which displays 18-fold fluorescence turn-off following Hg(II) coordination in water at pH 7.[90] Loss of the 368 nm absorption band, characteristic of anthracene, also occurs. This observation suggests that an aromatic interaction between Hg(II) and the anthracene unit causes fluorescence quenching rather than Hg(II) coordination to the linking secondary amine nitrogen atom. The dissociation constant of **31** for Hg(II) is ≤ 1 μM at neutral pH. Introduction of Cu(II) to aqueous solutions of **31** causes 4-fold fluorescence turn-off. The affinity of **31** for Cu(II) is relatively low, 56 μM. Other metal ions, including Al(III), Cr(III), Mn(II), Ni(II), Zn(II), Cd(II), Pb(II), various alkali and alkaline earth metals, and lanthanides do not interfere with the Hg(II)-induced response, even at 1 mM concentrations.

More recently, a dithia-dioxa-monoaza crown binding unit was linked to a phenoxazinone scaffold to provide turn-off Hg(II) detection in the visible region.[91] Compound **32** (Figure 6) exhibits a quantum yield of 0.08 in water, which decreases to 0.04 following addition of Hg(II). A blue-shift in the wavelength of maximum emission from 634 to 615 nm also occurs with Hg(II) coordination. Solution studies indicate 1:1 coordination, a dissociation constant for Hg(II) of 0.83 μM, reversibility, and a lower detection limit of 100 nM. This sensitivity is greater than that of many turn-off sensors described above that use macrocycles and can be partly attributed to the incorporation of a mixed donor atom chelate. The fluorescence response of **32** is Hg(II)-specific.

Dipyrrolylquinoxaline-bridged macrocycles **33** and **34** (Figure 6) exhibit fluorescence quenching upon Hg(II) addition in aqueous solution buffered at pH 4.5 (200 mM AcOH/NaOAc buffer).[92,93] Both macrocycles have maximum emission at ~506 nm ($\lambda_{ex} = 332$ nm) and coordination to Hg(II) induce blue-shifts in the wavelengths of maximum emission to ~460 nm with an ~5- (**33**) or ~8-fold (**34**) decrease in emission intensity at 506 nm. It is proposed that the fluorescence change upon Hg(II) binding results from a decrease of electron density on the fluorophore. Solution studies reveal 1:1 binding stoichiometry of **33** for Hg(II), an apparent dissociation constant of 2.6 μM, and a linear response up to 10 μM Hg(II). The turn-off response of **33** is Hg(II)-specific. A background mixture of Ca(II), Mn(II), Co(II), Ni(II), Cu(II), Zn(II), Cd(II), and Pb(II) has no effect on the emission of **33** and does not interfere with the Hg(II)-induced fluorescence response. Probe **34** has a similar selectivity profile and a Hg(II) K_d value of 2.9 μM. Because of the fluorophore, the apo sensors have dim emission; for instance, the quantum yield of **33** is only 0.006, which limits their utility.

(*E*)-1-(4-(Dimethylamino)benzylidene)thiosemicarbazide (DMABTS, **35**, Figure 6) gives turn-off Hg(II) detection in weakly acidic aqueous solution.[94] Addition of one equiv of Hg(II) to **35** causes a 99% reduction in emission intensity at 448 nm ($\lambda_{ex} = 353$ nm) at pH 5. The emission from **35** is essentially stable over the pH range of 4.6 to 10 and it is insensitive to most other metal ions except for Cu(II), which causes ~20% fluorescence quenching (10 equiv, pH 7). The probe has a K_d value of 0.13 μM for Hg(II). When 6.3 μM **35** is employed, a linear response up to 5.77 μM Hg(II) and a detection limit of 770 nM are observed at pH 5.

A supramolecular inclusion complex consisting of meso-tetraphenylporphyrin (TPP) and an alkylated cyclodextrin derivative has been employed for turn-off detection in aqueous solution at pH 8.[95] Addition of TPP to the cyclodextrin results in enhancement of TPP emission ($\lambda_{ex} =$ 424 nm, $\lambda_{em} =$ 608 and 653 nm). Rapid quenching of the 653 nm emission band occurs following Hg(II) addition and is attributed to an increased TPP metalation rate in the inclusion complex. The magnitude of quenching varieties with metal ion as Hg(II) > Zn(II) > Cd(II) > Ag(I) > Pb(II). Only negligible interference from K(I), Na(I), Ca(II), Mg(II), Ba(II), Pb(II), or Fe(II) occurs. The presence of anions (NO_3^-, NO_2^-, SO_4^{2-}, $CH_3CO_2^-$) and a variety of organic compounds also has little effect on the response of the inclusion complex to Hg(II). The TPP/cyclodextrin detector provides a linear response range from 50 nM – 20 μM of Hg(II) and a detection limit of 2 nM. Natural water samples spiked with Hg(II) were analyzed and good agreement between the spiked concentration (80 nM – 10 μM) and the value determined by the inclusion complex was found.

6. Intensity-Based "Turn-On" Small-Molecule Fluorescent Hg(II) Detectors

Designing fluorescent small-molecule sensors that provide turn-on response following Hg(II) recognition is a considerable challenge and a current focus in the Hg(II) sensing community. In the late 1990s and early 2000s, several turn-on Hg(II) detectors were characterized in organic solvents.[96,97]

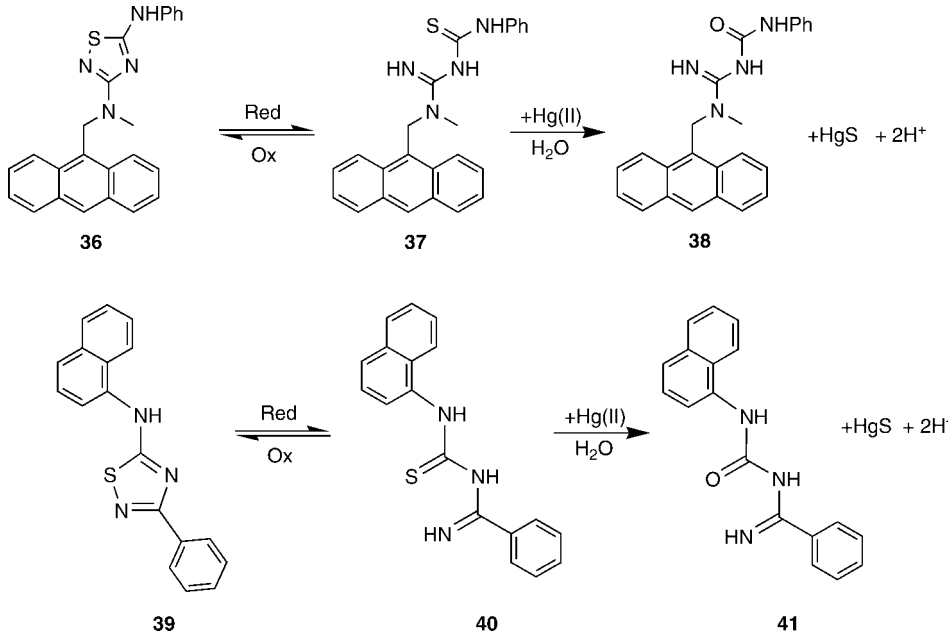

Figure 7. Redox-active detectors that give fluorescence enhancement following exposure to Hg(II) in MeCN.

Although more recent attention has addressed the need for sensors that operate in "real world" situations, the aqueous milieu in particular, many of the Hg(II) reporting strategies presented in early studies provide inspiration for current work. In this section, we chronicle the advances in the development and application of small-molecule Hg(II)-responsive probes that display fluorescence enhancement.

6.1. Turn-On in Organic Solution

Several redox-active sensor molecules with anthracene[96] and naphthalene[97] reporting groups afford turn-on detection of Hg(II) in acetonitrile (Figure 7). These systems both employ a redox-active thiadiazole/iminoylthiourea group. Anthracene **36** has a low quantum yield of 0.0027 that presumably results from PET quenching of the anthracene excited state by the tertiary amine nitrogen atom.[96] Addition of Hg(II) causes a 44-fold fluorescence increase with $\Phi_{Hg} = 0.12$. The response of **36** for Hg(II) exhibits good selectivity. Slight fluorescence enhancement also occurs upon addition of Cu(II) (2-fold) and Pb(II) (7.7-fold). Although the presence of 100-fold excess Pb(II) does not impede the Hg(II)-induced response, Cu(II) interference occurs. Compound **36** has a detection limit of approximately 10 μmol of Hg(II). Reduction of **36**, accomplished chemically by treatment with zinc in glacial acetic acid, affords iminoylthiourea **37**. This compound has a quantum yield of 0.039 and is a chemdosimeter for Hg(II) with a slow response time. Irreversible desulfurization of the iminoylthiourea group occurs, generating compound **38.** Approximately 5-fold fluorescence enhancement is observed one hour after addition of Hg(II) to **37**. The selectivity of **37** for Hg(II) is relatively low. Immediate fluorescence enhancement occurs following addition of Zn(II) or Cd(II) to **37**, which presumably results from metal-ion coordination and alleviation of PET quenching of anthracene emission.

The naphthalene-based system, comprising compounds **39–41**, displays some contrasting behavior.[97] In particular, emission from thiadiazole **39** ($\lambda_{em} = 405$ nm, $\Phi_{free} = 0.0019$) is essentially unaffected by Hg(II). Like the anthracenyl analog **37**, iminoylthiourea derivative **40** ($\lambda_{em} = 334$ nm, $\Phi = 0.0051$) is a chemodosimeter. It gives a robust, if slow, response to substoichiometric concentrations of Hg(II) as a result of an irreversible desulfurization reaction (Figure 7). A red-shift and increase in naphthalene emission occur immediately after Hg(II) addition. Following 48 h treatment with 0.1 equiv of Hg(II), 34-fold fluorescence enhancement occurs ($\lambda_{em} = 368$ nm, $\Phi_{free} = 0.17$). The dosimetric response of **40** to Hg(II) is sensitive to the Hg(II) concentration and is unstable in the presence of excess Hg(II). In particular, addition of 100 equiv of Hg(II) causes immediate fluorescence enhancement followed by gradual fluorescence quenching over 48 h.

Chemodosimeters consisting of 1,3-dithiole-2-thione moieties linked to anthracene reporters were documented more recently (Figure 8).[98] Probes **42** and **43** have low quantum yields of 0.01 in 20:1 THF/H_2O. Addition of Hg(II) causes a gradual 18-fold fluorescence enhancement over the course of 30 min ($T = 40$ °C), which results from the desulfurization reactions depicted in Figure 8. The quantum yields for the reaction products **44** and **45** are both 0.18. Analysis of the reduction potentials for a series of model complexes indicates that PET is more favorable for **42/43** than for the reaction products **44/45**. A detection limit of 50 nM for Hg(II) was obtained and the presence of other metal ions has negligible effect on the Hg(II)-induced fluorescence turn-on. Silver(I) ion does not promote desulfurization in this system.

Other organic solvent compatible turn-on Hg(II) detectors that utilize the anthracene chromophore are shown in Figure 9. Compound **46** exhibits 160-fold fluorescence enhancement following Hg(II) addition in MeCN.[99] Nevertheless, this probe is more appropriately categorized as a turn-on Cu(II) sensor because it gives 250-fold fluorescence turn-on following Cu(II) addition.

Sensor **47** (Figure 9) comprises two anthracene chromophores linked to an azacrown ether-functionalized *p-tert*-butylcalix[4]arene.[100] The emission from **47** is dim because the deprotonated amine groups effectively quench anthracene emission. Addition of Hg(II) alleviates PET quenching and causes fluorescence enhancement, the magnitude of which depends on the solvent composition (THF, 141-fold; 9:1

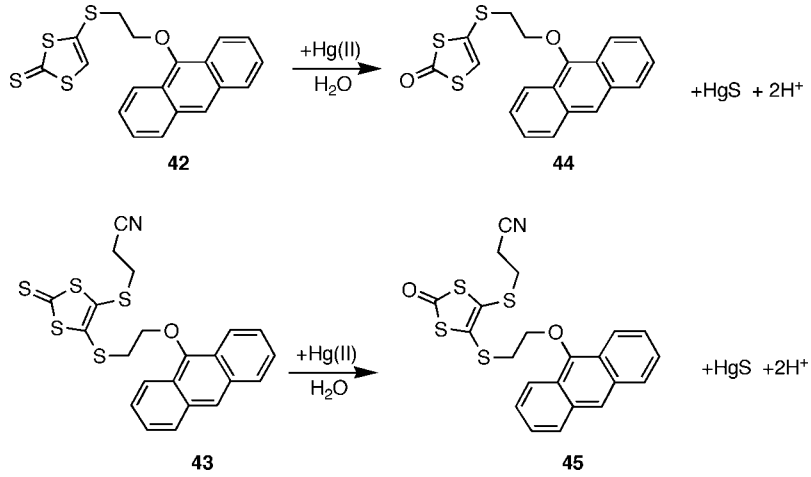

Figure 8. Anthracene-based chemodosimeters for Hg(II) that give fluorescence enhancement in THF.

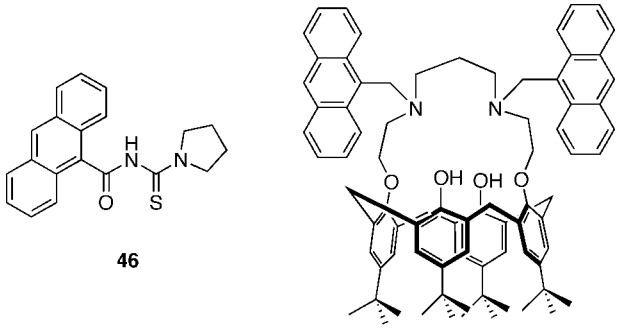

Figure 9. Turn-on probes for Hg(II) employing anthracene chromophores that operate in organic solution.

MeOH/THF, 87-fold). The selectivity of **47** for Hg(II) also varies with the solvent composition. In 9:1 MeOH/THF, Cu(II) and Pb(II) give some fluorescence enhancement, 16.8- and 9.9-fold, respectively, and essentially no fluorescence change occurs with addition of Co(II), Ni(II) and Zn(II). In 100% THF, Co(II) and Zn(II) give substantial fluorescence enhancement. Probe **47** binds Hg(II) with 1:1 stoichiometry and Hg(II) coordination is reversible by treatment with EDTA. Its affinity for Hg(II) is low and solvent-dependent (K_d = 556 μM in 9:1 MeOH/THF), and the detection limit for Hg(II) is 60 μM.

Macrocyclic chelates appended with nitrobenzoxadiazolyl (NBO), naphthalimide, boron dipyrromethene (BODIPY), and anthraquinone chromophores have also been employed for turn-on Hg(II) detection in organic solvents (Figure 10).[99,101–103] Compound **48** (Φ_{free} = 0.034, λ_{ex} = 476 nm, λ_{em} = 539 nm) exhibits fluorescence enhancement following Hg(II) addition in MeOH, but few other details regarding its photophysical properties and Hg(II) selectivity are documented.[99]

The macrocyclic chelates in **49–51** contain multiple thioether moieties, which help to provide selectivity and high affinity for soft metal ions such as Hg(II). Both sensors **49** and **50** exhibit fluorescence turn-on following Hg(II) coordination in MeCN and share a similar design strategy of decoupled donor and acceptor moieties.[101,102] Sensor **49** contains a naphthalimide acceptor linked to the 3-position of a 1,3,5-trisubstituted Δ^2-pyrazoline ring with an anilino NS_4 crown donor in the 5-position (Figure 10).[101] In the absence of Hg(II), the emission spectrum of **49** is weak (Φ = 0.007) and centered in the NIR region (λ_{em} = 680 nm). Coordination of Hg(II) reduces the donor strength of the macrocycle and inhibits electron transfer quenching of the fluorophore. A 13-nm blue-shift in the wavelength of maximum emission and a 20-fold enhancement in quantum yield following Hg(II) addition occur. Sensor **49** also responds to Ag(I) with a 15-fold enhancement in quantum efficiency.

Sensor **50** consists of an anilino thiaazacrown donor and a BODIPY acceptor (Figure 10).[102] The BODIPY chromophore itself provides bright emission, resulting from its high extinction coefficient and large quantum yield, relative to most other chromophores considered thus far. In the absence of metal ion, **50** shows a very low quantum yield of 1×10^{-4} in MeCN (λ_{em} = 509 nm). Addition of Hg(II) causes a two-nm red-shift in the wavelength of maximum emission and a dramatic 5900-fold enhancement in quantum yield. Metal-binding titrations indicate 1:1 stoichiometry for Hg(II) complexation. Because of the high affinity receptor, the large dynamic range and bright reporting group, ppb detection of Hg(II) is possible. Fluorescence enhancement also occurs following addition of Cu(II) (2500-fold) and Ag(I) (2200-fold) to **50** in MeCN and these metal ions can also be detected at ppb levels. Initial studies in mixed 1:3 MeCN/H_2O indicate that **50** gives turn-on Hg(II) detection in the presence of water, albeit with decreased dynamic range (223-fold increase in quantum yield), and that Hg(II) and Ag(I) can be differentiated by lifetime measurements. This system affords the largest fluorescence enhancement reported to date that results from Hg(II) coordination.

Sensor **51** is based on the anthraquinone chromophore and contains a sulfur-rich trithiacrown chelate (Figure 10).[103] The quantum yield of **51** increases from 0.0016 (λ_{em} = 481 nm) to 0.006 (λ_{em} = 522 nm) following addition of two equiv of Hg(II) in MeCN. The turn-on behavior is Hg(II)-specific. The affinity of **51** for Hg(II) was not reported, and Hg(II) binding titrations monitored by optical absorption spectroscopy reveal no isosbestic point. As a result, a model where formation of a 1:2 Hg(II):**51** sandwich complex occurs at relatively low Hg(II) concentration, and a 1:1 Hg(II):**51** complex at high Hg(II) concentration, was proposed.

Figure 11 displays several other fluorescent probes that give turn-on detection for Hg(II) in organic solvents. Spiropyran **52** has an ~20-fold fluorescence enhancement following addition of one equiv of Hg(II) (dissolved in EtOH) in benzene.[104] Some turn-on is also observed following addition of Zn(II) (~9-fold), Mg(II), and Cd(II) (3- to 4-fold).

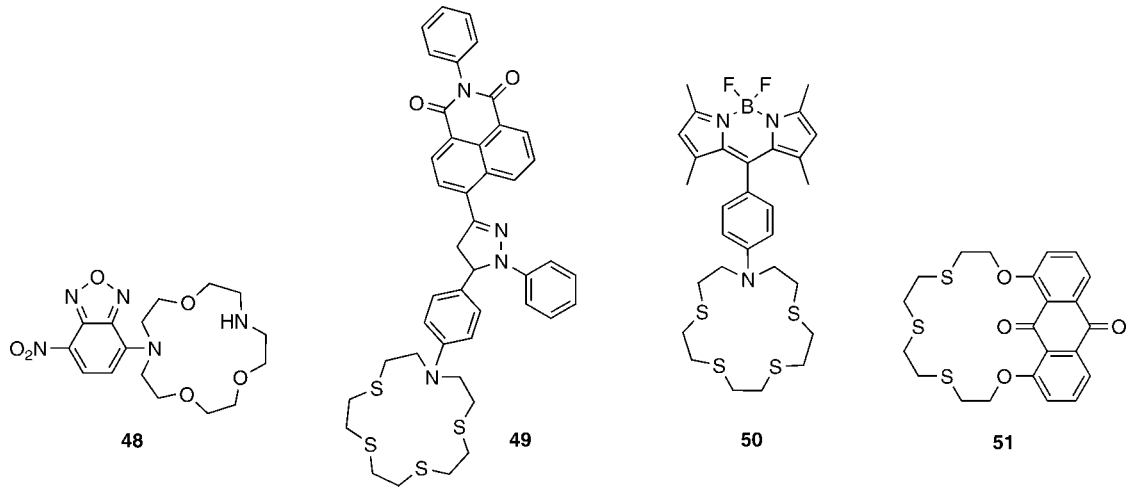

Figure 10. Hg(II) sensors with macrocyclic chelates that provide turn-on detection in organic solvents.

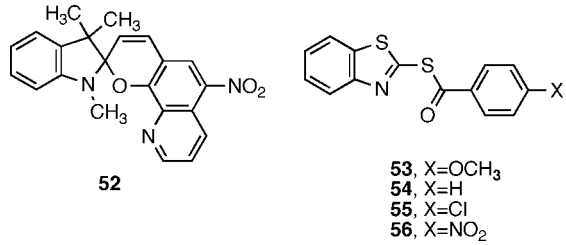

Figure 11. Other small molecules that provide fluorescence turn-on with Hg(II) addition in organic solution.

A series of 2-mercaptobenzothiazole (MBT) benzoates, **53–56**, provide varying degrees of fluorescence enhancement following addition of Hg(II) in THF.[105] The lone pair electrons of the carbonyl oxygen atom presumably quench emission from the nπ* state of the MBT moiety and Hg(II) coordination disrupts this pathway. Nevertheless, these probes show a greater response as a result of Zn(II) coordination and also give turn-on for Cd(II), Ag(II) and Pb(II), which renders them poor Hg(II) sensors.

6.2. Turn-On in Aqueous/Organic Solution

A number of turn-on Hg(II) detectors that operate in aqueous/organic solvent mixtures have been reported.[106–117] These probes, displayed in Figure 12, employ a variety of chromophores, metal-binding ligands and detection strategies, and some show promise for application in the environmental and biological milieus.

Compound **57** is one of the first examples of a Hg(II)-sensitive fluoroionophore that was characterized in a mixed solvent system.[106] Emission from the two 8-hydroxyquinoline groups is quenched in protic solvents because of excited-state proton transfer reactions involving the protonated hydroxyl moieties (λ_{em} = 540 nm, Φ = 0.00005). A 12-fold fluorescence enhancement occurs upon addition of one equiv of Hg(II) to **57** in 1:1 MeOH/H_2O at pH 7 (λ_{ex} = 423 nm, λ_{em}= 476 nm) and the quantum yield increases 20-fold to 0.001. Some fluorescence enhancement also occurs following addition of Cd(II) (3-fold) and Zn(II) (3.4-fold), but competition experiments confirm that the affinity of **57** is greater for Hg(II) than for Zn(II) or Cd(II). Furthermore, the presence of 100-fold excess alkali and alkaline earth metals has no effect on the Hg(II)-response of the probe. Metal-binding titrations indicate formation of a 1:1 Hg(II):**57** complex. The nitro group is essential for turn-on Hg(II) detection. Substitution of this moiety with chloride results in turn-on detection for Mg(II).

Sensor **58** has two NBO chromophores linked to a diazatetrathia crown ether chelate and provides maximum emission at 541 nm (λ_{ex} = 470 nm).[107] This sensor gives >10-fold fluorescence enhancement in 90:10 MeCN/H_2O following addition of 100 equiv of Hg(II) and the emission maximum undergoes a blue-shift to 529 nm. In this solvent mixture, **58** has a K_d value of 22 μM and a detection limit of 4.8 μM for Hg(II), and the turn-on fluorescence response is specific for Hg(II). The emission and Hg(II)-induced response of **58** are sensitive to water. Increasing the water content results in a decrease in emission intensity for both the apo and Hg(II)-bound forms.

Sensor **59** employs the NBO chromophore, which affords visible excitation and emission (λ_{ex} = 492 nm, λ_{em} = 536 nm), and a 3,6,12,15-tetrathia-9-azaheptadecane ligand, which provides a thioether-rich metal-binding unit that is well-suited for the coordination of soft metal ions (Figure 12).[108] An 18-nm blue-shift in the wavelength of maximum emission and an approximately 8-fold fluorescence enhancement occur upon addition of excess Hg(II) to **59** (dioxane/water mixtures). A linear fluorescence response to Hg(II) is obtained up to 15 μM (10 μM probe). Addition of Mn(II), Co(II), Ni(II), Cu(II), Zn(II), Cd(II), Pb(II), and Tl(I) has no effect on the emission spectrum of **59**. This probe binds Ag(I) readily and with higher affinity than Hg(II), but Ag(I) coordination elicits only negligible fluorescence enhancement. ^{1}H NMR studies indicate that Hg(II) binding decreases the π electron density on the nitrobenzoxadiazolyl chromophore, which presumably causes the fluorescence enhancement.

A Hg(II)-selective sensor based on the 4-aminonaphthalimide chromophore that operates in 9:1 H_2O/EtOH was described.[109] Sensor **60** contains a 2,6-bis(aminomethyl)pyridine-based receptor, two naphthalimide chromophores, two semirigid piperazine groups for PET quenching of the fluorophores, and two 2-(2-hydroxyethoxy)ethyl groups to enhance water solubility (Figure 12). The fluorescence of **60** is pH-dependent with a pK_a of ~5.2 and with minimum and stable fluorescence at pH > 6.5, which makes the sensor suitable for applications at neutral pH. Compound **60** exhibits visible emission (λ_{ex} = 548 nm) and a low quantum yield of 0.007. Addition of Hg(II) causes 17.4-fold fluorescence enhancement (Φ_{Hg} = 0.12) with a concomitant eight-nm red-shift in the wavelength of maximum emission. One equivalent of Hg(II) is sufficient to afford the maximum fluores-

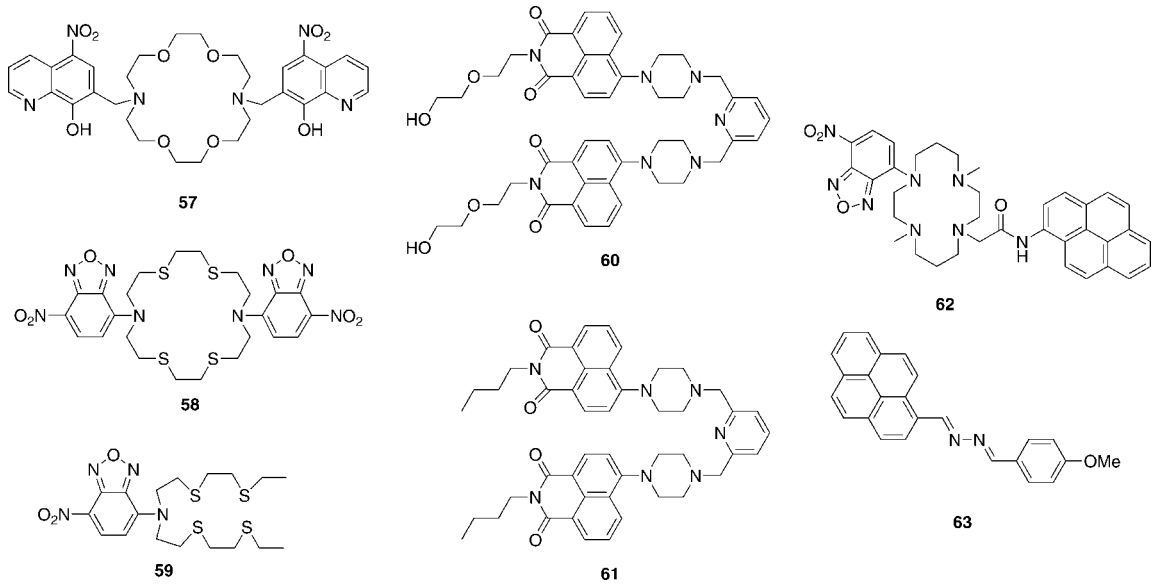

Figure 12. Fluorescent probes that give turn-on detection of Hg(II) in mixed aqueous/organic solvents.

cence change and a dissociation constant of ~6 μM was reported. When 1 μM probe is employed, 2 ppb of Hg(II) can be detected. Addition of other metal ions, including Zn(II), Cd(II), Pb(II), and Ag(I), causes slight fluorescence enhancements (<2.8-fold); however, these species, in addition to Fe(III), Co(II), Ni(II), Cu(II), Cr(III), and various alkali and alkaline earth metals, do not interfere with the Hg(II)-induced response. The origins of this selectivity are unclear. A derivative of this compound, **61**, has been applied to cultured human kidney proximal tubular epithelial cells for fluorescence monitoring of exogenous Hg(II) uptake and accumulation.[110] Although this preliminary work illustrates cell permeability and points to a role for **60** and **61** in practical applications, no chemical characterization of **61** was documented and control experiments were not provided to ensure the change in fluorescence signal resulted form Hg(II) binding and not photoactivation or some other competing phenomenon.

In more recent work, the nitrobenzoxadiazolyl chromophore was linked to a pyrene-appended cyclam for turn-on Hg(II) sensing in 90:10 MeCN/H_2O (acetate buffer, pH 4.8) (Figure 12).[111] Sensor **62** exhibits emission maxima centered at 385 and 538 nm attributed to pyrene and nitrobenzoxadiazolyl, respectively (λ_{ex} = 340 nm). Addition of Hg(II) to **62** causes an ~10-fold enhancement of the nitrobenzoxadiazolyl band with only negligible change in emission intensity of the pyrene monomer. The insensitivity of the pyrene band provides an internal calibration for determining the concentration of Hg(II). Although not described as such, **62** therefore provides single-excitation dual-emission ratiometric detection of Hg(II) by a comparison of intensity ratios at 385 and 538 nm before and after Hg(II) addition and can also be classified as a ratiometric sensor. Solutions of **62** change from orange to yellow with Hg(II) addition, which allows for detection by UV–vis spectroscopy. Probe **62** has a dissociation constant of 40 μM for Hg(II) and a detection limit of 7.9 μM. The sensor is reversible by addition of EDTA and its Hg(II) response is insensitive to millimolar concentrations of Na(I), K(I), Mg(II), and Ca(II). Addition of Cu(II) causes fluorescence quenching and **62** binds Cu(II) with greater affinity than Hg(II) (K_d = 0.12 μM).

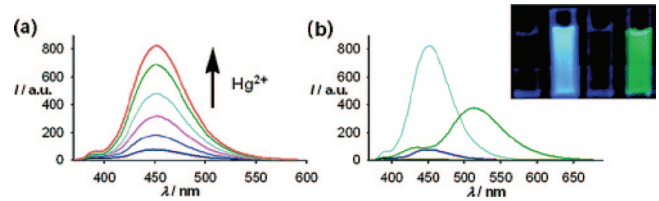

Figure 13. Fluorescence response of **63** to Hg(II). (a) Emission spectra corresponding to a titration of **63** with $Hg(ClO_4)_2$ in 7:3 MeCN/H_2O. (b) Emission response of **63** to Hg(II) in 7:3 MeCN/H_2O (blue line) and in pure MeCN (green line). The inset illustrates the fluorescence change of **63** upon addition of one equiv of Hg(II) in 7:3 MeCN/H_2O (leftmost cuvettes) or in pure MeCN (rightmost cuvettes). Reprinted with permission from ref 112. Copyright 2005 American Chemical Society.

The pyrene reporting group was also employed in the design of **63**, a fluorescent Hg(II) sensor that incorporates an unsymmetrical 1,4-disubstituted azine (Figure 12).[112] In 7:3 MeCN/H_2O, **63** has a quantum yield of 0.005 and 11-fold enhancement of the pyrene eximer emission band centered at 450 nm occurs upon addition of one equiv of Hg(II) (λ_{ex} = 350 nm). Coordination of Hg(II) presumably interferes with quenching of pyrene emission by the azine nitrogen atom lone pair electrons. The emission of **63** is insensitive to Ni(II), Na(I), K(I), Mg(II), Ca(II), Ni(II), Cu(II), Zn(II), Cd(II), and several lanthanide ions. Hg(II)-binding titrations monitored by fluorescence spectroscopy reveal a dissociation constant of 610 nM in MeCN and 1.1 μM in 7:3 MeCN/H_2O. The fluorescence properties of the Hg(II) complex depend on solvent composition. For instance, upon changing the solvent from mixed MeCN/H_2O to MeCN, the wavelength of maximum emission of the Hg(II) complex undergoes a dramatic red-shift from ~450 to ~510 nm (Figure 13). The sensor also provides colorimetric Hg(II) detection because solutions of **63** change from light-yellow to deep-orange following Hg(II) addition.

Several examples of Hg(II) detectors operating in aqueous/organic solvent mixtures that rely on chemical reactions have been reported (Figures 14 and 15).[113–115] These probes utilize Hg(II)-promoted cyclization and, as described above in Section 6.1, desulfurization reactions.

Irreversible and Hg(II)-promoted desulfurization and cyclization was employed in the design of thiocarbazone **64**

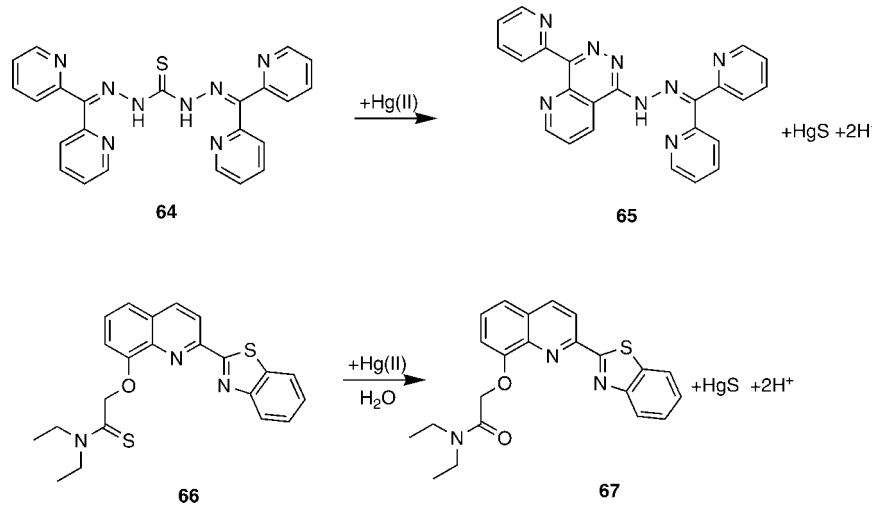

Figure 14. Irreversible chemodosimeters that give turn-on following reaction with Hg(II) in aqueous/organic solvent mixtures.

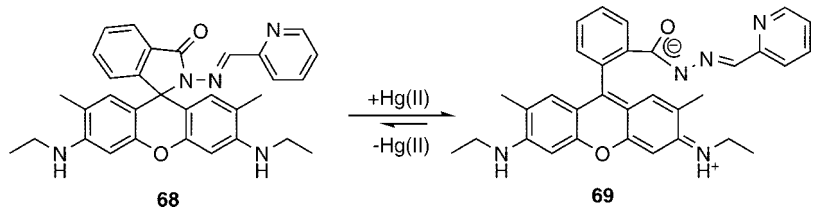

Figure 15. A rhodamine-based probe for Hg(II) that provides turn-on detection resulting from Hg(II)-induced opening of the spirolactam ring. Product **69** coordinates Hg(II) in a bidentate fashion and with 2:1 **69**:Hg(II) stoichiometry.

(Figure 14).[113] Emission from **64** is weak with $\Phi < 0.001$ ($\lambda_{em} = 530$ nm) in 90:10 H_2O/MeOH at pH 7 ($\lambda_{ex} = 380$ nm). Addition of one equiv of Hg(II) to **64** causes formation of the emissive triazanaphthalene **65**. Approximately 100-fold fluorescence enhancement occurs at 635 nm ($\Phi \sim 0.022$) following introduction of Hg(II) to solutions of **64**. The selectivity of this system for Hg(II) is high. Addition of five equiv of Zn(II) or Cd(II) to **64** causes slight fluorescence enhancement and five equiv of Cu(II) induces some fluorescence quenching, but the presence of these cations does not significantly affect the Hg(II)-induced fluorescence response. Reaction of **64** with $HgCl_2$ and subsequent X-ray crystallographic analysis of the product indicated that **65** forms a 1:1 complex with Hg(II). The Hg(II) center is five-coordinate with pyridyl, imine, and pyridazine nitrogen donor atoms and two chloride ions providing a distorted trigonal bipyramidal geometry. The Hg(II) complex has greater fluorescence relative to metal-free **65**, at least in DMSO. Dosimeter **66** operates in 30:70 MeCN/H_2O and relies on the irreversible conversion of the diethylthioamide to diethylamide **67** for turn-on Hg(II) detection (Figure 14).[114] Emission from **66** is centered at ~470 nm and weak, presumably because of intramolecular quenching of the hydroxyquinoline fluorophore by the thioamide. Product **67** exhibits maximum emission at 479 nm and has a quantum yield of 0.38 (30:70 MeCN/H_2O, pH 8.1). Addition of one equiv of Hg(II) to **66** causes 167-fold fluorescence enhancement. The performance of dosimeter **66** is sensitive to the solvent media. Although fluorescence enhancement occurs following addition of Hg(II) to **66** in pure water, the response is slow and 24 h are required to achieve a stable signal compared to approximately five min in 30:70 MeCN/H_2O. The dosimeter is essentially selective for Hg(II). Addition of Cd(II) to **66** results in some fluorescence enhancement, but the response is slow with one hour required for a 2.2-fold increase and one day for complete enhancement (20-fold). Furthermore, **66** responds to Hg(II) in the presence of Cd(II), although the turn-on is decreased by about 10%. Its detection limit for Hg(II) is estimated to be 540 nM.

Figure 15 depicts a recent Hg(II) detector that provides fluorescence enhancement in 1:1 DMF/H_2O following a chemical reaction.[115] Probe **68** integrates a carbohydrazone group into the rhodamine 6G chromophore and exists in the nonfluorescent spirolactam form. It employs a strategy previously described for fluorescent Pb(II) detection where metal-ion coordination causes ring-opening of the spirolactam and fluorescence turn-on.[116] Addition of Hg(II) to **68** affords >8-fold fluorescence enhancement centered at 560 nm ($\lambda_{ex} = 500$ nm, $\Phi = 0.42$). Ring-opened **69** coordinates Hg(II). Job plots and metal-binding titrations indicate formation of a 2:1 **69**:Hg(II) complex with an overall K_a of approximately 2.4×10^9 M^{-2}. X-ray crystallographic structural analysis of the product reveals that the Hg(II) is coordinated by two pyridylimine units in a bidentate fashion. The selectivity of **68** for Hg(II) is high because alkali and alkaline earth metals, first-row transition metal ions, Ag(I), and Cd(II) do not interfere with the Hg(II)-induced response of **68** and cause no or negligible (Zn(II), Ag(I)) fluorescence change. The sensitivity of **68** for Hg(II) is in the ppb range when 5 μM probe is employed. Although reversibility experiments were not reported, it is likely that **68** can detect Hg(II) reversibly based on related studies (*vide infra*).

A regenerative squaraine-based dosimeter for Hg(II) that operates in 1:4 MeCN/H_2O (0.01 M CHES buffer, pH 9.6) has been reported (Figure 33).[117] Although we choose to highlight this Hg(II) probe in the Section 8 (colorimetric), we note here that <2 ppb Hg(II) can be detected by fluorescence with 100 nM probe.

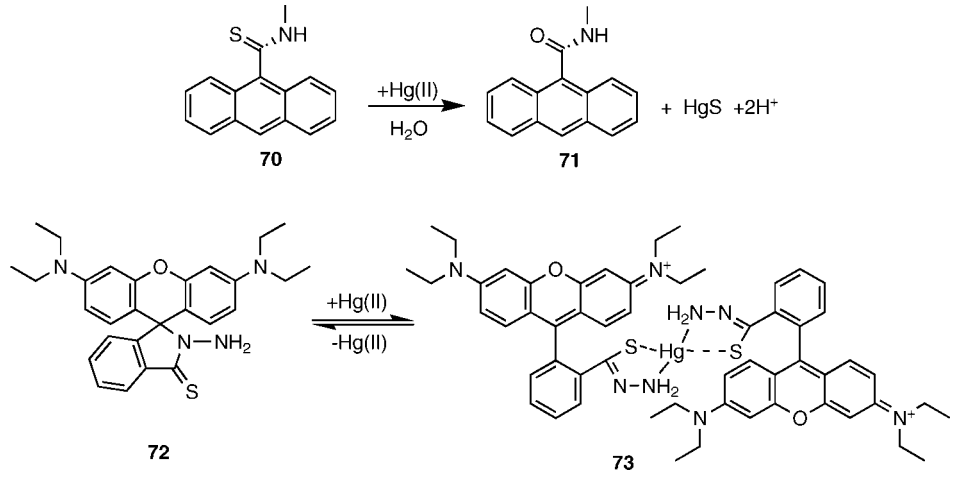

Figure 16. Mercury detectors that provide a turn-on response in aqueous solution by Hg(II)-induced chemical reactions.

6.3. Turn-On in Aqueous Solution

A recent goal in fluorescent Hg(II) sensor design is to synthesize probes that operate in aqueous solution, which will be of benefit for many practical applications. Since fluorescence turn-on is a preferable signal to turn-off, significant efforts have been made to design small molecule Hg(II) sensors that give turn-on in water, and major progress has been made in recent years. This objective requires the use of water-compatible chromophores and/or other solubilizing groups and, for practical applications, receptors with high Hg(II) selectivity. Several systems that operate in aqueous solution have been employed in applications that include quantifying Hg(II) content in digested fish samples and fluorescence imaging of exogenous Hg(II) uptake into neurons and zebra fish. Such advancements may ultimately have significant impacts on studies in environmental science and toxicology.

To the best of our knowledge, the first example of a water-compatible turn-on Hg(II) sensor was reported in 1992 by Czarnik.[118] Chemodosimeter **70** contains a thioamide group, which inhibits emission from the anthracene chromophore and affords a 56-fold reduction in fluorescence relative to **71** at 413.5 nm (Figure 16). Addition of Hg(II) to **70** promotes desulfurization and formation of anthrylamide **71**, which has a low affinity for Hg(II). This reaction results in a 55-fold fluorescence enhancement (10 mM HEPES, pH 7). Dosimeter **70** has a linear response to Hg(II) up to addition of one equiv of the ion and then exhibits saturation behavior. The desulfurization reaction is 87% complete after 10 min at room temperature, when one equiv of Hg(II) is employed, and irreversible. As exemplified by discussions throughout the present review, this sensing strategy has provided a design framework for many Hg(II) sensors that rely on chemical reactions.

In another approach that uses a chemical reaction, mercury-induced spiro-ring opening of rhodamine derivatives was employed for turn-on detection in water containing 1% 1,4-dioxane (pH 3.4).[119] Rhodamine **72** is essentially nonfluorescent and shows no absorption in the visible region because of the spirolactam (Figure 16). Addition of Hg(II) causes >7-fold fluorescence enhancement (λ_{ex} = 530 nm, λ_{em} = 582 nm) and an increase in absorption intensity at 561 nm (ε = 125,000 $M^{-1}cm^{-1}$). Titrations indicate formation of a 1:2 Hg(II):**72** complex and a detection limit of 50 nM. Addition of KI results in decomposition of the Hg(II) complex and a concomitant decrease in fluorescence emission. Introduction of additional Hg(II) restores the fluorescence turn-on, indicating that the sensor can be recycled. Characterization of **72** at physiological pH would provide insight into its potential for use in biological contexts.

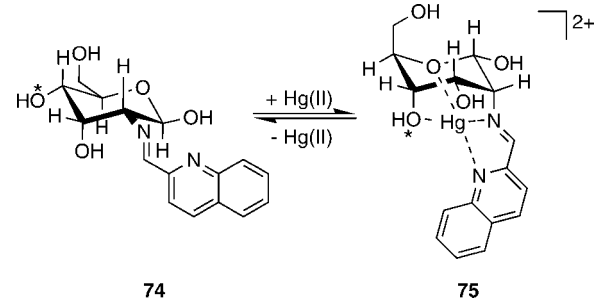

Figure 17. Sugar-appended quinoline for turn-on Hg(II) detection in water. The * indicates the glucosamine hydroxyl group involved in Hg(II) binding.

Difficulties with water-compatibility sometimes can be overcome by incorporating solubilizing groups into a sensor platform. For instance, sugars can enhance the solubility of a relatively nonpolar compound in aqueous media. Sensor **74** is a Schiff base comprising D-glucosamine appended to a quinoline reporting group (Figure 17).[120] The free ligand exhibits weak emission (λ_{ex} = 315 nm, λ_{em} = 480 nm) in aqueous solution and a quantum yield of 0.005. Addition of excess Hg(II) to solutions of **74** results in a 65-nm blue-shift of the emission band (λ_{em} = 415 nm) and ~10-fold fluorescence enhancement. The dramatic blue-shift is attributed to PCT from the hydroxyl group to the quinoline moiety, and the fluorescence enhancement to alleviation of PET. Glucosamine **74** shows maximum emission in the presence of ~20 equiv of Hg(II), forms a 1:1 complex with Hg(II), and has an apparent K_d value of 14 μM. Figure 17 depicts **75**, the proposed structure of the Hg(II) complex based on MS and NMR studies. This sensor shows excellent selectivity for Hg(II) over other cations. Excess Li(I), Na(I), K(I), Mg(II), Ca(II), Ba(II), Pb(II), Ag(I), Cu(II), Zn(II), Ni(II), Mn(II), Co(II), Cd(II), and Fe(II) do not interfere significantly with the Hg(II) response. The selectivity of **74** for Hg(II) over Cu(II) is an advantage over many Hg(II) sensors. The probe is pH-sensitive and operates in the range of 5 to 7.5.

Sensor **76** contains a polyarylpyridine fluorophore appended with phenylthiourea-capped methionine moieties that is linked to an Argogel™ resin (Figure 18).[121] Its

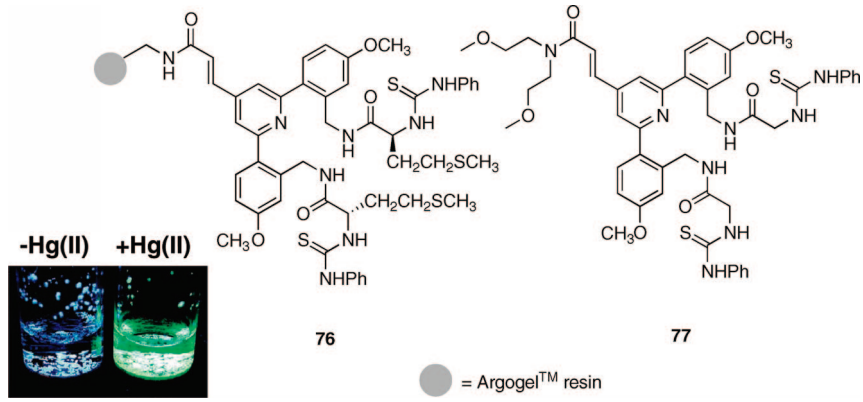

Figure 18. Mercury sensors obtained from a combinatorial library designed for producing metal-ion sensors. The grey circle represents an Argogel™ resin. The inset illustrates the fluorescence change that occurs following addition of Hg(II) to **76** in aqueous solution (MOPS, pH 7.5). The inset was reprinted with permission from ref 121. Copyright 2005 American Chemical Society.

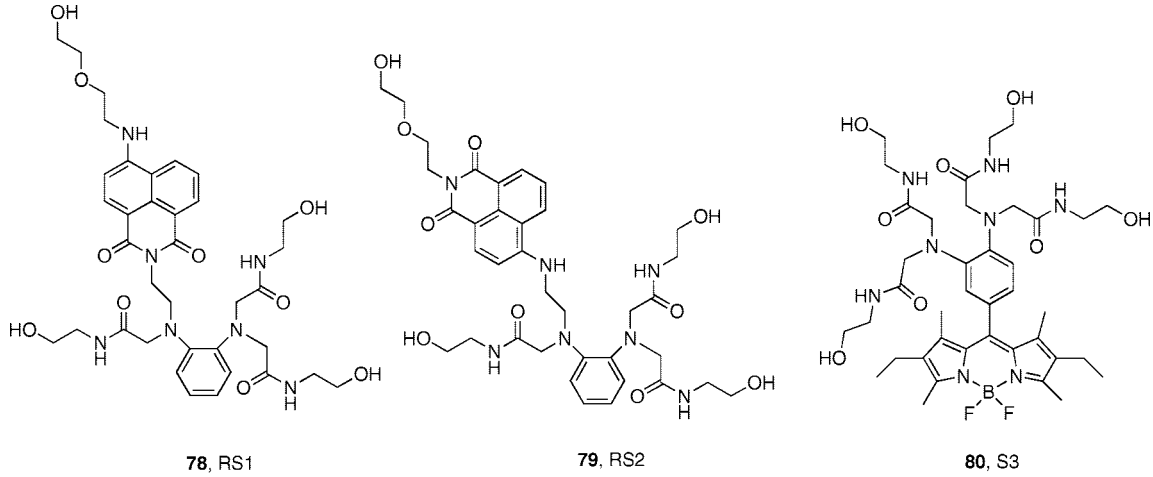

Figure 19. Turn-on Hg(II) sensors with polyamide receptors that operate in aqueous solution.

ability to detect Hg(II) was found during a screening of a combinatorial library designed for producing metal-ion sensors (pH 7.5, MOPS buffer). Substitution of the methionine with glycine or histidine also affords turn-on Hg(II) detection. A solution phase analog, **77**, was also prepared. It binds Hg(II) with 1:1 stoichiometry and gives fluorescence enhancement following addition of Hg(II) in MeCN, but lacks solubility in aqueous media. This observation points to an important role of the resin in providing water compatibility. This perhaps serendipitous observation provides a clue for making other systems compatible with aqueous milieu.

A trio of sensors with polyamide receptors that give turn-on Hg(II) detection in aqueous solution have been reported (Figure 19).[122,123] Sensors RS1, **78**, and RS2, **79**, contain the naphthalimide reporting group and exhibit weak fluorescence in the visible range at pH 7.5 (10 mM phosphate buffer) attributed to PET quenching of the chromophore by the *o*-phenylenediamine moieties.[122] Apo RS1 has a quantum yield of 0.032 ($\lambda_{em} = 545$ nm) and apo RS2 a quantum yield of 0.007 ($\lambda_{em} = 537$ nm). Addition of one equiv of Hg(II) to RS1 and RS2 causes 5.8- and 34.7-fold fluorescence enhancement, respectively, and the quantum yields for the Hg(II) complexes are 0.19 and 0.24. Metal-binding titrations and Job plots indicate formation of 1:1 RS:Hg(II) complexes. Both sensors bind Hg(II) with similar affinity ($K_d = 50$ nM, RS1; 79 nM, RS2). The fluorescence enhancement is selective for Hg(II), reversible by TPEN addition, and uninhibited by the presence of divalent first-row transition metals, various alkali and alkaline earth metals, Al(III), Ag(I), Pb(I), and Cd(II). In subsequent work, polyamide receptors were linked to the BODIPY chromophore, which offers superior photophysical properties relative to the naphthalimide dye employed in the design of RS1 and RS2 (Figure 19).[123] Sensor S3, **80**, provides 50-fold fluorescence enhancement ($\lambda_{ex} = 527$, $\lambda_{em} = 541$) immediately following Hg(II) addition (0.1 M phosphate buffer, pH 7.5) and the quantum yield increases from 0.012 to 0.61. Job plots indicate 1:2 **80**:Hg(II) binding stoichiometry. A dinuclear complex with a bridging water molecule is proposed where each Hg(II) ion is also coordinated by three nitrogen atoms of one diamide arm. The Hg(II)-induced fluorescence response is observable in the presence of two ppb Hg(II). Because of its brightness, Hg(II) selectivity and sensitivity, this probe has high potential for use in application-based contexts.

Fluoresceins and related xanthenone-based fluorophores are widely used in aqueous and biological contexts. Like the BODIPY and rhodamine fluorophores, fluorescein itself has a number of advantageous features for sensing purposes: water solubility, visible excitation and emission, maximum brightness at pH ≥ 7, and a high extinction coefficient and quantum yield. One drawback of fluorescein-based systems is that multistep syntheses are often required for functionalization,[124–126] although an elegant shortcut was recently described for "bottom" ring substituted probes where the chelate is attached to the phenyl or benzoate moiety.[127]

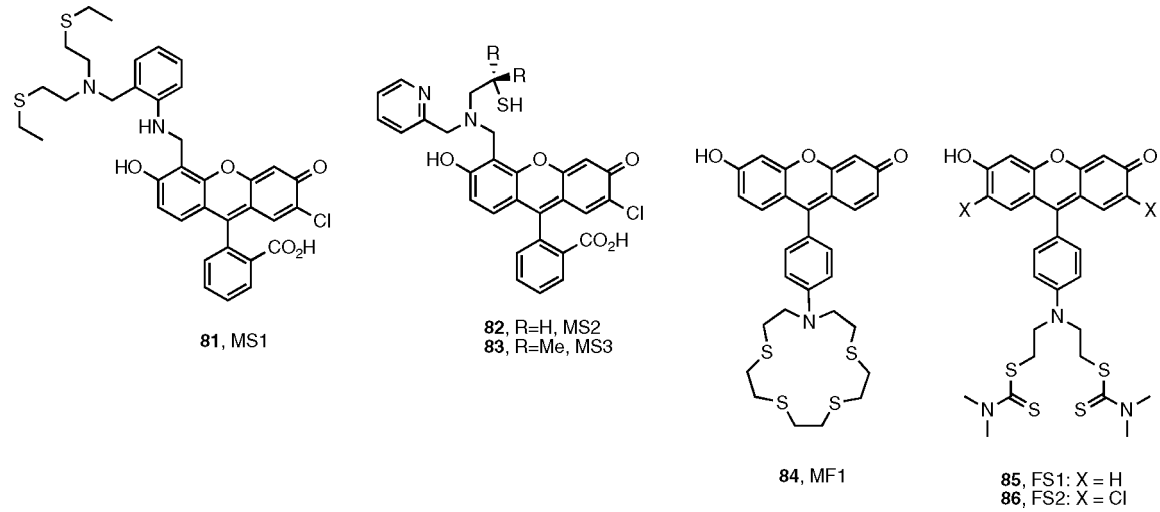

Figure 20. Top- (MS1-MS3) and bottom- (MF1, FS1 and FS2) ring substituted xanthenone sensors. These sensors provide turn-on detection of Hg(II) in aqueous solution at neutral pH.

Sensor MS1, **81**, was the first example of a fluorescein-based probe that responds selectively to Hg(II) (Figure 20).[128] Its design was based on several turn-on Zn(II) sensors prepared in our laboratory.[124,125] We anticipated that substitution of pyridyl groups, commonly employed in the design of high-affinity Zn(II) sensors, with soft sulfur donors would afford Hg(II) selectivity and turn-on Hg(II) detection. We therefore appended an aniline-based thioether-rich chelate to the "top" xanthenone moiety of an asymmetrical fluorescein platform. MS1 provides ~5-fold fluorescence enhancement immediately following addition of one equiv of Hg(II) at pH 7 (50 mM PIPES, 100 mM KCl). The apo sensor has a quantum yield of 0.04 attributed to PET quenching of fluorescein emission by the aniline moiety. Coordination of MS1 to Hg(II) results in enhancements of both quantum yield ($\Phi_{Hg} = 0.11$) and extinction coefficient (apo, $\epsilon_{505} = 61{,}300$ $M^{-1}cm^{-1}$; holo, $\epsilon_{501} = 73{,}200$ $M^{-1}cm^{-1}$). As anticipated given the N_2S_2O chelate, MS1 binds Hg(II) with 1:1 stoichiometry and high affinity, exhibiting an EC_{50} value of 410 nM (1 μM MS1). X-ray crystallographic characterization of a salicylaldehyde-based model complex confirms N_2S_2O coordination to the Hg(II) center. Addition of the heavy metal ion chelator TPEN or KI(aq) reverses the Hg(II)-induced fluorescence enhancement. When TPEN is employed, MS1 can be reversibly recycled by sequential addition of Hg(II) and TPEN at least six times. The fluorescence response of MS1 to Hg(II) is selective over alkali and alkaline earth metals, Mn(II), Co(II), Fe(II), Ni(II), Cr(III), Pb(II), and the Group 12 congeners Zn(II) and Cd(II). Cuprous and cupric ion both interfere with the Hg(II)-induced response of MS1. The affinity of MS1, and other thioether-rich detectors, for Cu(II) is not a surprise given previous thermodynamic and kinetics studies of similar chelates.[129] Like most PET-based sensors and fluorescein itself, the emission of MS1 is sensitive to pH. Protonation of the aniline moiety causes a slight ~2-fold fluorescence change with a fluorescent-dependent pK_a value of 7.1. Fluorescence quenching occurs in acidic solution because of protonation of the fluorescein moiety ($pK_a = 4.8$). The response of MS1 to Hg(II) shows chloride-ion dependence; the presence of chloride ion has no effect on the emission of the free sensor but provides an enhanced fluorescence response (~5-fold) to Hg(II) relative to its absence (~1.5-fold). We speculate that formation of a Hg—Cl bond or ion pair accounts for this behavior, but further studies are required to verify either claim. MS1 can detect two ppb Hg(II) in buffered aqueous solution.

Additional "top ring" substituted fluoresceins that give fluorescence enhancement following Hg(II) addition are MS2, **82**, and MS3, **83** (Figure 20).[130] These sensors have a tertiary amine-based ligand containing pyridyl and thiol moieties. Because tertiary amines generally quench fluorescein less efficiently than aniline-based ligands, MS2 and MS3 are inherently brighter in both the apo and Hg(II)-bound forms than MS1. At neutral pH, MS2 ($\Phi_{free} = 0.28$; $\epsilon_{500} = 62{,}000$ $M^{-1}cm^{-1}$) and MS3 ($\Phi_{free} = 0.27$; $\epsilon_{501} = 51{,}000$ $M^{-1}cm^{-1}$) provide modest ~1.5- (MS2, $\Phi_{Hg} = 0.27$, $\epsilon_{505} = 69{,}000$ $M^{-1}cm^{-1}$) and ~2-fold (MS3, $\Phi_{Hg} = 0.28$, $\epsilon_{507} = 59{,}000$ $M^{-1}cm^{-1}$) and selective turn-on detection of Hg(II) (50 mM PIPES, 100 mM KCl, pH 7). In both cases, the fluorescence enhancement results from brightness ($\Phi \times \epsilon$) enhancement because the extinction coefficients increase, not because of Hg(II)-induced alleviation of PET. The pH dependence of MS2/MS3 emission indicates that the tertiary amine nitrogen atom pK_a value is ~8 for both sensors and suggests that proton-induced background fluorescence compromises the MS2/MS3 response to Hg(II) at neutral pH. In accord with this notion, raising the pH to 9 affords a Φ_{free} value of 0.10 for MS2 and ~5-fold fluorescence enhancement ($\Phi_{Hg} = 0.28$). Both sensors bind Hg(II) reversibly and with 1:1 stoichiometry. EC_{50} values of 384 nM (MS2) and 1.6 μM (MS3) are obtained with 1 μM probe. Like MS1, these sensors display chloride-ion dependence with greater fluorescence enhancement observed in the presence of chloride. Mass spectrometric analyses of solutions containing equimolar MS2 and Hg(II) with and without chloride ion indicate that the MS2:Hg(II) complex readily associates with one or more chloride ions in solution. The selectivity of MS2 and MS3 parallels that of MS1 except that Ni(II), in addition to Cu(II), compromises the Hg(II)-induced fluorescence turn-on. This observation points to the importance of maintaining sulfur-rich chelates for preferentially binding Hg(II) over borderline divalent first-row transition metal ions.

Installation of a metal-binding unit on the "bottom" ring of fluorescein or a fluorescein derivative offers another route to assembling water-soluble Hg(II) sensors. Such bottom-ring substitution is commonly found in the Ca(II) and Zn(II) sensor literature.[131–133] Generally, bottom-ring substituted xanthenones exhibit lower quantum yields in the metal-free

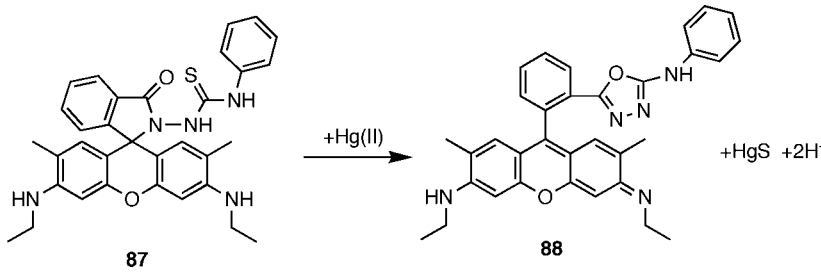

Figure 21. Rhodamine-based chemodosimeter for Hg(II) that operates in aqueous solution and has been applied to detect exogenous Hg(II) in a variety of cell types and in zebrafish.

forms and greater dynamic range than similar species where the ligand is installed in the 4′ and/or 5′ positions of the xanthenone platform. This design strategy has afforded water-compatible Hg(II) sensors with the greatest dynamic range to date.[127,134]

Sensor MF1 (**84**, Figure 20) contains a thioether-rich NS_4 macrocycle linked to a fluoran, 6-hydroxy-9-phenyl-3*H*-xanthen-3-one, reporter.[134] The apo sensor exhibits $\Phi_{free} < 0.001$ ($\lambda_{em} = 514$ nm) at pH 7 and Hg(II) coordination affords >170-fold fluorescence enhancement with $\Phi_{Hg} = 0.16$ ($\lambda_{em} = 517$ nm). MF1 binds Hg(II) with 1:1 stoichiometry, an EC_{50} value of 700 nM (1 μM probe), and has a detection limit of 60 nM for Hg(II). The known preference of the thioether-rich macrocycle for Hg(II) over Cu(II) overcomes the Cu(II)-interference observed for many Hg(II) sensors. Alkali and alkaline earth metals, other divalent first-row transition metal ions, and the Group 12 congeners do not interfere with the Hg(II)-induced fluorescence turn-on. MF1 was employed to detect Hg(II) extracted from digested fish samples. A strong linear correlation between MF1 fluorescence and Hg(II) concentration determined by atomic absorption (AA) spectroscopy was obtained, which points to its utility for quantifying bioaccumulated mercury in fish tissue.

In subsequent work, a carbamodithioate metal-binding unit was installed on the phenyl moieties of fluoran reporters (Figure 20).[127] Sensors FS1, **85**, and FS2, **86**, give ~90-fold fluorescence enhancement immediately following Hg(II) addition. The quantum yields of the free probes are <0.005 and increase to 0.29 (FS1) and 0.35 (FS2) with Hg(II) coordination (pH 7.2, 50 mM KCl). FS1 and FS2 bind Hg(II) reversibly and with 1:1 stoichiometry, show maximum fluorescence in the presence of one equiv of Hg(II), and have detection limits for Hg(II) of 20 ± 5 nM. Like MF1, these sensors also show Hg(II)-selective fluorescence enhancement. Slight (~3-fold) fluorescence enhancement occurs for Cd(II). To determine whether FS1 and FS2 can perform in the environmental milieu, water samples from several sources with known Hg(II) content, determined by AA spectroscopy, were collected, concentrated 100-fold and analyzed for Hg(II). Modest correlation was observed between the AA results and fluorescence data from FS1/FS2.

Lastly, we describe a rhodamine-based chemodosimeter for Hg(II) that has been employed for monitoring Hg(II) in several biological contexts (Figure 21).[135,136] Dosimeter **87** takes advantage of the known Hg(II)-promoted formation of 1,3,4-oxadiazoles from thiosemicarbazoles. Because of the spirolactam ring, rhodamine **87** is essentially nonfluorescent ($\lambda_{em} = 551$ nm). Addition of one equiv of Hg(II) to **87** causes formation of oxadiazole **88** ($t < 1$ min.) An ~30-fold fluorescence enhancement occurs and the solution changes from colorless to bright pink as a result of Hg(II) addition (pH 7.4). Product **88** exhibits maximum emission at 557 nm, has a quantum yield of 0.52 and a high extinction coefficient (46,700 $M^{-1}cm^{-1}$). Parts-per-billion levels of Hg(II) can be monitored. The cyclization reaction depicted in Figure 21 is selective for Hg(II). Of seventeen other metal ions screened, only Zn(II) and Ag(I) give slight fluorescence enhancement and eight hours are required to generate the full response of **87** to Ag(I). This sensor is cell permeable and Hg(II)-responsive in vivo (Figure 22). It was utilized to monitor exogenous Hg(II) uptake in C2C12 cells and in zebrafish in real time, and to image accumulated Hg(II) in zebra fish organs. This series of imaging experiments suggests that **87** will be a versatile Hg(II) imaging tool. The only obvious drawback

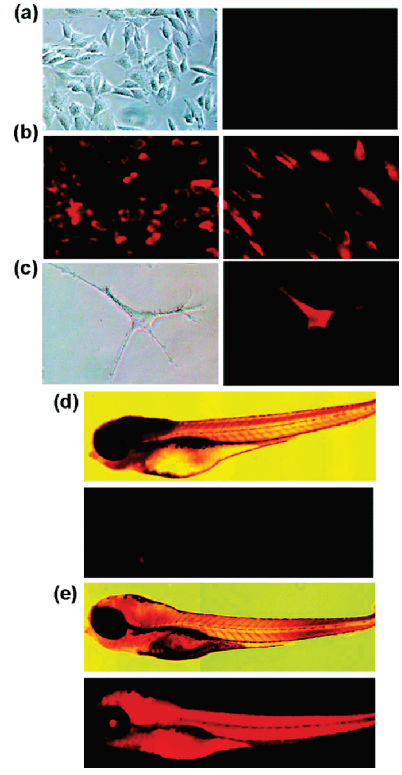

Figure 22. Fluorescence response of **87** (50 μM) to exogenous Hg(II) (50 μM) in a variety of cell types and zebrafish. The samples were treated with **87** for 20 min, washed with PBS, and then treated with $HgCl_2$ for 10 min. (a) C2C12 cells treated with **87** only. (b) Left: C2C12 cells following treatment with **87** and Hg(II). Right: Human muscle precursor cells treated with **87** and Hg(II). (c) Neurons from rat treated with **87** and Hg(II). (d) Zebrafish treated with **87**. (e) Zebrafish treated with both **87** and Hg(II). Reprinted with permission from ref 136. Copyright 2006 American Chemical Society.

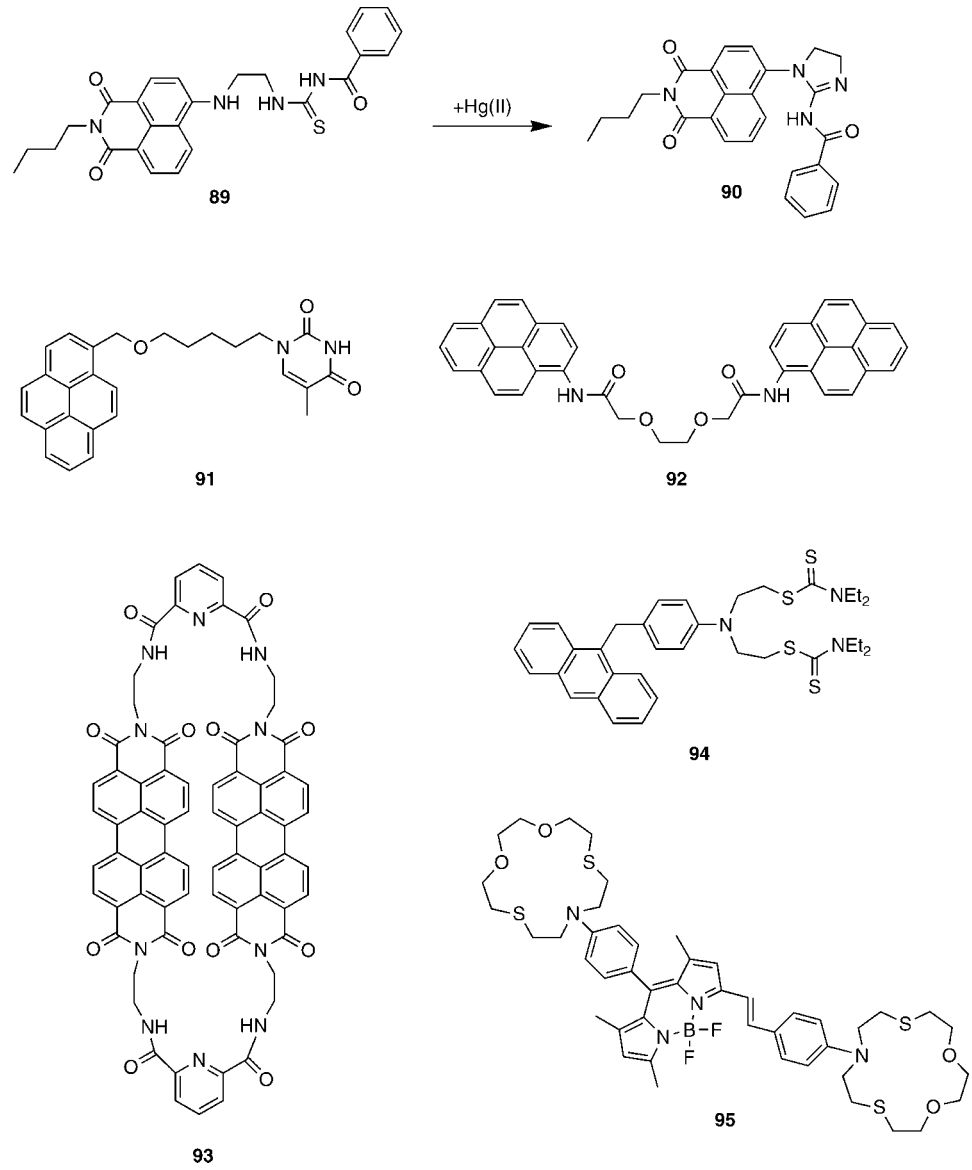

Figure 23. Ratiometric Hg(II) detectors that operate in mixed aqueous/organic solvents.

to this Hg(II) detector is that the Hg(II)-induced fluorescence increase is not reversible.

7. Ratiometric Small-Molecule Fluorescent Hg(II) Detectors

The majority of fluorescent Hg(II) probes described to date are intensity based, relying on fluorescence turn-off or turn-on following Hg(II) recognition. Ratiometric fluorescence monitoring, which involves a comparison of fluorescence intensities at two different wavelengths before and after analyte recognition, is an alternative approach. As illustrated by Ca(II) sensors such as Fura-2, ratiometric probes offer advantages in biological contexts because they facilitate analyte quantification, especially in inhomogeneous samples.[76] Although only a few examples of ratiometric Hg(II) detectors have been documented,[137–145] this technique is gaining attention in the mercury sensing community and provides an opportunity for further advances.

7.1. Ratiometric in Mixed Aqueous/Organic Solution

A ratiometric chemodosimeter for Hg(II) that operates in MeCN/H_2O solvent mixtures was achieved by taking advantage of the known Hg(II)-induced transformation of thiourea moieties into guanidine derivatives (Figure 23).[137] Benzoyl thiourea **89** (λ_{em} = 530 nm, Φ = 0.35) reacts with one equiv of Hg(II) to afford imidazoline **90** (λ_{em} = 475 nm, Φ = 0.48). As a result, emission from the solution changes from yellow-green to blue with an emission decrease and increase at 530 and 475 nm, respectively, and an isoemissive point at 510 nm (80:20 MeCN/H_2O). This behavior is attributed to changes in electronic delocalization on the chromophore. The thiourea receptor in **89** has little influence on the emission from the naphthalimide chromophore because of the ethylene spacer. Formation of the imidazoline results in loss of the spacer unit and a decrease in the electron-donating ability of the receptor portion. The selectivity of the dosimeter for Hg(II) is high. Some fluorescence enhancement occurs following addition of Ag(I),

but the reaction takes 20 h to reach completion compared to one hour for Hg(II). Other cations have no effect on its emission. Ratiometric behavior is also observed in the optical absorption spectra with an absorption increase at 350 nm, a decrease at 435 nm, and an isobestic point at ~391 nm.

Although described as a turn-on sensor, pyrene-thymine dyad **91** provides single-excitation dual-emission ratiometric detection of Hg(II) at pH 7 (20:1 H_2O/MeCN) (Figure 23).[138] In the absence of Hg(II), **91** displays emission from the pyrene monomer at ~375 and ~394 nm and weak eximer emission at 470 nm. Addition of Hg(II) causes an ~10-fold increase in the intensity of the eximer emission band and a relatively small decrease in pyrene monomer emission. A comparison of the I_{470}/I_{394} ratios before and after Hg(II) addition provides an ~19-fold ratiometric change. The response of **91** to Hg(II) is pH-dependent and optimal in the pH 6–8 range. The turn-on of **91** is selective for Hg(II) and occurs in the presence of mixtures that include Mn(II), Fe(II), Co(II), Ni(II), Cu(II), Zn(II), Pb(II), and various alkali and alkaline earth metal ions. Sensor **91** has a detection limit of 100 nM for Hg(II).

The pyrene chromophore was also employed in the design of dioxaoctanediamide-based sensor **92**, which provides single-excitation dual-emission ratiometric Hg(II) detection in 1:1 MeOH/H_2O (10 mM HEPES, pH 7) (Figure 23).[139] Emission from the pyrene eximer at 489 nm dominates the fluorescence spectrum of the free probe and its ratio of eximer/monomer emission, $\lambda_{489}/\lambda_{383}$, is 24.9. Addition of Hg(II) causes almost complete quenching of the eximer emission band ($I_{Hg}/I_{free} = 0.03$) and significantly less quenching of the monomer band ($I_{Hg}/I_{free} = 0.77$) and the $\lambda_{489}/\lambda_{383}$ ratio is 0.98. Comparison of the $\lambda_{489}/\lambda_{383}$ ratio before and after Hg(II) addition provides an ~25-fold ratiometric change with Hg(II) addition. The ratiometric response of **92** for Hg(II) is highly selective. Addition of 100 equiv of Na(I), K(I), Ca(II), Mg(II), Ni(II), Zn(II), Pb(II), or Cd(II) causes only negligible effects in the emission spectrum of **92**. Some fluorescence quenching occurs following introduction of Cu(II) to solutions of **92**, but the intensity changes are relatively small and of similar magnitude (489 nm, $I_{Cu}/I_{free} = 0.81$; 383 nm, $I_{Cu}/I_{free} = 0.80$), so there is no ratiometric response. A 1:1 **92**:Hg(II) binding model is proposed. NMR and mass spectrometric analysis indicate that deprotonation of the amide group occurs following Hg(II) coordination, and IR spectroscopy reveals a corresponding shift in carbonyl stretching frequency from 1678 to 1616 cm^{-1}. The dissociation constant of **92** for Hg(II) is 15.9 μM and the estimated detection limit is 1.6 μM. The fluorescence behavior is proposed to result from both disruption of the pyrene eximer by Hg(II) coordination and from the intrinsic ability of Hg(II) to quench fluorophore emission.

Perylene bisimide-based sensor **93** was presented as a "FEQ" sensor for simultaneous "fluorescence enhancement and quenching,"[140] but is more appropriately classified as ratiometric. Addition of Hg(II) to **93** causes an ~3.3-fold fluorescence increase at 365 nm and ~1.9-fold quenching at 557 nm (1:1 DMSO/H_2O). Two equiv of Hg(II) are required to elicit the complete fluorescence change and Job plots indicate 1:2 **93**:Hg(II) stoichiometry. Addition of K(I), Ca(II), Al(III), Fe(II), Co(II), Ni(II), Ag(I), Cd(II), or Pb(II) to **93** causes negligible effects on the emission spectrum. Some quenching occurs following Cu(II) coordination. The detection limit of **93** for Hg(II) is 10 nM (500 nM **93**). The probe can respond to Hg(II) in the presence of human serum albumin.

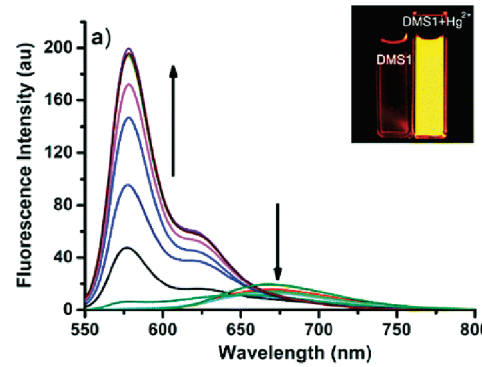

Figure 24. Ratiometric fluorescence response of 2 μM **95** (DMS1) to 0 – 40 μM Hg(II) in 30:70 THF/H_2O (20 mM HEPES, pH 7.2). Excitation was provided at 540 nm. Reprinted with permission from ref 142. Copyright 2007 American Chemical Society.

In **94**, anthracene is appended with two dithiocarbamate ligands and the construct provides ratiometric monitoring of Hg(II) in 1:1 MeCN/H_2O and 1:1 EtOH/H_2O.[141] In the latter solvent system, the emission spectrum of **94** exhibits two sharp maxima at ~390 and ~410 nm, characteristic of the anthracene chromophore, and a broad emission band centered at 525 nm attributed to charge transfer between the dithiocarbamate and anthracene moieties. Addition of Hg(II) to **94** inhibits charge transfer and the emission intensity at 525 nm decreases. Some fluorescence enhancement at ~390 and ~410 nm also occurs. This probe exhibits some fluorescence change following addition of Zn(II) and Cd(II). Substitution of the triethylamine moieties with morpholine abolishes the ratiometric response because only quenching of the charge transfer band is observed upon Hg(II) addition.

A BODIPY chromophore functionalized with two dithiadioxaaza macrocycles, **95**, was designed for the ratiometric detection of Hg(II) by both fluorescence and color changes (Figures 23 and 24).[142] In 30:70 THF/H_2O (20 mM HEPES, pH 7.2), emission from **95** is weak ($\Phi_{free} = 0.04$, $\lambda_{em} = 668$ nm) because of PET quenching of the BODIPY excited-state by the macrocyclic nitrogen atoms. Introduction of Hg(II) causes a slight decrease in emission at 668 nm and a dramatic increase at 578 nm ($\Phi_{Hg} = 0.33$). The I_{578}/I_{668} ratio increases ~30-fold with addition of 20 equiv of Hg(II). Addition of Mg(II), Fe(III), Co(II), Ni(II), Cu(II), Zn(II), Cd(II), Pb(II), Ag(I), or Al(III) to **95** results in negligible fluorescence change. Job plots indicate formation of a 1:2 **95**:Hg(II) complex, where one Hg(II) binds per macrocycle, with K_d values of 23 and 34 μM. Both PET and ICT were invoked to rationalize the fluorescence response of **95** to Hg(II). Red-shifted emission of **95** relative to unfunctionalized BODIPY occurs because of ICT from the donor nitrogen atom of the macrocycle to the BODIPY chromophore. Coordination of Hg(II) to the macrocyclic nitrogen atom decreases its electron-donating ability and disrupts ICT, which results in a hypsochromic shift of the emission band. In addition, Hg(II) complexation to **95** alleviates PET quenching of the BODIPY excited-state by the nitrogen lone pair electrons, which causes the fluorescence enhancement (Figure 24). Sensor **95** also provides colorimetric ratiometric Hg(II) detection. The optical absorption spectrum of **95** exhibits an absorption maximum at 606 nm (ϵ = 85,000 $M^{-1}cm^{-1}$), which is red-shifted by ~100 nm relative to that

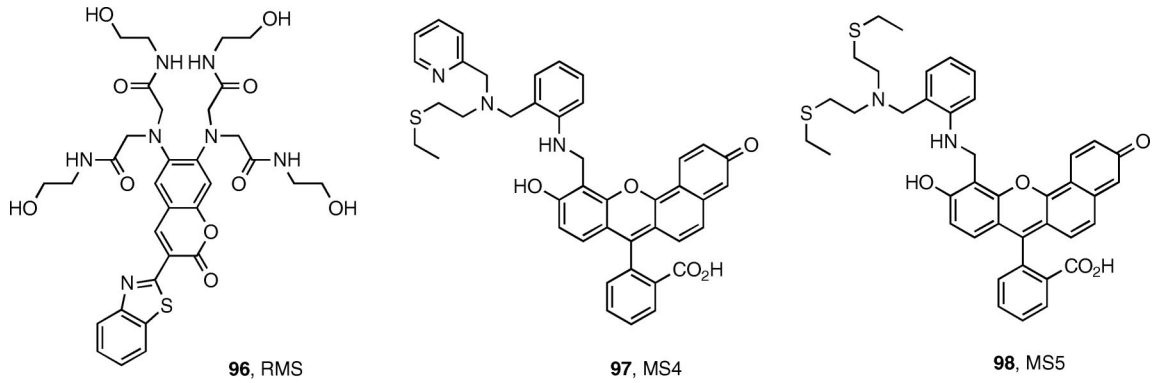

Figure 25. Ratiometric Hg(II) sensors that operate in aqueous solution.

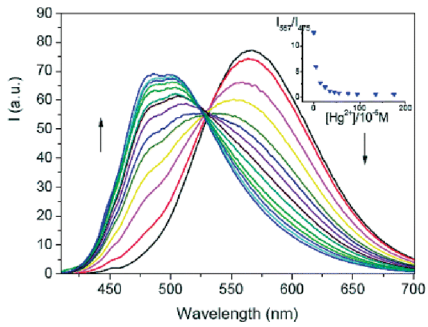

Figure 26. Ratiometric fluorescence response of **96** to Hg(II) in aqueous solution (pH 7.5). Reprinted with permission from ref 143. Copyright 2006 American Chemical Society.

of BODIPY itself and results from ICT. Addition of Hg(II) to **92** causes a hypsochromic shift of A_{max} to 564 nm (ϵ = 95,000 $M^{-1}cm^{-1}$), turning the solution color from purple to red-pink.

7.2. Ratiometric in Aqueous Solution

Only three examples of fluorescent ratiometric Hg(II) sensors that operate in aqueous solution have been reported (Figure 25).[143–145] One example employs a coumarin reporting group and the remaining two sensors, MS4 and MS5, are based on a seminaphthofluorescein platform. All three sensors afford single-excitation dual-emission ratiometric detection of Hg(II) with emission in the visible region of the electromagnetic spectrum.

The coumarin-based ICT fluorophore, **96**, comprises two electron-donating aniline groups and electron-accepting benzothiazolyl and carbonyl moieties.[143] Coordination of Hg(II) to the aniline nitrogen donor atoms disrupts charge transfer to the benzothiazolyl and carbonyl acceptors, thereby causing blue-shifts in the wavelengths of maximum absorption and emission (50 mM HEPES, pH 7.5). In the absence of Hg(II), **96** displays maximum emission at 567 nm (λ_{ex} = 390 nm) with a quantum yield of 0.051. Addition of increasing amounts of Hg(II) causes an ~100 nm blue-shift in the wavelength of maximum emission to 475 nm with essentially no change in quantum yield (Figure 26). The I_{567}/I_{475} ratio decreases from 11.9 to 0.4 with Hg(II) coordination, providing an almost 30-fold ratiometric change. Hg(II) binding causes an emission color change from yellow to cyan, visible by eye when a 10 μM solution of **96** ± Hg(II) is excited with 365 nm light by a hand-held UV lamp. Solution studies indicate 1:1 coordination of Hg(II) to **95** and a dissociation constant of 39 μM. From ^{1}H NMR spectroscopy, tetrahedral coordination of Hg(II) by the two aniline nitrogen atoms and two deprotonated amide nitrogen atoms is proposed. The selectivity of the yellow-to-cyan color change is very specific to Hg(II). Solutions of **96** remain yellow in the presence of Fe(III), Co(II), Ni(II), Cu(II), Zn(II), Cd(II), Ag(I), and Pb(II), and the Hg(II)-induced response is not compromised by the presence of 20 equiv of these metal ions. To date, this sensor provides the largest ratiometric response to Hg(II) in aqueous solution. Because ICT influences the optical absorption spectrum, **96** also provides colorimetric ratiometric Hg(II) detection.

MS4, **97**, is based on the seminaphthofluorescein platform and has an aniline-derivatized pyridyl-amine-thioether chelate (Figure 25).[144] At pH 8 (50 mM HEPES, 100 mM KCl), the optical absorption spectrum of MS4 has a maximum at 548 nm (ϵ = 9,000 $M^{-1}cm^{-1}$), which shifts to 545 nm (ϵ = 11,200 $M^{-1}cm^{-1}$) following addition of Hg(II). When excited at 499 nm, the emission spectrum of MS4 exhibits two local maxima at 524 and 613 nm (Φ_{free} = 0.05, pH 8). The intensity of the 613 nm band increases following addition of Hg(II) with no change in the 524 nm band, which affords single-excitation dual-emission ratiometric detection of this metal ion by comparison of the fluorescence intensity ratio (I_{624}/I_{524}) before and after Hg(II) addition. An ~4-fold ratiometric change occurs, with Φ_{Hg} = 0.10. The magnitude of the ratiometric response is pH-dependent with an ~2-fold increase at pH 7 and an ~8-fold enhancement at pH 11. Like MS1-MS3, Hg(II) coordination to MS4 is reversible and the maximum fluorescence response of MS4 to Hg(II) depends on chloride ion. The fluorescence response of MS4 is Hg(II)-specific and its selectivity for Hg(II) is similar to that of MS2 and MS3, with only Ni(II) and Cu(II) interfering with the Hg(II)-induced response. This observation provides further support for the notion that sulfur-rich chelates are valuable for achieving a high degree of Hg(II) selectivity.

MS5, **98**, employs the same thioether-derivatized aniline-based chelate as MS1 (MS5, Figure 25; MS1, Figure 20).[145] Combination of this ligand with the seminaphthofluorescein chromophore provides both turn-on and single-excitation dual-emission ratiometric sensing of Hg(II) in aqueous solution. Like MS4, the emission spectrum of apo MS5 exhibits two local maxima at ~520 and ~620 nm (λ_{ex} = 499 nm). The nature of the fluorescence response of MS5 to Hg(II) varies with pH. At pH 7, enhancement of both emission bands occurs, which provides ~4-fold turn-on detection (Φ_{free} = 0.018; Φ_{Hg} = 0.032). At pH > 8, Hg(II) coordination gives rise to a larger change in integrated emission (pH 8, ~9-fold; pH 9, ~11-fold), which arises from enhancement of the ~620 nm emission band. Only negligible changes in the ~520 nm emission band occur. This feature

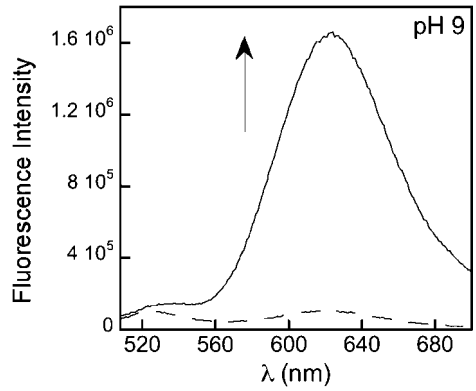

Figure 27. Fluorescence response of MS5 (5 μM) to 25 equiv of Hg(II) at pH 9 (50 mM CHES, 100 mM KCl) with excitation provided at 499 nm. Reprinted with permission from ref 145. Copyright 2007 American Chemical Society.

provides ratiometric detection through a comparison of (I_{624}/I_{524}) before and after Hg(II) addition and an ~13-fold ratiometric change occurs at pH 9 (Φ_{free} = 0.010; Φ_{Hg}= 0.086) (Figure 27). As expected based on MS1–4, chloride ion influences the magnitude of fluorescence turn-on observed for MS5. The fluorescence response of MS5 is Hg(II)-specific and reversible, and the sensor selectivity mirrors that of MS1 with only copper interfering with Hg(II) signaling. MS5 provides maximum fluorescence enhancement in the presence of ~10 equiv of Hg(II) and its EC_{50} for Hg(II) is 910 nM (1 μM probe; 50 mM PIPES, 100 mM KCl, pH 7), higher than that of MS1 (EC_{50} = 410 nM, pH 7) despite a conserved metal-binding unit. This variation may reflect differences in the protonation states of the seminaphthofluorescein and fluorescein platforms, with phenolate coordination to Hg(II) for MS1 and phenol coordination for MS5. The detection limit for Hg(II) is 50 nM when 500 nM probe is employed. MS5 can be used in conjunction with a low-affinity Zn(II) sensor QZ2[146] for simultaneously reporting Hg(II) and Zn(II) in buffered aqueous solution (pH 7). MS5 also responds to Hg(II) in spiked samples of natural water, which suggests that the chloride dependence will not be a limiting factor for its use.

8. Colorimetric Small-Molecule Hg(II) Detectors

Colorimetric Hg(II) detection has been pursued by several laboratories. This sensing approach has clear application in the development of commercial Hg(II) indicators, such as paper test strips, that can be evaluated visually without illumination. Water solubility is arguably a less important criterion for colorimetric probes than for fluorescent ones, which are better suited for in vivo work. As long as the colorimetric indicator responds to Hg(II) in the presence of water and can be absorbed onto a paper strip or into a membrane or film, it has potential. For this reason, in part, we choose not to group colorimetric sensors according to their solvent compatibility.

Figure 28 depicts colorimetric probes designed for Hg(II) detection that contain a wide variety of chromophores and chelates.[147–151] Sensor **99** consists of two 2,4-dinitrophenylazophenol reporting groups embedded into a *p-tert*-butylcalix[4]arenediaza-crown ether.[147] In chloroform, the optical absorption spectrum of **99** exhibits a dominant band centered at 424 nm due to the azophenol groups and **99** forms a yellow-colored solution. This probe can be employed in liquid/liquid extraction experiments. When an aqueous solution containing Hg(II) is vigorously mixed with a solution of **99** in chloroform, the color of the organic phase changes from yellow to red (A_{max} = 500 nm). Extraction of the red organic phase with EDTA reverses the color change. A colorimetric response also occurs following Cd(II) coordination. The detection limit of **99** for Hg(II) is estimated to be 10 μM.

Hemicyanine dye **100** consists of an aniline donor and benzothiazolium acceptor and provides colorimetric detection of Hg(II) in mixed EtOH/H_2O (1:10) at neutral pH.[148] Addition of Hg(II) to **100** causes an ~100 nm blue-shift in the wavelength of maximum absorption from ~550 to ~450 nm, with an isosbestic point at ~480 nm. As a result, solutions of **100** change from pink to green upon introduction of Hg(II) (Figure 29). This color change is selective for Hg(II). No color change occurs following addition of Na(I), Mg(II), Fe(II), Ni(II), Cu(II), Zn(II), Cd(II), or Pb(II). The absorption spectrum of **100** displays some pH dependence, with a red-shift of 25 nm in A_{max} in alkaline solution and with a decrease in extinction coefficient in acidic media. The response of **100** to Hg(II) also depends on pH and is optimal at pH 7. Job plots reveal a 1:1 stoichiometry for the **100**:Hg(II) complex and the K_d value for Hg(II) is 100 nM. Although a detection limit using optical absorption spectroscopy has not been not reported, ~85% fluorescence quenching occurs following Hg(II) addition to **100**. Fluorimetric analysis provides a detection limit of 100 ppb.

Sensors **101** and **102** were designed as "push-pull" systems for Hg(II) detection and each contain two amine receptors (Figure 28).[149] Coordination of Hg(II) to one of the amine groups causes metal-induced intramolecular charge transfer (MICT) where the free amine is the donor. As a result, addition of Hg(II) to solutions of **101** and **102** results in a dramatic red-shift in the wavelength of maximum absorption from ~400 to ~500 nm and the color changes from light yellow to red (MeCN). The color change is specific for Hg(II). Addition of thiourea to solutions of **101/102** and Hg(II) causes disappearance of the red color, indicating that the probes bind to Hg(II) reversibly. Metal-binding titrations reveal formation of 1:1 complexes and ^{1}H NMR studies confirm Hg(II) coordination to the amine nitrogen atom and not to the azine bridge. To determine whether **101** can detect Hg(II) dissolved in aqueous solution, test strips were prepared by treating filter paper with solutions of **101** in dichloromethane. After air drying and submersion into an aqueous solution of 25 μM Hg(II) (pH 7), the test strips change color from yellow to red.

Several aza-oxo open chain receptors appended to aromatic chromophores provide colorimetric Hg(II) detection (Figure 28).[150,151] Sensor **103** comprises an aza-oxo open chain receptor appended to a nitrophenylazophenyl reporting group.[150] It exhibits a charge transfer band centered at 460 nm in dioxane, causing its yellow-orange color. Addition of Hg(II) to **103** in dioxane induces a bathochromic shift in A_{max} of ~50 nm, and the solution turns red. Of twenty metal ions screened, only Hg(II) causes this color change. Although no binding constant was reported for the **103**:Hg(II) complex, ^{1}H NMR investigations indicate a strong interaction between Hg(II) and the aza-oxo chain.

In subsequent work, a linear aza-oxo chain was appended to a 1,3,5-triarylpent-2-en-1,5-dione to provide colorimetric Hg(II) detection in a dioxane/H_2O mixture (70:30, pH 6).[151] When appended to anilinium moieties, such diones undergo cyclizations to form the corresponding pyrilium cations upon

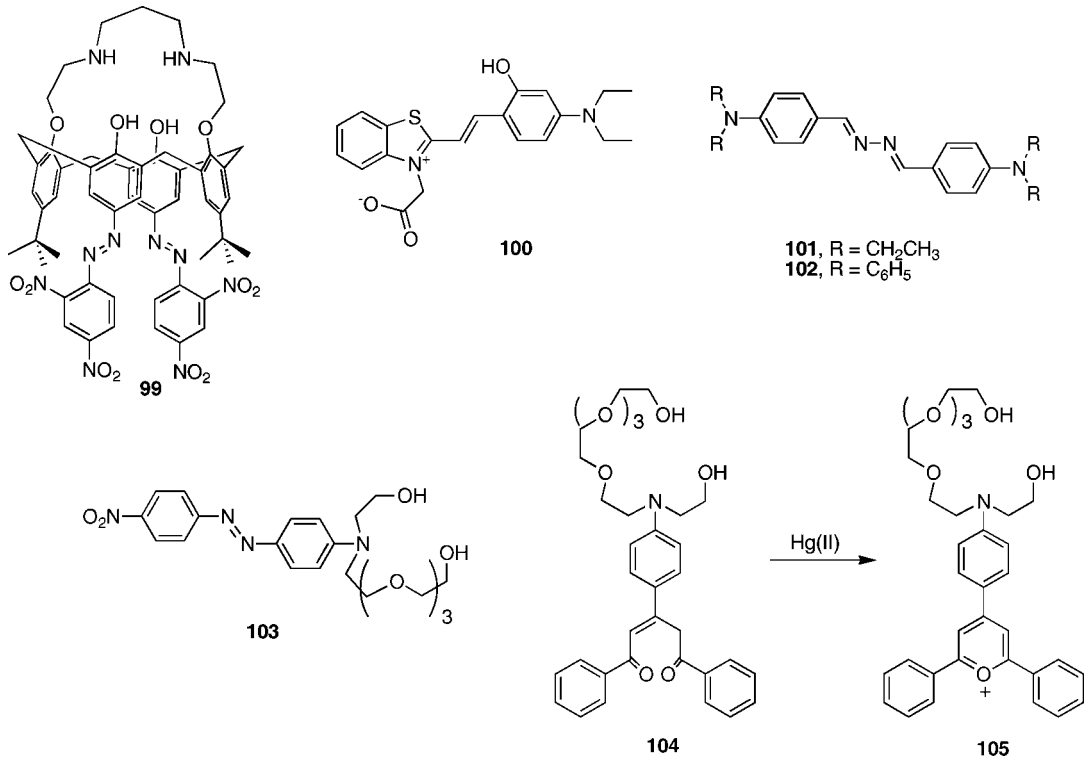

Figure 28. Miscellaneous colorimetric Hg(II) probes.

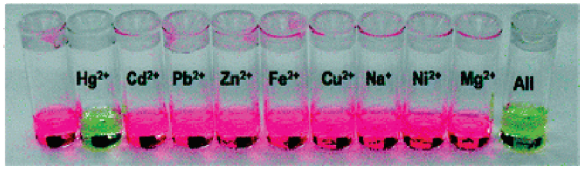

Figure 29. Digital image of the colorimetric response of **100** to Hg(II) in 1:10 EtOH/H_2O (pH 7, HEPES buffer). Reprinted with permission from ref 148. Copyright 2006 American Chemical Society.

protonation of the aniline moiety. Protonation alters the electronic character of the C_1 atom and allows for electrophilic attack by C_1 on the hydroxylic oxygen of the enol tautomer. To extend this work to metal-ion sensing, **104** was designed, which incorporates an aniline moiety into a linear aza-oxo chelate receptor. Introduction of one equiv of Hg(II) to a solution of **104** causes the color to change from yellow to magenta, indicative of ring closure and formation of **105**. The color change is visible by-eye at a probe concentration of 100 μM. Of eighteen other metal ions screened, only Fe(III) provides slight color change. Extraction experiments employing dichloromethane solutions of **104** and aqueous solutions of Hg(II) provide 10 ppb detection of Hg(II) following four min of shaking. When conducted in the presence of other metal ions, only Fe(III) competes with Hg(II) in the extraction experiments. Nevertheless, protonation of the aniline moiety also induces the yellow-to-magenta color change and may afford a false positive.

Phosphorodithioate **106** is a colorimetric Hg(II) precipitator (Figure 30).[152] Addition of Hg(II) to **106** instantaneously causes the solution color to change from yellow to red, which is visible to the naked eye when >8 μM **106** and >5 μM Hg(II) are employed. Precipitation of a red powder, a 2:1 **106**:Hg(II) complex, follows (MeCN/H_2O mixtures), which effectively bleaches the solution. This detector shows good selectivity for Hg(II). Although a number of other metal ions cause color changes, only Hg(II) causes immediate bleaching

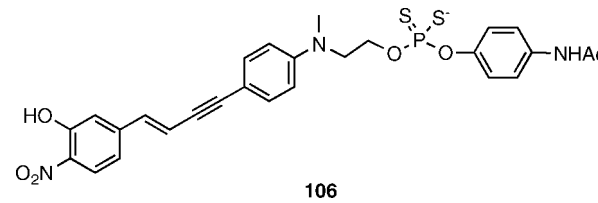

Figure 30. A colorimetric Hg(II) precipitator.

by precipitation. The affinity of **106** is highest for Hg(II) (K_d = 1.6 nM) with Hg(II) > Pb(II) > La(III) ~ Eu(III) ~ Gd(III) ~ Tb(III) > Cd(II) > Co(II). When monitored with a UV–vis spectrophotometer, a detection limit of 1 μM Hg(II) is obtained. In subsequent work, the authors developed a Hg(II) precipitator with 0.3 ppb sensitivity for Hg(II) that does not require attachment of a chromophore.[153]

Several colorimetric Hg(II) detectors utilize the squaraine reporter, which provides intense absorption in the visible and near-IR spectral regions. The probes depicted in Figure 31 respond to Hg(II) by bleaching of the chromophore.[154,155] Squaraine **107** has two dithiadioxaaza crown ether macrocycles as receptors.[154] In pure MeCN, the probe displays an absorption maximum at 640 nm. When increasing amounts of water are added to a solution of **107** in MeCN, face-to-face π stacking and aggregate formation occurs, which results in a decrease in absorption intensity and a blue-shift of A_{max} to 560 nm ($H_2O \geq 67\%$). In 20:80 MeCN/H_2O, **107** displays absorption from both the monomeric (~650 nm) and aggregate (~560 nm) forms and the solution is purple. Coordination of Hg(II) to **107** perturbs π-delocalization across the squaraine and the purple solution becomes colorless (Figure 32). The bleaching effect is selective for Hg(II). The alkali and alkaline earth metals, divalent first-row transition metal ions, the Group 12 congeners Zn(II) and Cd(II), and Pb(II) induce no significant change in the absorption bands of **107**. Addition of Ag(I) disrupts aggregate formation, causing the absorption at 647 nm to increase and

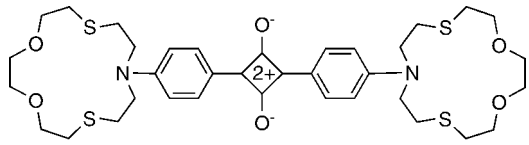

107

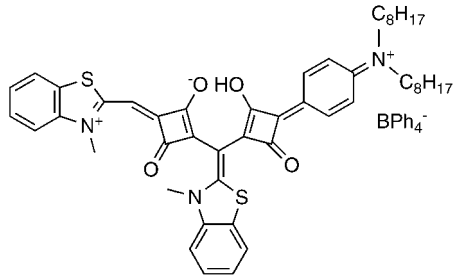

108

Figure 31. Colorimetric Hg(II) probes that operate via bleaching of squaraine absorption.

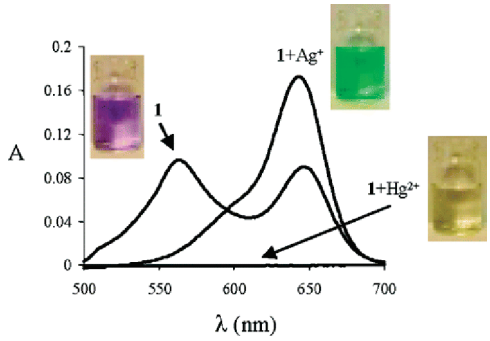

Figure 32. Colorimetric response of squaraine **107**, designated by "**1**" in the diagram, to Hg(II) and Ag(I) in 80:20 H_2O/MeCN. Reprinted with permission from ref 154. Copyright 2004 American Chemical Society.

the solution to turn green (Figure 32). The detection limit of **107** for Hg(II) varies with the MeCN/H_2O ratio of the solvent system. With 67% or less water content, the detection limit is <10 nM, below the EPA drinking water limit for inorganic Hg(II).

Bleaching of squaraine absorption also occurs for compound **108** following Hg(II) addition (Figure 31).[155] In dichloromethane, **108** exhibits an intense absorption band centered at ~782 nm. Addition of Hg(II) causes a decrease in and slight hypsochromic shift of A_{max} to 770 nm and formation of a new absorption band at 551 nm. The solution color changes from green to pink following introduction of Hg(II). Job plots indicate 2:1 **108**:Hg(II) binding stoichiometry and density functional calculations at the B3LYP/6–31G* level of theory suggest tetrahedral coordination of Hg(II) by the squaraine oxygen atoms. Similar changes in the optical absorption spectrum of **108** occur following introduction of Pb(II), but most other cations do not cause any change and **108** detects Hg(II) in the presence of Cu(II).

Squaraine has also been employed as the reporting group in a regenerative chemodosimeter containing a thioether moiety and two linear azacrown ethers (Figure 33).[117] Compound **109** is colorless in solution and exhibits two weak absorption bands centered at ~265 and ~305 nm attributed to the dialkylanilino and dialkylaminophenylhydroxycyclobut-2-enone groups, respectively. Formation of squaraine **110** is triggered by Hg(II)-induced loss of the thioether moiety, which provides intense absorption at 642 nm (1:4 MeCN/H_2O, pH 9.6) with ε_{642} > 100,000 $M^{-1}cm^{-1}$. The blue color that occurs upon Hg(II) addition is visible by eye. Spectrophotometrically, 20 ppb Hg(II) can be detected. The Hg(II)-induced conversion of **109** to **110** can also be monitored by fluorescence, and this methodology yields a detection limit below 10 nM (MeCN/H_2O mixture, pH 9.6). Derivative **111** was absorbed onto powdered silica and used in the preparation of films for "dip-stick" testing. The films turn blue after being submerged in an aqueous solution of Hg(II) for several seconds, which indicates a high potential for practical applications. Addition of propanethiol allowed for recycling of the dosimeter. This feature is an advantage over the chemodosimeters that rely on irreversible chemical reactions. Furthermore, compared to other strategies involving squaraine, this one is superior because a color enhancement results from Hg(II) detection instead of bleaching.

9. Mercury Detectors Based on Biomolecules

Biomolecules are alternatives to small-molecule detectors and have been applied in a variety of sensing applications. Often the specificity of a given biomolecule can be exploited to provide a probe that selectively responds to the analyte of interest. Other advantages include the water-solubility of biomolecules and that they generally function at neutral pH and under physiological conditions. Several types of biomolecules have been employed for Hg(II) detection, including proteins,[156,157] oligonucleotides,[158] DNAzymes,[159] and an antibody.[160] We include Hg(II)-responsive organisms[161–163] in this section and begin with a discussion of live bacteria engineered to provide fluorescent detection of mercury.

9.1. Recombinant Whole-Cell Bacterial Hg(II) Detectors

Many bacteria harbor genetically encoded resistance systems that allow them to survive in environments contaminated with various toxins, including heavy metals. The genes of the *mer* operon, *merTP(C)A(B)D,* are responsible for mercury resistance in several bacterial strains.[164] The regulatory protein MerR, encoded by the *merR* gene, suppresses transcription of the *mer* operon in the absence of Hg(II).[165–168] When bacteria encounter Hg(II), its binding to MerR results in a conformational change and transcription occurs, causing the synthesis of mercuric reductase. This enzyme converts inorganic Hg(II) to Hg(0), the latter of which is volatile and lost from the cells. Bacteria containing the *merB* gene also produce organomercurial lyase, which cleaves C—Hg bonds and thereby allows for the detoxification of organomercurial compounds. Live bacterial Hg(II) detectors that have been described to date are based on the receptor-reporter concept whereby a strictly Hg(II)-regulated promoter controls the expression of a reporter gene.[169] In most systems, the reporting firefly luciferase gene (*lucFF*) is controlled by the operator/promoter for the *mer* operon.[161–163,170,171] In the presence of Hg(II), MerR activates transcription and expression of firefly luciferase results. This enzyme catalyzes the ATP-dependent oxidative decarboxylation of D-luciferin to oxyluciferin, the latter of which is luminescent (λ_{max} = 560 nm). Recombinant bacteria lacking the *merB* gene exhibit narrow-range specificity and are only sensitive to inorganic Hg(II) whereas those containing the *merB* gene are broad-range and also detect organomercurials.[162] The sensitivity of these live

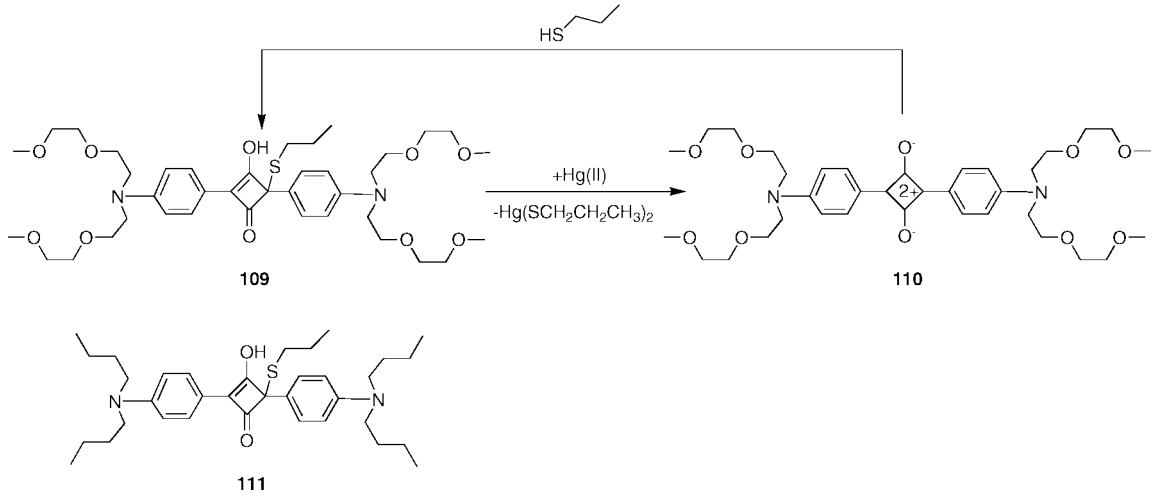

Figure 33. Regenerative colorimetric chemodosimeter for Hg(II) based on the squaraine chromophore that provides color development with Hg(II) detection.

cell Hg(II) detectors depends on the strain, but concentrations as low as 0.1 fM Hg(II) are detected by *E. coli* MC1061/pCSS810.[161] Because of the specificity of MerR for Hg(II), these microbe-based detectors are insensitive to other metal ions including Zn(II), Cu(II), Mn(II), and Co(II). Some emission enhancement results when micro- to millimolar concentrations of Cd(II) are present. The *mer/lucFF* systems have been applied to the analysis of water and soil samples[170–172] and have been installed in fiber optic devices.[173] In all cases, the systems report on bioavailable mercury instead of total mercury. Most protocols for employing the live bacterial sensors include incubation of the microbes with the sample of interest and subsequent addition of D-luciferin followed by spectrophotometric analysis. Because no complicated sample preparation is required and the bacteria can be lyophilized and stored frozen for at least 6 months, the approach is cost-effective. One potential drawback is that relatively long and temperature-dependent incubation times for both the sample and D-luciferin treatment are required to generate the luminescent signal. It should also be noted that false negatives occur in the presence of elevated mercury concentrations (~100 nM to ~1 μM depending on the mercury source) or other unknown toxins resulting from bacterial cell death. In related work, *E. coli* RBE27–13, a mercury-sensing strain containing the *lacZ* reporter gene under the control of the heavy metal-responsive gene promoter *zntA*, was employed in a fiber optic array to report on Hg(II).[174] After one hour incubation with 100 nM Hg(II) and treatment with fluorescein di-β-D-galactopyranoside, a 44% increase in fluorescence was observed, indicating an enhancement of LacZ expression relative to control cells where no Hg(II) was added. A 149% fluorescence change occurred when 5 μM Hg(II) was employed.

9.2. Protein-Based Hg(II) Detectors

In a separate strategy involving members of the *mer* gene cluster, *E. coli* MerR was overexpressed and combined with a 31-mer DNA duplex containing the MerR binding sequence and pyrrolo-C, depicted in red, a fluorescent analog of cytosine (Figure 34).[156] Pyrrolo-C itself emits at ~445 nm (λ_{ex} = 350 nm), but its fluorescence is quenched when it is attached to a DNA duplex because it hydrogen bonds with guanine to form a base pair. Addition of Hg(II) to solutions containing MerR and the 31-mer DNA duplex results in fluorescence turn-on because Hg(II) binding to MerR causes the enzyme to unwind the DNA duplex and disrupt base-pairing, which alleviates quenching of pyrrolo-C. An ~4-fold fluorescence enhancement immediately results following addition of one equiv of Hg(II) to the Mer/DNA mix. The detection system is >100-fold more sensitive to Hg(II) than other metal ions, in agreement with the known selectivity of MerR.[164] A detection limit for Hg(II) was not provided. Given the nanomolar sensitivity of MerR itself for Hg(II), this system or modifications thereof, particularly one with a brighter fluorophore, has the potential to respond to low Hg(II) concentrations. The DNA distortion mechanism provides a general strategy for developing fluorescent sensors for various analytes based on MerR family members and has been extended to Cu(II) and Pb(II).[156]

In subsequent work, the Mer/DNA approach was modified to afford ratiometric Hg(II) detection.[157] Two pyrene moieties, one on each oligonucleotide and adjacent to an abasic site, were incorporated into the center of a 31-mer duplex DNA containing the MerR binding sequence (Figure 34). In the absence of Hg(II), the pyrenes are in close proximity and emission is predominantly from the eximer (λ_{em}~ 480 nm). Once again, MerR coordination to Hg(II) causes a distortion in the DNA duplex, which separates the pyrene groups and disrupts eximer formation. An ~5-fold decrease in pyrene eximer and an ~3.3-fold increase in pyrene monomer emission (λ_{em}~ 380 nm) occur following addition of one equiv of Hg(II) to solutions containing MerR/DNA, which results in an overall ~15-fold ratiometric response. This fluorescence change is observable by-eye following addition of 1 μM Hg(II) if a hand-held UV lamp is employed. The detection limit for Hg(II) is ~10 nM and the metal-ion selectivity is like that of the pyrrolo-C analog described above.

9.3. Oligonucleotide-Based Hg(II) Detector

An oligodeoxyribonucleotide-based Hg(II) detector[158] was designed that takes advantage of the known ability of mercuric ion to bind to thymine-thymine (T-T) mispairs in DNA, resulting in stabilization of the duplex.[175] This sensor consists of an oligodeoxyribonucleotide (ODN) containing multiple thymine moieties that is linked to a dabcyl quencher (D) on the 5′ end and a fluorescein (F) on the 3′ end (Figure 35). In the absence of Hg(II), the D-ODN-F sensor is randomly oriented in aqueous solution and emission from

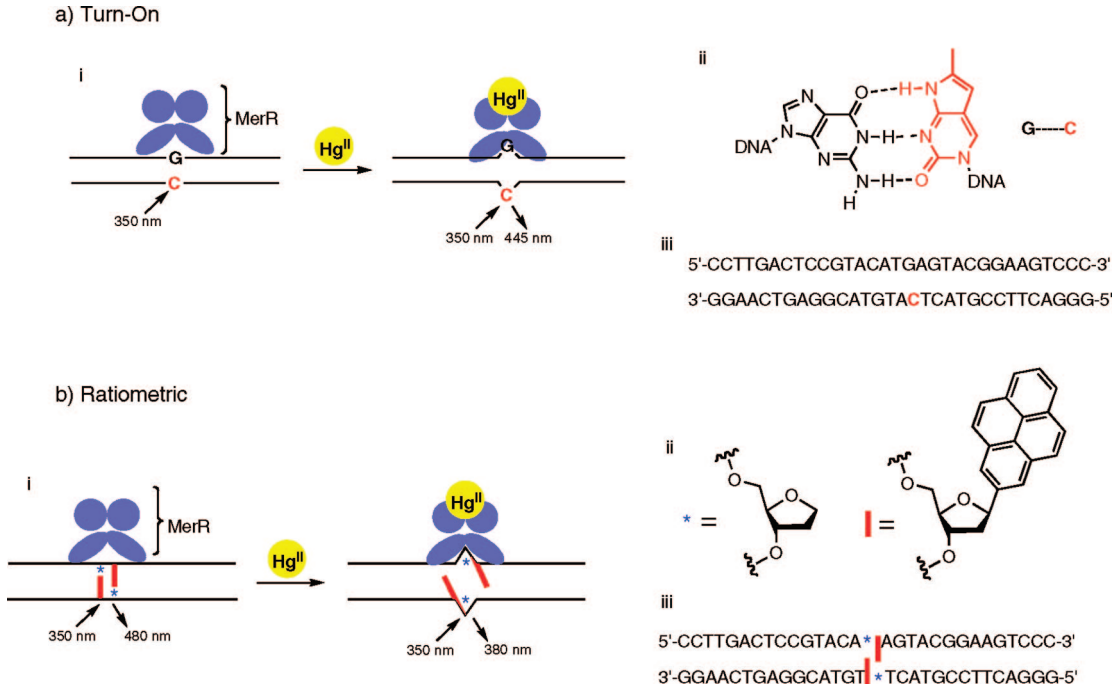

Figure 34. Hg(II) detectors that utilize the MerR-induced distortion of DNA. (a) Turn-on response to Hg(II): (i) Addition of Hg(II) causes MerR to distort a 31-mer DNA duplex containing a pyrrolo-C (red) chromophore and emission results. (ii) The hydrogen bonding and base-pairing that occur between guanine (G) and pyrrolo-C (red C) in the absence of Hg(II), which quenches pyrrolo-C emission. (iii) The 31-mer duplex DNA used in this study. (b) Ratiometric response to Hg(II): (i) Addition of Hg(II) causes the MerR to distort the 31-mer DNA duplex, which disrupts pyrene eximer formation. (ii) The abasic site (blue star) and pyrene (red bar) moieties employed. (iii) The 31-mer DNA duplex with pyrene and abasic sites employed.

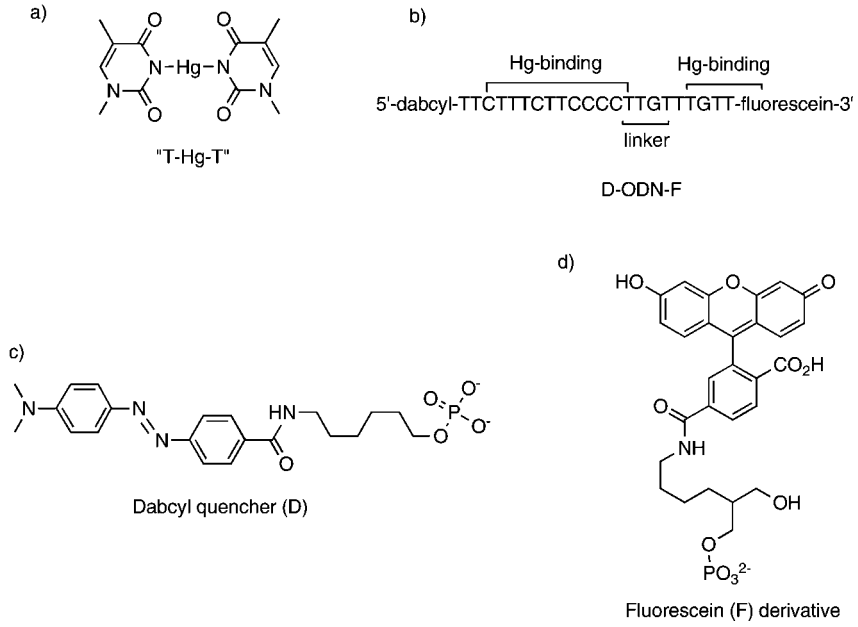

Figure 35. Components of the oligonucleotide Hg(II) detector. (a) Schematic of T-Hg-T pairs. (b) Structure and design of the D-ODN-F probe. (c) Structure of the dabcyl quencher. (d) Structure of the fluorescein derivative employed.

fluorescein is observed. Upon addition of Hg(II), the T-Hg-T adduct forms and produces a hairpin structure. The dabcyl moiety and fluorescein come into close proximity and fluorescence quenching results. This detector operates in aqueous solution at neutral pH, gives a linear response in the range of 40 to 100 nM of Hg(II), and has a lower detection limit of 8 ppb (40 nM). Because other metal ions do not promote similar stabilization of DNA duplexes containing T-T mispairs,[175] the response of this probe is highly selective for Hg(II). Detailed studies of Hg(II)-binding stoichiometry were not reported, but coordination of multiple Hg(II) ions is presumably necessary to form the hairpin structure. Because fluorescence quenching can result from other, unknown species in an environmental sample, an antisense approach was designed whereby a probe lacking both quencher and fluorophore was employed. If the D-ODN-F sensor exhibits fluorescence quenching in the absence of the antisense probe (as-ODN) and fluoresces brightly in the presence of excess as-ODN, the response can be attributed to Hg(II) complexation.

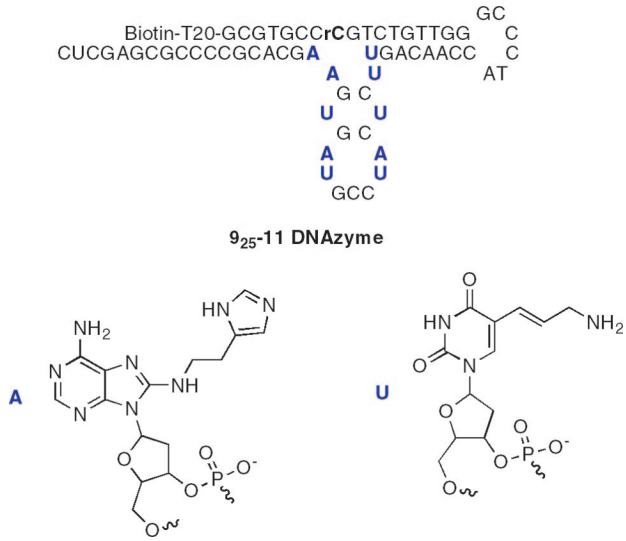

Figure 36. The 9_{25}-11 DNAzyme, which is a reversible sensor for Hg(II). Coordination of Hg(II) to the DNAzyme results in the inhibition of self-cleavage activity.

9.4. DNAzyme-Based Hg(II) Detectors

DNAzymes are nucleic acids that exhibit catalytic activity. Many of these deoxyribozymes have cleavage activity, promoting DNA or RNA strand scission. The 9_{25}-11 DNAzyme depicted in Figure 36 contains several unnatural nucleic acids appended with imidazole and amine groups that are important for catalytic activity.[159] In the absence of any metal ion, this species exhibits RNAase-A-like activity and self-cleaves an embedded ribophosphodiester linkage (rC in Figure 36). Addition of Hg(II) to the 9_{25}-11 DNAzyme results in its inhibition, which is attributed to chelation of Hg(II) by the imidazole groups. The inhibitory effect is visible by gel electrophoresis. A Hill plot analysis indicates that only one Hg(II) ion is required for inhibition and the apparent K_d value for Hg(II) is 110 ± 9 nM. Inhibition of the self-cleavage reaction by Hg(II) is reversible following addition of EDTA or DTT. Many other transition metal and rare earth metal ions were screened. Some of these show inhibitory effects in the order Hg(II) > Cu(II) > Yb(III) > Zn(II) ~ Y(III) ~ Eu(III) for the most potent inhibitors at 100 μM metal ion. The DNAzyme has a 25-fold weaker apparent K_d for Cu(II) relative to Hg(II), and the presence of Cu(II) has no apparent effect on the kinetics of the Hg(II)-induced cleavage inhibition. Drawbacks of the current system include: (i) it relies on inhibition rather than cleavage for Hg(II) detection and (ii) gel electrophoresis is required to analyze the products. Modification of this approach to afford an optical readout would be worthwhile. More recently, an in vitro selection approach was used to obtain Hg(II)-selective DNAzymes from a random population (10^{15} members) of oligonucleotides.[176] Eight cycles of selection and amplification afforded a population exhibiting a 54% enhancement in Hg(II)-induced cleavage efficiency, suggesting that in vitro selection may prove useful for discovering new Hg(II)-specific oligos.

9.5. Antibody-Based Hg(II) Detector

Chemically programmed monoclonal antibodies offer a means of fluorescent Hg(II) detection. 19G2 is a monoclonal antibody against *trans*-stilbene hapten EP-2 (**112**, Figure 37), and the EP2–19G2 complex emits blue fluorescence (λ_{ex} = 327 nm, λ_{em} = 410 nm, Φ = 0.78).[177] Modification of the stilbene moiety to include an arylboronic acid (Figure 37) maintains the blue emission characteristic of the EP2–19G2 complex in buffered aqueous solution, although the intensity is diminished to some degree and the emission maximum red-shifts to 445 nm (λ_{ex} = 300 nm). Addition of four equiv of Hg(II) to solutions of 19G2 and boronic acid **113**, which undergoes transmetalation with Hg(II) to form the aryl mercuric chloride, **114**, provides up to 93% fluorescence quenching.[160] This system is selective for Hg(II) over many other metal ions in aqueous solution. Alkali and alkaline earth metals, divalent first-row transition metal ions, Cd(II), Pb(II), and Pt(II) do not cause any fluorescence response. Addition of 10 equiv of Pd(II) results in ~65% fluorescence quenching. The detection limit of **113**-19G2 for Hg(II) is less than 6 nM.

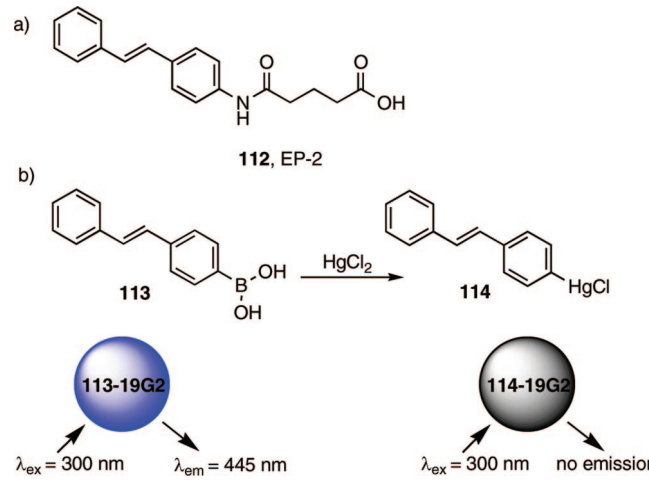

Figure 37. Components of a Hg(II) detection system that relies on the 19G2 antibody. (a) The stilbene hapten EP-2. (b) The 19G2 antibody fluoresces in the presence of the arylboronic acid. Addition of Hg(II) results in formation of the aryl mercuric chloride and quenching of antibody emission occurs.

10. Mercury Detectors Based on Materials

In this section, we highlight progress that has been made in the design and use of optical Hg(II) probes that employ materials as either the sensory unit or as a medium for harboring a Hg(II)-responsive element. These approaches vary widely and include soluble polymers,[178–183] heterogeneous systems that comprise membranes, films, and fibers,[184–190] and a variety of functionalized nanoparticles.[191–195]

10.1. Soluble and Fluorescent Polymers

Conjugated polymers (CPs) or "molecular wires" have been employed for the detection of many analytes, including biomolecules, explosives, and other small molecules.[196,197] An advantage of CPs over small molecules is that signal amplification occurs from electronic communication along the polymer backbone.[197] As a result, a single CP provides enhanced optical response relative to one of its monomer units. In recent years, CPs have been employed either alone or in conjunction with biomolecules for Hg(II) detection.

The poly[*p*-(phenyleneethylene)-*alt*-(thienyleneethynylene)] (PPETE) conjugated polymer functionalized with *N*,*N*,*N*′-trimethylethylenediamino (tmeda) groups affords turn-on Hg(II) detection in organic solution (**115**, Figure 38).[178] This polymer emits at 488 nm with a low quantum yield of 0.09. Addition of micromolar quantities of Hg(II)

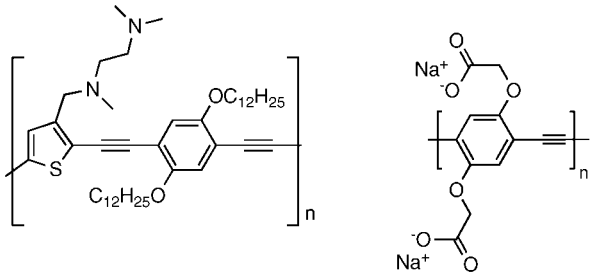

115 116, PPE

Figure 38. Conjugated polymers used for Hg(II) detection. CP **115** provides turn-on detection in THF. CP **116** gives a turn-off response to Hg(II) when combined with papain in an agglutination assay.

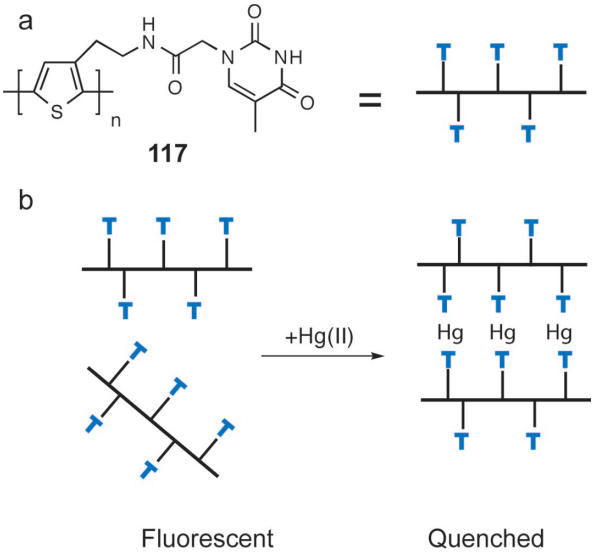

Figure 39. (a) A thymine-appended oligothiophene employed for Hg(II) detection. (b) Schematic of the Hg(II) sensing system. Addition of Hg(II) to **117** causes interpolymer stacking as a result of T-Hg-T interactions. Quenching of the CP emission results.

to **115** causes 2.7-fold fluorescence enhancement in THF. The polymer also responds to Ca(II), Zn(II), and protons, all of which afford 1.6- to 1.8-fold fluorescence turn-on. Because the PPETE polymer itself has a quantum yield of 0.54,[198] a PET mechanism is used to explain the low emission of **115** and the turn-on resulting from Hg(II) addition. In this model, the lone pairs of the tmeda nitrogen atoms quench emission from the PPETE polymer. Mercury coordination to the nitrogen atoms disrupts this pathway and gives fluorescence enhancement. This explanation is consistent with many experimental observations, including the proton and Zn(II) sensitivity to **115**, but a model study employing a PPETE-tmeda monomer would provide helpful insight into the details of Hg(II) coordination and subsequent turn-on. Although the fluorescence change is small and the Hg(II) affinity low (not quantified), this work provides a foundation for the design of turn-on conjugated polymers with enhanced Hg(II) affinity and selectivity.

Conjugated polymers have been used in conjunction with biomolecules for Hg(II) detection (Figures 38 and 39).[179,180] In one example, a hydrolytic enzyme was added to improve the sensitivity of a negatively charged CP, poly(*para*-phenyleneethynylene) (PPE), **116**, for Hg(II). Emission from **116** is sensitive to a number of metal ions, including Ca(II), Fe(II), Ni(II), Zn(II), Pb(II), and Hg(II), with the greatest fluorescence quenching observed following Hg(II) addition.

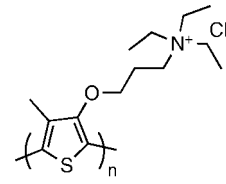

118, PMNT

5'-CATTTCTTTCTTCCCCTTGTTTGTTTCA-3'

119, MSO

Figure 40. The CP and mercury sensitive oligonucleotide, which provide colorimetric and turn-on fluorescent detection of Hg(II) in aqueous solution.

Papain, a positively charged hydrolase enzyme, coordinates Hg(II) and forms an electrostatic complex with **116** in solution. Addition of 20 μM Hg(II) to a 1:1 mixture of **116** and papain results in agglutination, precipitation, and a nonfluorescent solution phase. This turn-off effect only occurs for Hg(II). It is proposed that the **116**-papain complex is more susceptible to agglutination than are its individual constituents. The fluorescence change can be observed by eye using a hand-held UV lamp when 5 μM 1:1 **116**:papain and 20 μM Hg(II) are employed. This agglutination and precipitation behavior is observed with other proteins including histone (cationic) and BSA (anionic), but >100 μM Hg(II) is required to elicit the response. With significantly improved sensitivity, this strategy may afford a useful method for quick Hg(II) detection in the laboratory.

A conjugated polymer functionalized with nucleic acids has been employed for Hg(II) detection in aqueous solution.[180] Taking advantage of the characterized interaction of Hg(II) with thymine (see Section 9.3),[175] a poly(thiophene) conjugated polymer with one thymine moiety per monomer unit was designed (**117**, Figure 39). In the absence of Hg(II), the CPs are separated and exhibit strong emission at 550 nm (λ_{ex} = 415 nm, 4:1 EtOH/DMSO). Addition of mercuric acetate results in interpolymer stacking and aggregate formation because of T-Hg-T interactions between separate polymer chains. A 63% decrease in fluorescence intensity at 550 nm results. Coordination to Hg(II) also induces a 5-nm red-shift in the wavelength of maximum absorption. The emission of CP **117** exhibits some sensitivity to Cu(II) and Zn(II) (~25% and ~8% quenching observed, respectively). Other cations, including Ca(II), Mg(II), Co(II), and Ni(II), elicit little or no response and **117** can detect Hg(II) in their presence. The sensor responds to Hg(II) in the 30 to 300 μM range.

Most recently, a mixture containing a cationic CP, poly(3-(3′-*N,N,N*-triethylamino-1′-propyloxy)-4-methyl-2,5-thiophene hydrochloride) (PMNT, **118**), and an oligonucleotide (MSO, **119**) was used to provide colorimetric and turn-on fluorescent detection of Hg(II) in water (Figure 40).[181] The 28-base oligonucleotide is thymine-rich and serves as the Hg(II) probe. Solutions of **118** are yellow and exhibit maximum absorption centered at 392 nm. In the absence of Hg(II), **118** and the oligonucleotide form an electrostatic complex. Addition of oligonucleotide **119** to an aqueous solution of CP **118** causes the solution to turn red. A decrease in the 392 nm absorption band and formation of a new band of slightly greater intensity centered at 520 nm occur. Addition of Hg(II) causes the oligonucleotide to undergo a conformational change; like the oligonucleotide illustrated in Figure 35,[158] it adopts a stem-loop structure as a result of

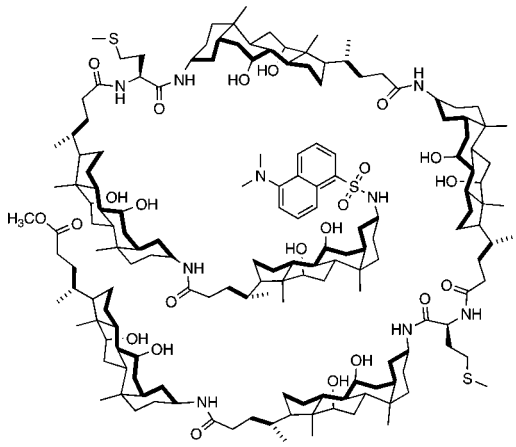

120

Figure 41. A cholate-based foldamer containing two methionine moieties for Hg(II) coordination and a dansyl reporting group.

Hg(II) coordination and formation of T-Hg-T linkages. This conformational change modulates the electrostatic interaction between **118** and **119**, and the solution color returns to yellow, which provides colorimetric detection of Hg(II). The Hg(II)-induced red-to-yellow color change is visible to the eye at 12.5 μM Hg(II) and at 2.5 μM with a spectrophotometer. Emission from **118** is also influenced by **119** and Hg(II). Addition of the oligonucleotide to aqueous solutions of the CP results in ~5-fold fluorescence quenching with no apparent change in the wavelength of maximum emission (λ_{em} = 533 nm). Subsequent addition of Hg(II) to this mixture restores ~50% of **118** emission. A detection limit of 42 nM is obtained by fluorescence. Other metals including Ca(II), Mg(II), Mn(II), Co(II), Cu(II), Zn(II), and Pb(II) cause negligible color and fluorescence change. The optical changes that result from Hg(II) addition are attributed to a new interaction between the **118** and the Hg(II)-bound oligonucleotide. Nevertheless, the red-to-yellow color change and fluorescence turn-on could also arise from breakdown of the electrostatic CP-oligonucleotide complex.

Foldamers are another class of polymers that have been employed for Hg(II) detection. The cholate/methionine foldamer **120** is appended with a dansyl fluorophore at one chain terminus (Figure 41).[182,183] When dissolved in nonpolar media containing a trace amount of polar solvent, foldamer **120** can adopt a helical structure with a central cavity. Addition of Hg(II) to **120** in such a "folding-friendly" solvent system (2:1:hexane/EtOAc with 5% methanol) results in ~2-fold fluorescence quenching. The fluorescence change is attributed to Hg(II) coordination to the two methionine thioether moieties of **120**, which are in close proximity as a result of folding, and quenching of dansyl emission by Hg(II). Job plots indicate that the foldamer binds Hg(II) with 1:1 stoichiometry. A K_d value of 67 nM and a detection limit of 20 nM were obtained in this solvent system. The affinity of **120** could be systematically decreased by almost 4 orders of magnitude by changing the solvent composition to disfavor folding, which separates the thioether donors. The fluorescence response of **120** to Hg(II) is relatively high. Other metal ions, including Mg(II), Co(II), Ni(II), Cu(II), Zn(II), Pb(II), and Ag(I), were screened and **120** only showed a fluorescence response for Ag(I) (4%). In subsequent work, **120** was treated with surfactant micelles for application in aqueous solution.[183] A combination of **120** and anionic SDS micelles proves to be optimal for Hg(II) detection in aqueous

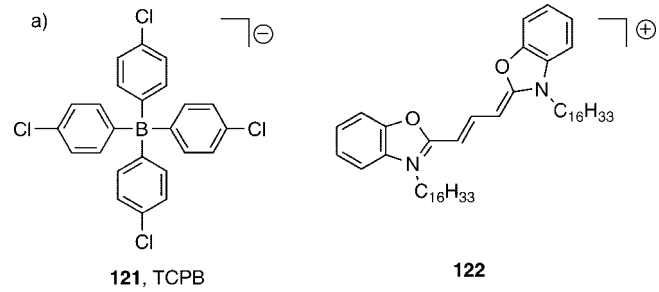

121, TCPB **122**

b)

$$B(C_6H_5)_4^- + 4Hg^{2+} + 3H_2O = 4C_6H_5Hg^+ + 3H^+ + B(OH)_3$$

$$B(C_6H_5)_4^- + 2Hg^{2+} + 3H_2O = 2(C_6H_5)_2Hg + 3H^+ + B(OH)_3$$

Figure 42. Components and reactivity of a Hg(II)-sensitive membrane. (a) Fluorescent and reactive components of the system. The membrane also contains the PVC polymer and DOS plasticizer. (b) Decomposition of tetraphenylborates by Hg(II).

solution, although the affinity for Hg(II) drops significantly (K_d = ~1.5 to ~9 μM depending on SDS concentration) and the detection limit increases to 1 μM.

10.2. Membranes, Films, and Fibers

A turn-off Hg(II) detection system based on a cation-sensitive membrane, a potential-sensitive fluorophore, and the known decomposition of borate by Hg(II) has been described.[184,185] The cation-sensitive membrane contains a mixture of poly(vinyl chloride) (PVC), bis-(2-ethylhexyl)sebacate (DOS), potassium tetrakis(4-chlorophenyl)borate (PTCPB, **121**), and the 3,3′-dihexadecyldicarbocyanine fluorophore (**122**, Figure 42) dried on a Mylar support. 3,3′-Dihexadecyldicarbocyanine is lipophilic and exhibits solvent-dependent emission with fluorescence in moderately polar media, including the PVC membrane, and quenching in aqueous solution. It forms an ion-pair with **121** in the membrane. When immersed in aqueous solution, the **121–122** ion-pairs reside in the membrane, which thereby fluoresces (λ_{ex} = 492 nm; λ_{em} = 512 nm). When Hg(II) is introduced into the aqueous solution and enters the membrane, borate decomposition occurs (Figure 42), disrupting the borate-dye ion-pairs and causing partial expulsion of **122** from the membrane. Consequently, fluorescence quenching occurs when **122** encounters aqueous solution and aggregates. This system provides a linear response to Hg(II) in the concentration range of 0.1 to 5 μM, which is insensitive to pH in the 4 to 6 range. The specificity of the membrane for Hg(II) is high. Addition of Zn(II) or Ag(I) results in slight fluorescence quenching, <10% of the total observed for Hg(II). Negligible emission change occurs following addition of Na(I), K(I), Ca(II), Mg(II), Ni(II), Cu(II), Cd(II), or Al(III). Although decomposition of borate by Hg(II) is irreversible, the membrane can be recycled by a soak in borate solution. Because of its two hexadecyl tails, fluorophore **122** remains associated with the polymer and the cationic portion will re-enter following borate treatment.

A number of films and fibers have been employed for Hg(II) detection with varying degrees of success. The small-molecule Hg(II) probes embedded in these materials are shown in Figure 43.[186–190,199] In the 1990s, an approach for detecting cations that employs distearylphosphatidylcholine (DSPC) bilayers doped with synthetic lipid-appended reporters was developed.[199] Mercury detection in aqueous solution (MOPS buffer, pH 7.4) was achieved by using hydrated films containing DSPC and a synthetic lipid, **123**, appended with

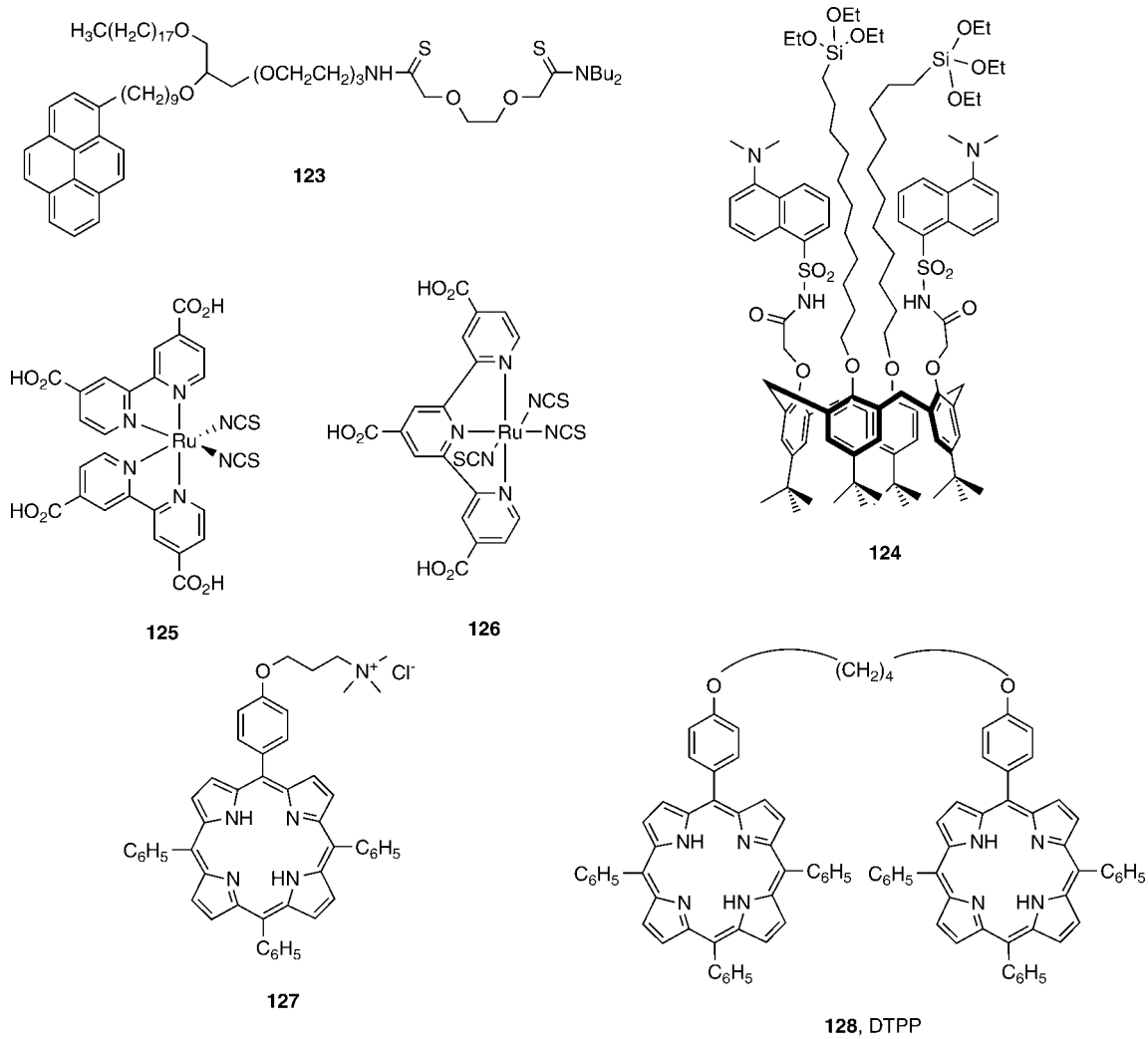

Figure 43. Small molecules employed in membranes, films and fibers for Hg(II) detection.

both a dithioamide receptor and a pyrene reporting group (Figure 43). The hydrophobic pyrene moieties are embedded inside of the DSPC interior and the dithioamide receptors reside at the bilayer surface. In the absence of Hg(II), emission from both the pyrene monomer ($\lambda_{em} = 376$ nm) and eximer ($\lambda_{em} = 470$ nm) occurs with a monomer/eximer (M/E) intensity ratio of 2.2. The eximer emission results from a high local concentration of pyrene in the bilayer, which facilitates aggregation. Introduction of Hg(II) causes a decrease in eximer and increase in monomer emission, attributed to reorganization of **123** in the bilayer and disruption of eximer formation. The sensing response of the DSPC/**123** bilayer is therefore ratiometric, although it was not described as such in the initial report. Its response to Hg(II) occurs immediately after mixing. The change in M/E ratio is linear (semilogarithmic plot) over a Hg(II) concentration range of 100 nM to 100 μM and the detection limit for Hg(II) is 100 nM. DSPC/**123** is unresponsive to mM concentrations of Na(I), Li(I), K(I), Mn(II), Ni(II), Ca(II), Cr(III), Co(II), and Pb(II). Both Cu(II) and Cd(II) generate some fluorescence response, but the sensitivities are 10- and 1000-fold lower than that of Hg(II). Addition of EDTA restores the M/E ratio characteristic of the unbound form and the bilayer can be recycled.

Mesoporous materials offer an alternative means of immobilizing small molecules and have been employed for the detection of heavy metal ions. Calixarene-based sensor **21** (Figure 4) was modified to include triethoxysilane groups (**124**, Figure 43) suitable for grafting onto SBA-15, an ordered mesoporous silica with an average pore size of 66 Å.[186] When grafted onto SBA-15 and suspended in water (pH 4.0), the emission spectrum of **124** exhibits a maximum at 540 nm ($\lambda_{ex} = 350$ nm). Following introduction of Hg(II) into the aqueous solution, the emission from **124**-SBA-15 decreases ~50% and a 12-nm blue-shift in the wavelength of maximum emission occurs. Metal-binding titrations monitored by fluorescence spectroscopy indicate that one Hg(II) binds per **124** on the SBA-15 support with a K_d value of 2 μM (pH 4). The linear response range of **124**-SBA-15 extends to 4 μM Hg(II) and its detection limit for Hg(II) is 330 nM. **124**-SBA-15 gives some fluorescence response to Cu(II) (turn-off) and to Na(I) and Pb(II) (turn-on). The material responds to Hg(II) within a few seconds following Hg(II) addition and can be recycled. Addition of excess EDTA regenerates the emission of apo **124**-SBA-15.

Two ruthenium-based compounds with pyridyl and thiocyanate ligands provide colorimetric Hg(II) detection in solution both as free molecules and when appended to mesoporous nanocrystalline TiO_2 films (Figure 43).[187,188] Aqueous solutions of **125** change from dark red-purple to orange upon addition of Hg(II) with a decrease in 530 and an increase in 480 nm absorption. This color change is visible by eye at 1.5 ppm Hg(II), and 20 ppb Hg(II) can be detected by UV–vis spectroscopy.[188] X-ray crystallographic studies

indicate that Hg(II) binds to the sulfur atoms of the NCS groups and forms an insoluble coordination polymer $[Ru(N_2C_{12}O_4H_8)_2(NCS)_2]_n^{n+}$ under the conditions for crystal growth. When **125** is absorbed onto TiO_2 and exposed to aqueous solutions of Hg(II), a red-purple-to-orange color change occurs in seconds at millimolar concentrations of Hg(II) and in minutes for micromolar concentrations. This color change is specific for Hg(II). Other metal ions, including Ca(II), Mg(II), Mn(II), Fe(II), Co(II), Ni(II), Cu(II), Zn(II), Cd(II), and Pb(II), do not cause any an optical change (20 μM metal ion, 10 min), and no interference from different anions (F^-, Cl^-, Br^-, I^-, AcO^-, NO_3^-, and SO_4^{2-}) occurs. The film sensitivity is less than that of the free Ru(II) complex, with 0.5 ppm detection being achievable with the use of a spectrophotometer. Importantly for practical applications, the TiO_2 films can be recycled by washing with KI and subsequently reused for Hg(II) detection. A second-generation Ru(II)-based sensor, **126**, was also prepared.[188] Solutions of **126** exhibit a greater colorimetric change from dark green to pink following Hg(II) addition resulting from a decrease in the 625 nm charge transfer band and an increase in absorption at 560 nm. As observed for **125**, the color change of **126** is Hg(II)-specific; this sensor provides a linear response from 0.5 to 600 nmol of Hg(II) and a detection limit of ~100 ppb. As for **125**, TiO_2 films soaked with **126** provide a Hg(II)-specific colorimetric change when dipped in aqueous solutions containing Hg(II). Low ppm concentrations of Hg(II) are visible by-eye with this film.

Porphyrin films deposited on glass surfaces have been used for turn-off Hg(II) detection in water.[189] Films formed by depositing porphyrin **127** (Figure 43) on hexamethyldisiloxane-treated glass slides exhibit an optical absorption band at 420 nm and emission bands at 652 and 720 nm (λ_{ex} = 420 nm). Following immersion into an aqueous solution of 10 μM Hg(II), the porphyrin emission decreases ~10-fold. A bathochromic shift in the absorption spectrum also occurs, which indicates Hg(II) coordination to the porphyrin. The heavy metal ion chelator TPEN, **13** (Figure 1), effectively removes Hg(II) from the porphyrin and restores the original fluorescence of the film. Through consecutive dipping into Hg(II) or TPEN solutions, the film can be recycled at least six times. The film is stable in the pH 5–9 range and <100 μM concentrations of other metal ions, including Cu(II), Cd(II), and Pb(II), have negligible effect on film emission. A flow-through fluorescence cell was fabricated using **127** and fluorescence quenching occurs when a Hg(II)-containing solution was passed through the device. The degree of quenching was linearly correlated to the concentration of Hg(II) in the 0 – 250 μM range. In related work, 5,10,15-tris(pentafluorophenyl)corrole was embedded in a PVC membrane and used to sense Hg(II) by fluorescence quenching in the pH 5–8 range.[200]

Optical fibers[201,202] are useful Hg(II) sensing platforms because they accommodate multiplexing and can be delivered to remote locations such as deep sea waters. A lipophilic diporphyrin, 5-*p*-[[4-(10′,15′,20′-triphenyl-5′-porphinato)-phenyloxyl]-1-butyloxyl]phenyl-10,15,20-triphenylporphine (DTPP) (**128**, Figure 43), was incorporated into PVC containing sodium tetraphenylborate and DOS, and the mixture was coated onto a quartz plate for use in a bifurcated optical fiber.[190] The porphyrin dominates the fluorescent properties of the fiber, which exhibits two peaks of maximum emission at ~652 and ~717 nm (λ_{ex} = 421.5 nm). Addition of Hg(II) causes ~2-fold fluorescence quenching. The working concentration range is from 0.52 to 310 μM Hg(II) and the 1:1 DTPP/Hg(II) complex has an apparent K_d of 46 μM. Emission from the fiber is pH-insensitive from 2.4 to 8, which makes it suitable for use in natural waters. It is selective for Hg(II) over millimolar concentrations of Cd(II), Co(II), Cu(II), Ni(II), Pb(II), Zn(II), and Fe(III) (pH 5.4), and the Hg(II)-induced fluorescence quenching can be reversed by washing the membrane with dilute HCl. Consequently, the fiber can be recycled >30 times and can be stored for at least one month without compromising its integrity. To determine the ability of the fiber to detect Hg(II) in relatively complex media, water samples from the Xiang River (China) were spiked with 2 – 10 μM Hg(II). In all cases, fluorescence quenching was observed. This experiment points to potential utility of the fiber in real-life applications, but the relatively low Hg(II) affinity will be a limitation for detecting pM and nM variations in Hg(II) concentrations in natural waters.

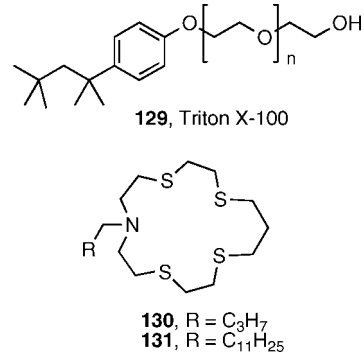

129, Triton X-100

130, R = C_3H_7
131, R = $C_{11}H_{25}$

Figure 44. Components of Triton X-100 micelles for Hg(II) detection.

10.3. Micelles

Triton X-100, **129**, micelles containing pyrene and thioether-rich macrocyclic chelates functionalized with alkyl chains, **130–131**, give turn-off or turn-on detection for Hg(II) in water depending on the length of the alkyl chain and solution pH.[203] The dodecyl macrocycle **131** (Figure 44) is lipophilic and resides inside of the Triton X-100 micelle. At pH < 4, its nitrogen atom is protonated and does not quench emission from the pyrene moieties that also reside in the micelle. Addition of Hg(II) to the micelles that contain **131** and pyrene causes fluorescence quenching. The turn-off effect is attributed to formation of a **131**:Hg(II) complex, which remains in the micelle because of the hydrophobic alkyl chain and quenches pyrene emission. When **130**, a macrocycle functionalized with a shorter alkyl chain, is employed, turn-on Hg(II) detection can be achieved (pH > 7). Under these conditions, the macrocycle is not protonated and it quenches pyrene emission in the absence of Hg(II). Introduction of Hg(II) causes formation of the **130**:Hg(II) complex, which is sufficiently hydrophilic to leave the micelle. Pyrene emission is thereby restored. This work provides a proof of concept that micelles can be employed to encapsulate components of an Hg(II) sensing system. It would have been preferable, however, for the system to be covalently linked rather than having so many individual components.

10.4. Nanoparticles

Interest in using nanoparticles for Hg(II) detection is growing. They offer strong emission and stability to photo-

bleaching, and they can be functionalized with solubilizing groups and/or chelates to afford water compatibility and increased Hg(II) specificity.[6,204–206] Several types of nanoparticles have been employed for Hg(II) detection to date and include CdTe and InP nanocrystals,[191,192] gold nanoparticles,[194] and gold nanorods.[193]

CdTe nanocrystals stabilized with mercaptopropionic acid (MPA) having a particle diameter of 3.0 ± 0.2 nm show ~68% fluorescence quenching following addition of Hg(II) in aqueous solution at pH 7.4 (λ_{em} ~540 nm).[191] The nanocrystals provide a linear response to Hg(II) at concentrations below ~130 nM and a lower detection limit of 0.5 nM. The carboxyl groups of the MPA moieties may coordinate Hg(II). The Hg(II)-induced turn-off was attributed to electron transfer from MPA to Hg(II) or to Hg(II)-induced nonradiative decay of the nanocrystal, but more work is required to support either possibility. The response of the CdTe nanocrystals shows good selectivity for Hg(II). Only ≤8% fluorescence quenching is observed following introduction of Na(I), K(I), Ba(II), Ca(II), Mn(II), Fe(III), Zn(II), Cd(II), Pb(II), or Al(III) (47 nM) and ~30% turn-off occurs with Cu(II) addition.

In subsequent work, fluorescence enhancement was observed following addition of Hg(II) to InP nanocrystals capped with mercaptoacetic acid (MAA).[192] These nanocrystals have a median diameter of 8 nm, emit in the near-infrared region with two local maxima centered at 750 and 826 nm, and exhibit ~2-fold fluorescence turn-on with Hg(II) addition. The Hg(II)-induced fluorescence response is linear from 0.5 to 8 μM and a detection limit of 0.1 μM was reported. As suggested for the CdTe nanocrystals described above, Hg(II) may coordinate to the mercaptoacetic acid moieties on the nanocrystal surface. But the Hg(II)-induced fluorescence enhancement is attributed to the formation of HgS particles on the nanoparticle surface, which are electron–hole recombination centers and can eliminate nonradiative decay of the excited InP electrons. No experimental evidence was provided to support this notion, however. Like the CdTe nanocrystals, emission from the InP/MAA system is apparently insensitive to most other metal ions; some fluorescence enhancement occurs from Cu(II) and Ag(I).

Gold nanorods have been employed to detect dissolved mercury by optical absorption spectroscopy.[193] The nanorods have an average aspect ratio of 1.6 and, in water, exhibit absorption bands at 520 and 612 nm attributed to the transversal and longitudinal modes, respectively. In the presence of sodium borohydride ($NaBH_4$), which reduces all dissolved Hg(II) to Hg(0), amalgamation between Hg(0) and gold occurs. Amalgamation induces changes in the optical absorption spectrum of the nanorods. The absorption peak resulting from the longitudinal mode, which is centered at 599 nm in the presence of $NaBH_4$, undergoes a blue-shift that directly correlates to Hg(II) concentration at low, ~10^{-11} M, levels. At higher concentrations (~10^{-4} M), only one absorption band centered at 530 nm is observed, consistent with conversion of the nanorods to nanospheres. The nanorods respond to Hg(0) in less than 10 min and ppt levels of Hg(0) can be monitored.

More recently, 13-nm diameter gold nanoparticles (AuNPs) functionalized with rhodamine B (RB) chromophores have been utilized for turn-on Hg(II) detection in aqueous media.[194] Emission from the RB-AuNPs is weak (λ_{ex} = 510 nm, λ_{em} = 575 nm) because AuNPs quench organic chromophores effectively by both energy- and electron-transfer processes. Addition of Hg(II) to the AuNPs causes ~400-fold fluorescence enhancement, which results from Hg(II)-induced release of the rhodamine chromophores from the AuNP surfaces. When the AuNPs are only functionalized with RB, fluorescence turn-on also occurs for many other metal ions including Mn(II), Fe(II), Cr(III), Cd(II), and Pb(II). Additional functionalization of the AuNPs with thiophilic chelates, including MPA, helps promote Hg(II) selectivity. When the AuNP surfaces are ~20% covered by a thiophilic chelate, they exhibit reduced sensitivity to Mn(II), Fe(II) and Cr(III) and remain responsive to Hg(II), Pb(II), and Cd(II). Introduction of pyridine-2,6-dicarboxylic acid (PDCA) to solutions of RB-AuNP-MPA provides a Hg(II)-selective response. The RB-AuNP-MPA detectors provide a linear response to Hg(II) from 15 to 250 nM and have a lower detection limit of 10 nM (2 ppb). The RB-AuNP-MPA constructs were used to determine the concentration of Hg(II) in spikes samples of pond water and in batteries. In instances, 90–95% correlation was found with the data from fluorescence and ICPMS.

Lastly, DNA-functionalized AuNPs (DNA-AuNPs) have been employed for colorimetric Hg(II) detection.[195] Individual DNA-AuNPs with complementary sequences form DNA-linked aggregates when combined in aqueous solution.[207] The aggregates have sharp melting temperatures (T_m) and they provide a color change from purple to red upon dissociation. These features were utilized in the design of a Hg(II) detection method that employs two DNA-AuNPs, with thiolated DNA sequences 5′-HS-C_{10}-A_{10}-T-A_{10}-3′ and 5′-HS-C_{10}-T_{10}-T-T_{10}-3′, that exhibit a T-T mismatch. Because (i) T_m values are sensitive to base-pair mismatches and decrease relative to the T_m values of perfectly complementary stands, (ii) Hg(II) has a high affinity for T-T mispairs, and (iii) addition of Hg(II) to a DNA duplex containing T-T mispairs results in stabilization of the duplex, Hg(II) addition to the DNA-AuNP aggregates harboring a T-T mismatch causes an increase in the T_m that is linearly dependent on the concentration of Hg(II). It increases ~5 °C per 1 μM Hg(II). As a result, a purple-to-red color change occurs, resulting from deaggregation of the DNA-AuNPs, at a particular Hg(II)-dependent temperature. The response is selective for Hg(II) because K(I), Ca(II), Mg(II), Ba(II), Mn(II), Fe(II), Fe(III), Co(II), Ni(II), Cu(II), Zn(II), and Cd(II) have no effect on the T_m value. Addition of Pb(II) to the DNA-AuNP aggregates causes a negligible increase in the T_m of ~0.8 °C. The detection limit for Hg(II) is 100 nM.

11. Perspectives

Remarkable progress in the design, synthesis and characterization of Hg(II)-responsive probes has occurred over the past several years. Dozens of new small-molecule fluorescent and colorimetric Hg(II) detectors, in addition to probes based on biomolecules and materials, have been published that exhibit a range of characteristics. Through both rational design and serendipity, a number of these probes exhibit features amenable for practical applications and a few have been tested in real-world samples. Nevertheless, from the standpoint of Hg(II) sensor design, many avenues require further elaboration. In particular, ratiometric Hg(II) detection in water lags behind other small-molecule approaches and warrants further investigation and novel design strategies. Mechanistic and theoretical studies aimed at providing detailed explanations of how individual sensors provide optical feedback are often lacking. The results of such

investigations will help guide the design of future generations of probes with improved characteristics. Arguably none of the reported Hg(II) sensors have been rigorously tested in the environmental and biological realms. Doing so, and hence achieving the ultimate goal of providing effective tools for application-based work, requires substantial effort and cross-disciplinary interactions.

Many issues regarding mercury speciation and detection exist. With few exceptions, the detectors reported thus far respond to Hg(II). This analyte is important for water quality analysis and studies of Hg(II) toxicity, and it also provides the indirect detection of mercury derivatives, including organomercurials, in fish tissue following digestion and extraction. As a result, the monitoring of Hg(0) has been overlooked although it also deserves attention. Hg(0)-specific sensors will be beneficial for monitoring fluctuations in Hg(0) emissions from smokestacks and from natural disasters. The former application would be useful in preventing unintentional anthropogenic release. Methylmercury is of particular concern because of its ability to bioaccumulate and its potent neurotoxicity. With the exception of several chromatographic methods described in Section 3, little effort has been made to design optical probes for this mercury derivative. One reason for this dearth is clear – handling methylmercury is perilous to the investigator – and the necessity of direct methylmercury detection is also subject to debate. Procedures for its extraction from tissue and conversion to Hg(II) exist, which facilitate its indirect detection with Hg(II)-sensitive probes. Direction detection of methylmercury would be worthwhile for in vivo toxicology studies and cellular/tissue imaging, but the evaluation of putative methylmercury-sensitive probes poses significant and serious safety risks that must be weighed before embarking on any work in this area. Two recent studies addressing the nature of methylmercury in fish point to the existence of a methylmercury cysteine complex.[29,32] Toxicology studies have shown that methylmercury passes through the blood-brain barrier as a complex with L-cysteine.[43] These observations suggest that probes capable of detecting and differentiating various CH_3HgX species would be necessary, which adds an additional layer of complexity.

Some of the mercury detectors described above, in addition to sensors in the immediate and distant pipeline, will provide the scientific community with a versatile toolkit for monitoring this metal ion in a wide variety of contexts. The fundamental chemistry may also provide new frameworks for addressing related problems, such as the design of new drugs for the treatment of accidental mercury overexposure and environmental remediation. We intend for this review to provide a comprehensive account of progress in mercury ion detection through mid-2007 and to be a major reference for future work. We look forward to seeing the results of such forthcoming endeavors and their translation into devices for practical applications.

12. Addendum

New approaches based on small molecules, biomolecules, and nanparticles for detecting Hg(II) have been reported since mid-2007. In this section, we provide a brief account of some recent developments through February of 2008.

12.1. Small Molecules

A variety of new Hg(II)-responsive probes that utilize fluorescence detection have been described (Figure 45). The anthracene-derivatized dioxocyclam **132** provides turn-off detection of Hg(II) and Cu(II) in 95:5 MeCN/H_2O (acetate buffer, pH 4.8; λ_{em} = 428 nm).[208] Depending on the protonation state, thioether-containing macrocycles **133** and **134** exhibit enhancement or quenching of anthracene emission following addition of Hg(II) in dichloromethane.[209] Because of the low water solubility of **133**:Hg(II), **133** was successfully employed in Hg(II) extraction experiments in which an aqueous solution of Hg(II) at pH 8 was vortexed with a solution of **133** in dichloromethane. Anthracene was also employed as the reporting group in cholic acid–based Hg(II) sensors **135** and **136**, both of which contain two dithiocarbamate ligands.[210] In 1:1 MeCN/H_2O, **135** and **136** respectively provide 6.6- and 4-fold fluorescence enhancement following Hg(II) addition, bind Hg(II) with 1:1 stoichiometry, and exhibit K_d values for Hg(II) of 190 and 649 nM. Sensor **135** also responds to methylmercury, with ~2-fold fluorescence enhancement in 1:1 MeCN/H_2O. Chemodosimeter **137** displays 73-fold fluorescence enhancement following Hg(II)-induced oxadiazole formation in 2:8 MeCN/H_2O at pH 7.4.[211] Bisnaphthyl azadiene **138** provides fluorescence turn-on when in the presence of >0.5 equiv Hg(II) in acetonitrile.[212]

Compounds **139–142** (Figure 45) are rhodamine derivatives that provide optical and fluorescence turn-on following addition of Hg(II), which results from opening of the spirolactam ring.[213–215] In MeCN, **139** exhibits ~600-fold fluorescence enhancement following addition of 5 equiv of Hg(II); however, its selectivity for Hg(II) is poor because Fe(II), Fe(III), and Pb(II) each provide a response similar in magnitude to that of Hg(II).[213] The Hg(II) selectivity of **140** is also relatively low because Pb(II), Zn(II) and Cd(II) also generate substantial fluorescence enhancement.[214] In contrast, **141** provides essentially Hg(II)-selective turn-on (>100-fold, MeCN; $K_d \sim 3.1\ \mu M$).[214] Sensor **142** contains rhodamine, hydroxyquinoline, and ferrocene moieties, and it provides colorimetric, fluorescent, and electrochemical Hg(II) detection.[215] In 1:1 EtOH/H_2O (HEPES buffer, pH 7.2), **142** exhibits ~105-fold fluorescence enhancement following addition of 15 equiv of Hg(II). The fluorescence enhancement is reversible following addition of KI and the affinity of **142** for Hg(II) is 270 μM. Because **142** responds to Hg(II) relatively rapidly (t < 2 min) and is soluble in 98% PBS (5 μM), its ability to detect Hg(II) in live Caov-3 cells was investigated. Greater fluorescence was observed in cells pretreated with $Hg(NO_3)_2$ (10 μM, 2.5 h) compared to Hg(II)-free cells.

Rhodamine was also used as the reporting group in a FRET-based Hg(II) detector.[216] In **143**, a tris(2-aminoethyl)amine moiety links two pyrene-appended calix[4]arenes and a ring-closed rhodamine fluorophore (Figure 45). Because the pyrene eximer and rhodamine exhibit spectral overlap in the ~450 – 600 nm range, they constitute a potential FRET pair with a pyrene donor and rhodamine acceptor. In MeCN and in the absence of Hg(II), excitation of the pyrene chromophore (λ_{ex} = 343 nm) results in emission from the both the pyrene monomer and eximer at <400 and ~475 nm, respectively. No rhodamine emission is observed because of the spirolactam ring. Addition of Hg(II) causes opening of the spirolactam ring and hence an increase in rhodamine absorption and emission. When

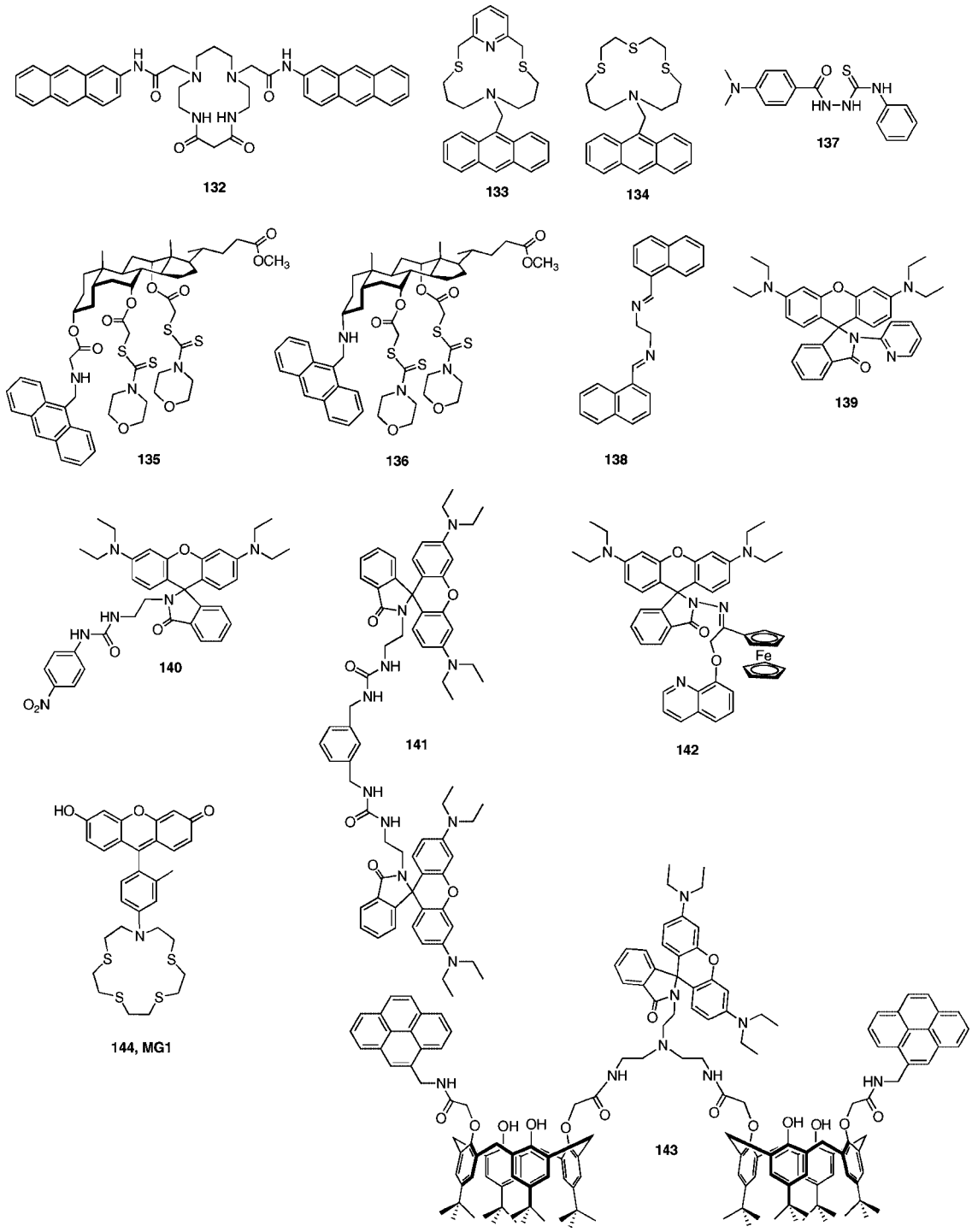

Figure 45. Some recently reported small-molecule fluorescent Hg(II) detectors.

solutions of **143** and Hg(II) are excited at 343 nm, some emission enhancement centered at ~575 nm occurs. This increase is attributed to energy transfer from the pyrene eximer to the ground-state of the ring-opened rhodamine. Although use of FRET for small-molecule Hg(II) detection is novel and this study illustrates proof of principle, it is very questionable whether this design provides any benefit over direct monitoring of the turn-on change in rhodamine emission that results from Hg(II) addition.

Modification of MF1 (**84**, Figure 20) by introduction of an *ortho*-methyl moiety onto the phenyl group provides Hg(II) sensor MG1 (**144**, Figure 45).[217] At neutral pH, MG1 ($\Phi_{free} = 0.02$) provides ~44-fold fluorescence enhancement, Φ_{Hg} being 0.72. Both the Φ_{free} and Φ_{Hg} values of MG1 are significantly greater than those of MF1 ($\Phi_{free} < 0.001$; $\Phi_{Hg} = 0.16$). Although the dynamic range of MG1 is smaller than that of parent MF1, it exhibits superior detection of low Hg(II) concentrations. When MG1 encounters 2 ppb Hg(II), 72 ± 10% turn-on occurs. This probe can be used to quantify Hg(II) in digested samples of fish muscle and to detect exogenous Hg(II) in HEK cells by fluorescence microscopy.

Lastly, we describe a recent report of several benzoylthiourea derivatives that contain azo moieties and are colorimetric and ratiometric dosimeters for Hg(II) (**145**–**147**, Figure 46).[218] Addition of Hg(II) to **145**–**147** results in

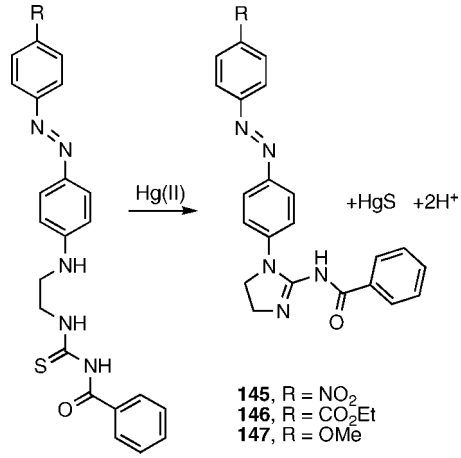

Figure 46. Recent colorimetric and ratiometric dosimeters for Hg(II).

desulfurization and subsequent cyclization. For instance, in 4:1 DMSO/H_2O, **145** exhibits maximum absorption at 486 nm ($\epsilon = 3.3 \times 10^4$ $M^{-1}cm^{-1}$). Addition of Hg(II) causes a decrease in 486 nm absorption and a concomitant absorption increase at 406 nm ($\epsilon = 2.7 \times 10^4$ $M^{-1}cm^{-1}$) with an isosbestic point at 433 nm. As a result, the solution color changes from pink to yellow, which is visible by-eye with a 1 μM solution of **145**. The color change is specific for Hg(II) and occurs in the presence of other metal ions. The colorimetric response is insensitive in the 4 to 9 pH range (4:1 DMSO/H_2O).

12.2. Biomolecules

An allosteric DNAzyme that provides fluorescence turn-on following Hg(II)-induced cleavage was reported.[219] The probe is based on a previously described DNAzyme, isolated by in vitro selection, that requires uranium (UO_2^{2+}) for activity.[220] Several base pair substitutions and additions are incorporated into the uranium-specific DNAzyme, allowing the introduction of one to six T-T mismatches, such that addition of Hg(II) causes the DNAzyme to fold into its active conformation. Gel-based studies indicate that Hg(II) promotes strand cleavage within one min and the amount of cleavage correlates with the number of T-T mismatches. When UO_2^{2+} is added to solutions of the DNAzymes and Hg(II), the rate of cleavage increases with increasing T-T mismatches, but the opposite behavior occurs when Hg(II) is introduced to solutions containing the DNAzyme and UO_2^{2+}. To obtain a fluorescent signal, a fluorescein moiety and two quenchers were attached to a DNAzyme containing five T-T mismatches. In the absence of Hg(II), a mixture of the DNAzyme and UO_2^{2+} emits only weakly. Addition of Hg(II) to this mixture causes the DNAzyme to adopt its active conformation. Subsequent coordination of UO_2^{2+} promotes strand cleavage and release of the fluorescein-labeled fragment. An ~50-fold increase in fluorescein emission results when the DNAzyme encounters 500 nM Hg(II). Hill plot analysis indicates that coordination of two Hg(II) ions is sufficient to promote strand cleavage. The probe is highly selective for Hg(II) and it has a low Hg(II) detection limit of 2.4 nM. Because of its water-compatability, favorable response time, and sub-ppb Hg(II) selectivity, this method may be useful for analyzing environmental samples. But one hurdle will be to convince regulatory agencies and the public that the use of UO_2^{2+} is acceptable from a health perspective.

12.3. Materials

Several new nanoparticle-based approaches to Hg(II) detection were reported in mid-to-late 2007. L-Carnitine-capped CdSe/ZnS quantum dots ($\lambda_{em} \sim 560$ nm) exhibit fluorescence quenching following Hg(II) addition in EtOH with a detection limit of 180 nM.[221] Solutions of gold nanoparticles functionalized with 11-mercaptoundecanoic acid (11-MUA-AuNPs) exhibit aggregation, which results in fluorescence quenching, following of addition of Hg(II) (borate buffer, pH 9.2).[222] Pb(II) and Cd(II) also quench emission from the 11-MUA-AuNPs, but this behavior can be overcome by addition of PDCA. When PDCA is added to aqueous solutions of 11-MUA-AuNPs, Hg(II)-specific quenching occurs and 5 nM (1 ppb) Hg(II) can be detected. The Hg(II) content in a pond water sample was measured with PDCA/11-MUA-AuNPs and compared to the amount determined by ICPMS. The two methods agree to better than 90%, with Hg(II) concentrations of 3.49 and 3.2 ppb, respectively. Lastly, a combination of gold nanoparticles derivatized with MPA, homocystine, rhodamine B, and the PDCA chelator provides a turn-on fluorescence Hg(II) sensing method that was fabricated into a small device that employs a battery-powered laser pointer as the excitation source.[223] The device was used to quantify Hg(II) content in samples of soil, water, and fish from the Mississippi River. This system provides Hg(II) detection at the 2 ppt level.

13. List of Abbreviations

AA	atomic absorption
AcOH	acetic acid
AuNP	gold nanoparticle
BODIPY	boron dipyrromethene
BPBA	bis(pyrrol-2-ylmethyleneamine)
BSA	bovine serum albumin
CdTe	cadmium telluride
CP	conjugated polymer
CT	charge transfer
D	Dabcyl quencher
DMABTS	*p*-dimethylaminobenzaldehyde thiosemicarbazone
DOS	bis-(2-ethylhexyl)sebacate
DSPC	distearylphosphatidylcholine
DTPP	5-*p*-[4-(10′,15′,20′-triphenyl-5′-porphinato)phenyl-oxyl-1-butyloxyl]-phenyl-10,15,20-triphenylporphiene
DTT	dithiothreitol
EC_{50}	the concentration of Hg(II) required for 50% of the total fluorescence change for a given probe concentration
EDTA	ethylenediaminetetraacetic acid
ET	electron transfer
F	fluorescein
FRET	fluorescence resonance energy transfer
GI	gastrointestinal tract
HEK	human embryonic kidney
HEPES	4-(2-hydroxyethyl)-1-piperazineethanesulfonic acid
HPLC	high performance liquid chromatography
ICPMS	inductively coupled plasma mass spectrometry
ICT	internal charge transfer
InP	indium phosphorous
IR	infrared
K_d	dissociation constant
MAA	mercaptoacetic acid
MABT	*N*-methyl-*N*-9-(methylanthracene)-*N*′-benzoylthiourea

MICT	metal-induced charge transfer
MPA	mercaptopropionic acid
MSO	mercury-sensitive oligonucleotide
$NaBH_4$	sodium borohydride
NaOAc	sodium acetate
NBO	nitrobenzoxadiazolyl
ng	nanogram
NIR	near infrared
NMR	nuclear magnetic resonance
ODN	oligodeoxyribonucleotide
PBS	phosphate-buffered saline
PCT	photoinduced charge transfer
PDCA	pyridine-2,6-dicarboxylic acid
PET	photoinduced electron transfer
PIPES	piperazine-1,4-bis(2-ethanesulfonic acid)
PPETE	poly[*p*-phenyleneethylene)-*alt*-(thienyleneethynylene)
PMNT	poly(3-(3′-*N*,*N*,*N*-triethylamino-1′-propyloxy)-4-methyl-2,5-thiophenehydrochloride)
ppm	parts per million
ppb	parts per billion
ppt	parts per trillion
PTCPB	potassium tetrakis(4-chlorophenyl)borate
PVC	polyvinylchloride
RB	rhodamine B
TBAF	tetrabutylammonium fluoride
TiO_2	titanium oxide
T_m	melting temperature
tmeda	*N*,*N*,*N*′-trimethylethylenediamino
TPP	tetraphenylporphyrin

14. Acknowledgments

Work on mercury ion sensing was supported by Grant GM65519 from the National Institute of General Medical Sciences.

15. References

(1) Czarnik, A. W. *Acc. Chem. Res.* **1994**, *27*, 302.
(2) de Silva, A. P.; Gunaratne, H. Q. N.; Gunnlaugsson, T.; Huxley, A. J. M.; McCoy, C. P.; Rademacher, J. T.; Rice, T. E. *Chem. Rev.* **1997**, *97*, 1515.
(3) de Silva, A. P.; Fox, D. B.; Huxley, A. J. M.; Moody, T. S. *Coord. Chem. Rev.* **2000**, *205*, 41.
(4) Prodi, L.; Bolletta, F.; Montalti, M.; Zaccheroni, N. *Coord. Chem. Rev.* **2000**, *205*, 59.
(5) Callan, J. F.; de Silva, A. P.; Magri, D. C. *Tetrahedron* **2005**, *61*, 8551.
(6) Prodi, L. *New J. Chem.* **2005**, *29*, 20.
(7) Krawczyk, T. K.; Moszczyńska, M.; Trojanowicz, M. *Biosens. Bioelectron.* **2000**, *15*, 681.
(8) Vlasov, Y. G.; Ermolenko, Y. E.; Kolodnikov, V. V.; Ipatov, A. V.; Al-Marok, S. *Sens. Actuators, B* **1995**, *24–25*, 317.
(9) Bonfil, Y.; Brand, M.; Kirowa-Eisner, E. *Anal. Chim. Acta* **2000**, *424*, 65.
(10) Han, S.; Zhu, M.; Yuan, Z.; Li, X. *Biosens. Bioelectron.* **2001**, *16*, 9.
(11) Manivannan, A.; Seehra, M. S.; Tryk, D. A.; Fujishima, A. *Anal. Lett.* **2002**, *35*, 355.
(12) Zhao, Q.; Cao, T.; Li, F.; Li, X.; Jing, H.; Yi, T.; Huang, C. *Organometallics* **2007**, *26*, 2077.
(13) Caballero, A.; Lloveras, V.; Curiel, D.; Tárraga, A.; Espinosa, A.; García, R.; Vidal-Gancedo, J.; Rovira, C.; Wurst, K.; Molina, P.; Veciana, J. *Inorg. Chem.* **2007**, *46*, 825.
(14) Muthukumar, C.; Kesarkar, S. D.; Srivastava, D. N. *J. Electroanal. Chem.* **2007**, *602*, 172.
(15) Guo, T.; Baasner, J.; Gradl, M.; Kistner, A. *Anal. Chim. Acta* **1996**, *320*, 171.
(16) Bloom, N.; Fitzgerald, W. F. *Anal. Chim. Acta* **1988**, *208*, 151.
(17) Method 1631 Revision B: Mercury in Water by Oxidation, Purge and Trap, and Cold Vapor Atomic Fluorescence Spectrometry. EPA-821-R-99-005; EPA, Office of Water: Washington, DC, May 1999.
(18) Fitzgerald, W. F.; Gill, G. A. *Anal. Chem.* **1979**, *51*, 1714.
(19) Nendza, M.; Herbst, T.; Kussatz, C.; Gies, A. *Chemosphere* **1997**, *35*, 1875.
(20) Renzoni, A.; Zino, F.; Franchi, E. *Environ. Res., Sect. A* **1998**, *77*, 68.
(21) Boening, D. W. *Chemosphere* **2000**, *40*, 1335.
(22) Malm, O. *Environ. Res., Sect. A* **1998**, *77*, 73.
(23) Mercury Update: Impact of Fish Advisories. EPA Fact Sheet EPA-823-F-01-011; EPA, Office of Water: Washington, DC, 2001.
(24) Gustin, M. S.; Coolbaugh, M. F.; Engle, M. A.; Fitzgerald, B. C.; Keislar, R. E.; Lindberg, S. E.; Nacht, D. M.; Quashnick, J.; Rytuba, J. J.; Sladek, C.; Zhang, H.; Zehner, R. E. *Environ. Geol.* **2003**, *43*, 339.
(25) Chu, P.; Porcella, D. B. *Water, Air, Soil Pollut.* **1995**, *80*, 135.
(26) Mason, R. P.; Morel, F. M. M.; Hemond, H. F. *Water, Air, Soil Pollut.* **1995**, *80*, 775.
(27) Celo, V.; Lean, D. R. S.; Scott, S. L. *Sci. Total Environ.* **2006**, *368*, 126.
(28) Mason, R. P.; Reinfelder, J. R.; Morel, F. M. M. *Water, Air, Soil Pollut.* **1995**, *80*, 915.
(29) Harris, H. H.; Pickering, I. J.; George, G. N. *Science* **2003**, *301*, 1203.
(30) Kraepiel, A. M. L.; Keller, K.; Chin, H. B.; Malcolm, E. G.; Morel, F. M. M. *Environ. Sci. Technol.* **2003**, *37*, 5551.
(31) Burger, J.; Gochfeld, M. *Environ. Res.* **2004**, *96*, 239.
(32) Kuwabara, J. S.; Arai, Y.; Topping, B. R.; Pickering, I. J.; George, G. N. *Environ. Sci. Technol.* **2007**, *41*, 2745.
(33) Johnson, D. W.; Lindberg, S. E. *Water, Air, Soil Pollut.* **1995**, *80*, 1069.
(34) Forman, J.; Moline, J.; Cernichiari, E.; Sayegh, S.; Torres, J. C.; Landrigan, M. M.; Hudson, J.; Adel, H. N.; Landrigan, P. J. *Environ. Health Perspect.* **2000**, *108*, 575.
(35) Silbergeld, E. K.; Silva, I. A.; Nyland, J. F. *Toxicol. Appl. Pharmacol.* **2005**, *207*, S282.
(36) Newby, C. A.; Riley, D. M.; Leal-Almeraz, T. O. *Ethn. Health* **2006**, *11*, 287.
(37) Drexler, H.; Schaller, K.-H. *Environ. Res., Sect. A* **1998**, *77*, 124.
(38) Factor-Litvak, P.; Hasselgren, G.; Jacobs, D.; Begg, M.; Kline, J.; Geier, J.; Mervish, N.; Schoenholtz, S.; Graziano, J. *Environ. Health Perspect.* **2003**, *111*, 719.
(39) Dye, B. A.; Schober, S. E.; Dillon, C. F.; Jones, R. L.; Fryar, C.; McDowell, M.; Sinks, T. H. *Occup. Environ. Med.* **2005**, *62*, 368.
(40) Magos, L. *J. Appl. Toxicol.* **2001**, *21*, 1.
(41) Pichichero, M. E.; Cernichiari, E.; Lopreiato, J.; Treanor, J. *Lancet* **2002**, *360*, 1737.
(42) Clarkson, T. W.; Magos, L.; Myers, G. J. *New Engl. J. Med.* **2003**, *349*, 1731.
(43) Clarkson, T. W.; Magos, L. *Crit. Rev. Toxicol.* **2006**, *36*, 609.
(44) Magos, L.; Clarkson, T. W. *Ann. Clin. Biochem.* **2006**, *43*, 257.
(45) Takeuchi, T.; Morikawa, N.; Matsumoto, H.; Shiraishi, Y. *Acta Neuropathologica* **1962**, *2*, 40.
(46) Harada, M. *Crit. Rev. Toxicol.* **1995**, *25*, 1.
(47) Akagi, H.; Grandjean, P.; Takizawa, Y.; Weihe, P. *Environ. Res. Sec. A* **1998**, *77*, 98.
(48) Eto, K.; Tokunaga, H.; Nagashima, K.; Takeuchi, T. *Toxicol. Pathol.* **2002**, *30*, 714.
(49) Bakir, F.; Damluji, S. F.; Amin-Zaki, L.; Murtadha, M.; Khalidi, A.; Al-Rawi, N. Y.; Tikriti, S.; Dhahir, H. I.; Clarkson, T. W.; Smith, J. C.; Doherty, R. A. *Science* **1973**, *181*, 230.
(50) Amin-Zaki, L.; Majeed, M. A.; Clarkson, T. W.; Greenwood, M. R. *Br. Med. J.* **1978**, *1*, 613.
(51) McKeown-Eyssen, G. E.; Ruedy, J.; Neims, A. *Am. J. Epidemol.* **1983**, *118*, 470.
(52) Davidson, P. W.; Myers, G. J.; Cox, C.; Shamlaye, C. F.; Marsh, D. O.; Tanner, M. A.; Berlin, M.; Sloane-Reeves, J.; Cernichiari, E.; Choisy, O.; Choi, A.; Clarkson, T. W. *Neurotoxicol.* **1995**, *16*, 677.
(53) Grandjean, P.; Weihe, P.; White, R. F.; Debes, F. *Environ. Res. Sec. A* **1998**, *77*, 165.
(54) Bolger, P. M.; Schwetz, B. A. *New Eng. J. Med.* **2002**, *347*, 1735.
(55) Counter, S. A.; Buchanan, L. H. *Toxicol. Appl. Pharmacol.* **2004**, *198*, 209.
(56) Kaur, P.; Aschner, M.; Syversen, T. *Neurotoxicol.* **2006**, *27*, 492.
(57) Milaeva, E. R. *J. Inorg. Biochem.* **2006**, *100*, 905.
(58) Shanker, G.; Mutkus, L. A.; Walker, S. J.; Aschner, M. *Mol. Brain Res.* **2002**, *106*, 1.
(59) Zalups, R. K.; Ahmad, S. *J. Am. Soc. Nephrol.* **2004**, *15*, 2023.
(60) Zalups, R. K.; Lash, L. H. *Toxicol. Appl. Pharmacol.* **2006**, *214*, 88.
(61) Unterreitmaier, E.; Schuster, M. *Anal. Chim. Acta* **1995**, *309*, 339.
(62) Lombardo, M.; Vassura, I.; Fabbri, D.; Trombini, C. *J. Organomet. Chem.* **2005**, *690*, 588.
(63) Liu, L.; Lam, Y.-W.; Wong, W.-Y. *J. Organomet. Chem.* **2006**, *691*, 1092.
(64) Liu, L.; Wong, W.-Y.; Lam, Y.-W.; Tam, W.-Y. *Inorg. Chim. Acta* **2007**, *360*, 109.
(65) Westöö, G. *Acta Chem. Scand.* **1966**, *20*, 2131.
(66) Medina, I.; Rubí, E.; Mejuto, M. C.; Cela, R. *Talanta* **1993**, *40*, 1631.

(67) Hardy, S.; Jones, P. *J. Chromatography A* **1997**, *791*, 333.
(68) Jones, P.; Hardy, S. *J. Chromatography A* **1997**, *765*, 345.
(69) Saito, S.; Sasamura, S.; Hoshi, S. *Analyst* **2005**, *130*, 659.
(70) Kasha, M. *J. Chem. Phys.* **1952**, *20*, 71.
(71) El-Sayed, M. A. *Acc. Chem. Res.* **1968**, *1*, 8.
(72) Koziar, J. C.; Cowan, D. O. *Acc. Chem. Res.* **1978**, *11*, 334.
(73) Svejda, P.; Maki, A. H.; Anderson, R. R. *J. Am. Chem. Soc.* **1978**, *100*, 7138.
(74) Masuhara, H.; Shioyama, H.; Saito, T.; Hamada, K.; Yasoshima, S.; Mataga, N. *J. Phys. Chem.* **1984**, *88*, 5868.
(75) Burress, C. N.; Bodine, M. I.; Elbjeirami, O.; Reibenspies, J. H.; Omary, M. A.; Gabbai, F. P. *Inorg. Chem.* **2007**, *46*, 1388.
(76) Tsien, R. Y.; Poenie, M. *Trends in Biol. Sci.* **1986**, *11*, 450.
(77) Costero, A. M.; Andreu, R.; Monrabal, E.; Martínez-Máñez, R.; Sancenón, F.; Soto, J. *J. Chem. Soc., Dalton Trans.* **2002**, 1769.
(78) Zhu, X.-J.; Fu, S.-T.; Wong, W.-K.; Guo, J.-P.; Wong, W.-Y. *Angew. Chem., Int. Ed.* **2006**, *45*, 3150.
(79) Wu, Z.; Zhang, Y.; Ma, J. S.; Yang, G. *Inorg. Chem.* **2006**, *45*, 3140.
(80) Wu, Z.; Chen, Q.; Xiong, S.; Xin, B.; Zhao, Z.; Jiang, L.; Ma, J. S. *Angew. Chem., Int. Ed.* **2003**, *42*, 3271.
(81) Métivier, R.; Leray, I.; Valeur, B. *Chem. Eur. J.* **2004**, *10*, 4480.
(82) Chen, Q.-Y.; Chen, C.-F. *Tetrahedron Lett.* **2005**, *46*, 165.
(83) Kim, J. H.; Hwang, A.-R.; Chang, S.-K. *Tetrahedron Lett.* **2004**, *45*, 7557.
(84) Kim, S. H.; Song, K. C.; Ahn, S.; Kang, Y. S.; Chang, S.-K. *Tetrahedron Lett.* **2006**, *47*, 497.
(85) Moon, S.-Y.; Youn, N. J.; Park, S. M.; Chang, S.-K. *J. Org. Chem.* **2005**, *70*, 2394.
(86) Park, S. M.; Kim, M. H.; Choe, J.-I.; No, K. T.; Chang, S.-K. *J. Org. Chem.* **2007**, *72*, 3550.
(87) Youn, N. J.; Chang, S.-K. *Tetrahedron Lett.* **2005**, *46*, 125.
(88) Kim, Y.-H.; Youk, J. S.; Moon, S. Y.; Choe, J.-I.; Chang, S.-K. *Chem. Lett.* **2004**, *33*, 702.
(89) Ha-Thi, M.-H.; Penhoat, M.; Michelet, V.; Leray, I. *Org. Lett.* **2007**, *9*, 1133.
(90) Yoon, J.; Ohler, N. E.; Vance, D. H.; Aumiller, W. D.; Czarnik, A. W. *Tetrahedron Lett.* **1997**, *38*, 3845.
(91) Descalzo, A. B.; Martínez-Máñez, R.; Radeglia, R.; Rurack, K.; Soto, J. *J. Am. Chem. Soc.* **2003**, *125*, 3418.
(92) Wang, L.; Wong, W.-K.; Wu, L.; Li, Z.-Y. *Chem. Lett.* **2005**, *34*, 934.
(93) Wang, L.; Zhu, X.-J.; Wong, W.-Y.; Guo, J.-P.; Wong, W.-K.; Li, Z.-Y. *J. Chem. Soc., Dalton Trans.* **2005**, 3235.
(94) Yu, Y.; Lin, L.-R.; Yang, K.-B.; Zhong, X.; Huang, R.-B.; Zheng, L.-S. *Talanta* **2006**, *69*, 103.
(95) Yang, R.; Li, K.; Wang, K.; Liu, F.; Li, N.; Zhao, F. *Anal. Chim. Acta* **2002**, *469*, 285.
(96) Hennrich, G.; Sonnenschein, H.; Resch-Genger, U. *J. Am. Chem. Soc.* **1999**, *121*, 5073.
(97) Hennrich, G.; Walther, W.; Resch-Genger, U.; Sonnenschein, H. *Inorg. Chem.* **2001**, *40*, 641.
(98) Zhang, G.; Zhang, D.; Yin, S.; Yang, X.; Shuai, Z.; Zhu, D. *Chem. Commun.* **2005**, 2161.
(99) Resch, U.; Rurack, K.; Bricks, J. L.; Slominski, J. L. *J. Fluorescence* **1997**, *7*, 231S.
(100) Cha, N. R.; Kim, M. Y.; Kim, Y. H.; Choe, J.-I.; Chang, S.-K. *J. Chem. Soc. Perkin Trans. 2* **2002**, 1193.
(101) Rurack, K.; Resch-Genger, U.; Bricks, J. L.; Spieles, M. *Chem. Commun.* **2000**, 2103.
(102) Rurack, K.; Kollmannsberger, M.; Resch-Genger, U.; Daub, J. *J. Am. Chem. Soc.* **2000**, *122*, 968.
(103) Kadarkaraisamy, M.; Sykes, A. G. *Polyhedron* **2007**, *26*, 1323.
(104) Winkler, J. D.; Bowen, C. M.; Michelet, V. *J. Am. Chem. Soc.* **1998**, *120*, 3237.
(105) Feng, L.; Chen, Z. *Sensors and Actuators B* **2007**, *120*, 665.
(106) Prodi, L.; Bargossi, C.; Montalti, M.; Zaccheroni, N.; Su, N.; Bradshaw, J. S.; Izatt, R. M.; Savage, P. B. *J. Am. Chem. Soc.* **2000**, *122*, 6769.
(107) Kim, S. H.; Youn, N. J.; Park, J. Y.; Choi, M. G.; Chang, S.-K. *Bull. Korean Chem. Soc.* **2006**, *27*, 1553.
(108) Sakamoto, H.; Ishikawa, J.; Nakao, S.; Wada, H. *Chem. Commun.* **2001**, 2395.
(109) Guo, X.; Qian, X.; Jia, L. *J. Am. Chem. Soc.* **2004**, *126*, 2272.
(110) Zhang, Z.; Guo, X.; Qian, X.; Liu, Z.; Liu, F. *Kidney Int.* **2004**, *66*, 2279.
(111) Kim, S. H.; Kim, J. S.; Park, S. M.; Chang, S.-K. *Org. Lett.* **2006**, *8*, 371.
(112) Caballero, A.; Martínez, R.; Lloveras, V.; Ratera, I.; Vidal-Gancedo, J.; Wurst, K.; Tárraga, A.; Molina, P.; Veciana, J. *J. Am. Chem. Soc.* **2005**, *127*, 15666.
(113) Zhao, Y.; Lin, Z.; He, C.; Wu, H.; Duan, C. *Inorg. Chem.* **2007**, *46*, 1538.
(114) Song, K. C.; Kim, J. S.; Park, S. M.; Chung, K.-C.; Ahn, S.; Chang, S.-K. *Org. Lett.* **2006**, *8*, 3413.
(115) Wu, D.; Huang, W.; Duan, C.; Lin, Z.; Meng, Q. *Inorg. Chem.* **2007**, *46*, 1538.
(116) Kwon, J. Y.; Jang, Y. J.; Lee, Y. J.; Kim, K. M.; Seo, M. S.; Nam, W.; Yoon, J. *J. Am. Chem. Soc.* **2005**, *127*, 10107.
(117) Ros-Lis, J. V.; Marcos, M. D.; Martínez-Máñez, R.; Rurack, K.; Soto, J. *Angew. Chem., Int. Ed.* **2005**, *44*, 4405.
(118) Chae, M.-Y.; Czarnik, A. W. *J. Am. Chem. Soc.* **1992**, *114*, 9704.
(119) Zheng, H.; Qian, Z.-H.; Xu, L.; Yuan, F.-F.; Lan, L.-D.; Xu, J.-G. *Org. Lett.* **2006**, *8*, 859.
(120) Ou, S.; Lin, Z.; Duan, C.; Zhang, H.; Bai, Z. *Chem. Commun.* **2006**, 4392.
(121) Mello, J. V.; Finney, N. S. *J. Am. Chem. Soc.* **2005**, *127*, 10124.
(122) Wang, J.; Qian, X. *Chem. Commun.* **2006**, 109.
(123) Wang, J.; Qian, X. *Org. Lett.* **2006**, *8*, 3721.
(124) Burdette, S. C.; Frederickson, C. J.; Bu, W.; Lippard, S. J. *J. Am. Chem. Soc.* **2003**, *125*, 1778.
(125) Nolan, E. M.; Burdette, S. C.; Harvey, J. H.; Hilderbrand, S. A.; Lippard, S. J. *Inorg. Chem.* **2004**, *43*, 2624.
(126) Hirano, T.; Kikuchi, K.; Urano, Y.; Nagano, T. *J. Am. Chem. Soc.* **2002**, *124*, 6555.
(127) Meng, X.-M.; Liu, L.; Hu, H.-Y.; Zhu, M.-Z.; Wang, M.-X.; Shi, J.; Guo, Q.-X. *Tetrahedron Lett.* **2006**, *47*, 7961.
(128) Nolan, E. M.; Lippard, S. J. *J. Am. Chem. Soc.* **2003**, *125*, 14270.
(129) Cooper, T. H.; Mayer, M. J.; Leung, K.-H.; Ochrymowycz, L. A.; Rorabacher, D. B. *Inorg. Chem.* **1992**, *31*, 3796.
(130) Nolan, E. M.; Racine, M. E.; Lippard, S. J. *Inorg. Chem.* **2006**, *45*, 2742.
(131) Jiang, P.; Guo, Z. *Coord. Chem. Rev.* **2004**, *248*, 205.
(132) Chang, C. J.; Lippard, S. J. *Met. Ions Life Sci.* **2006**, *1*, 281.
(133) Takahashi, A.; Camacho, P.; Lechleiter, J. D.; Herman, B. *Physiol. Rev.* **1999**, *79*, 1089.
(134) Yoon, S.; Albers, A. E.; Wong, A. P.; Chang, C. J. *J. Am. Chem. Soc.* **2005**, *127*, 16030.
(135) Yang, Y.-K.; Yook, K.-J.; Tae, J. *J. Am. Chem. Soc.* **2005**, *127*, 16760.
(136) Ko, S.-K.; Yang, Y.-K.; Tae, J.; Shin, I. *J. Am. Chem. Soc.* **2006**, *128*, 14150.
(137) Liu, B.; Tian, H. *Chem. Commun.* **2005**, 3156.
(138) Wang, Z.; Zhang, D.; Zhu, D. *Anal. Chim. Acta* **2005**, *549*, 10.
(139) Kim, J. S.; Choi, M. G.; Song, K. C.; No, K. T.; Ahn, S.; Chang, S.-K. *Org. Lett.* **2007**, *9*, 1129.
(140) Feng, L.; Chen, Z. *Sensors and Actuators B* **2007**, *122*, 600.
(141) Cheung, S.-M.; Chang, W.-H. *Tetrahedron* **2006**, *62*, 8379.
(142) Yuan, M.; Li, Y.; Li, J.; Li, C.; Liu, X.; Lv, J.; Xu, J.; Liu, H.; Wang, S.; Zhu, D. *Org. Lett.* **2007**, *9*, 2313.
(143) Wang, J.; Qian, X.; Cui, J. *J. Org. Chem.* **2006**, *71*, 4308.
(144) Nolan, E. M.; Lippard, S. J. *J. Mater. Chem.* **2005**, *15*, 2778.
(145) Nolan, E. M.; Lippard, S. J. *J. Am. Chem. Soc.* **2007**, *129*, 5910.
(146) Nolan, E. M.; Jaworski, J.; Okamoto, K.-I.; Hayashi, Y.; Sheng, M.; Lippard, S. J. *J. Am. Chem. Soc.* **2005**, *127*, 16812.
(147) Choi, M. J.; Kim, M. Y.; Chang, S.-K. *Chem. Commun.* **2001**, 1664.
(148) Tatay, S.; Gaviña, P.; Coronado, E.; Palomares, E. *Org. Lett.* **2006**, *8*, 3857.
(149) Fu, Y.; Li, H.; Hu, W. *Eur. J. Org. Chem.* **2007**, 2459.
(150) Sancenón, F.; Martínez-Máñez, R.; Soto, J. *Tetrahedron Lett.* **2001**, *42*, 4321.
(151) Sancenón, F.; Martínez-Máñez, R.; Soto, J. *Chem. Commun.* **2001**, 2262.
(152) Brümmer, O.; La Clair, J. J.; Janda, K. D. *Org. Lett.* **1999**, *1*, 415.
(153) Dickerson, T. J.; Reed, N. N.; LaClair, J. J.; Janda, K. D. *J. Am. Chem. Soc.* **2004**, *126*, 16582.
(154) Ros-Lis, J. V.; Martínez-Máñez, R.; Rurack, K.; Sancenón, F.; Soto, J.; Spieles, M. *Inorg. Chem.* **2004**, *43*, 5183.
(155) Basheer, M. C.; Thomas, A. K. G.; Suresh, C. H.; Das, S. *Tetrahedron* **2006**, *62*, 605.
(156) Chen, P.; He, C. *J. Am. Chem. Soc.* **2004**, *126*, 728.
(157) Wegner, S. V.; Okesli, A.; Chen, P.; He, C. *J. Am. Chem. Soc.* **2007**, *129*, 3474.
(158) Ono, A.; Togashi, H. *Angew. Chem., Int. Ed.* **2004**, *43*, 4300.
(159) Thomas, J. M.; Ting, R.; Perrin, D. M. *Org. Biomol. Chem.* **2004**, *2*, 307.
(160) Matsushita, M.; Meijler, M. M.; Wirsching, P.; Lerner, R. A.; Janda, K. D. *Org. Lett.* **2005**, *7*, 4943.
(161) Virta, M.; Lampinen, J.; Karp, M. *Anal. Chem.* **1995**, *67*, 667.
(162) Ivask, A.; Hakkila, K.; Virta, M. *Anal. Chem.* **2001**, *73*, 5168.
(163) Yamagata, T.; Ishii, M.; Narita, M.; Huang, G.-C.; Endo, G. *Water Sci. Technol.* **2002**, *46*, 253.
(164) Barkay, T.; Miller, S. M.; Summers, A. O. *FEMS Microbiol. Rev.* **2003**, *27*, 355.
(165) O'Halloran, T. V.; Walsh, C. T. *Science* **1987**, *235*, 211.
(166) Heltzel, A.; Gambill, D.; Jackson, W. J.; Totis, P. A.; Summers, A. O. *J. Bacteriol.* **1987**, *169*, 3379.

(167) Shewchuk, L. M.; Verdine, G. L.; Walsh, C. T. *Biochemistry* **1989**, *28*, 2331.
(168) Helmann, J. D.; Wang, Y.; Mahler, I.; Walsh, C. T. *J. Bacteriol.* **1989**, *171*, 222.
(169) Lewis, J. C.; Feltus, A.; Ensor, C. M.; Ramanathan, S.; Daunert, S. *Anal. Chem.* **1998**, *70*, 579A.
(170) Lappalainen, J. O.; Karp, M. T.; Nurmi, J.; Juvonen, R.; Virta, M. P. J. *Environ. Toxicol.* **2000**, *15*, 443.
(171) Ivask, A.; Virta, M.; Kahru, A. *Soil Biology and Biochemistry* **2002**, *34*, 1439.
(172) Bernaus, A.; Gaona, X.; Ivask, A.; Kahru, A.; Valiente, M. *Anal. Bioanal. Chem.* **2005**, *382*, 1541.
(173) Hakkila, K.; Green, T.; Leskinen, P.; Ivask, A.; Marks, R.; Virta, M. *J. Appl. Toxicol.* **2004**, *24*, 333.
(174) Biran, I.; Rissin, D. M.; Ron, E. Z.; Walt, D. R. *Anal. Biochem.* **2003**, *315*, 106.
(175) Miyake, Y.; Togashi, H.; Tashiro, M.; Yamaguchi, H.; Oda, S.; Kudo, M.; Tanaka, Y.; Kondo, Y.; Sawa, R.; Fujimoto, T.; Machinami, T.; Ono, A. *J. Am. Chem. Soc.* **2006**, *128*, 2172.
(176) Vannela, R.; Adriaens, P. *Environ. Eng. Sci.* **2007**, *24*, 73.
(177) Simeonov, A.; Matsushita, M.; Juban, E. A.; Thompson, E. H. Z.; Hoffman, T. Z.; Beuscher, A. E.; Taylor, M. J.; Wirsching, P.; Rettig, W.; McCusker, J. K.; Stevens, R. C.; Millar, D. P.; Schultz, P. G.; Lerner, R. A.; Janda, K. D. *Science* **2000**, *290*, 307.
(178) Fan, L.-J.; Zhang, Y.; Jones, W. E. *Macromolecules* **2005**, *38*, 2844.
(179) Kim, I.-B.; Bunz, U. H. F. *J. Am. Chem. Soc.* **2006**, *128*, 2818.
(180) Tang, Y.; He, F.; Yu, M.; Feng, F.; An, L.; Sun, H.; Wang, S.; Li, Y.; Zhu, D. *Macromol. Rapid Commun.* **2006**, *27*, 389.
(181) Liu, X.; Tang, Y.; Wang, L.; Zhang, J.; Song, S.; Fan, C.; Wang, S. *Adv. Mater.* **2007**, *19*, 1471.
(182) Zhao, Y.; Zhong, Z. *J. Am. Chem. Soc.* **2006**, *128*, 9988.
(183) Zhao, Y.; Zhong, Z. *Org. Lett.* **2006**, *8*, 4715.
(184) Mohr, G. J.; Murkovic, I.; Lehmann, F.; Haider, C.; Wolfbeis, O. S. *Sensors and Actuators B* **1997**, *38–39*, 239.
(185) Murkovic, I.; Wolfbeis, O. S. *Sensors and Actuators B* **1997**, *38–39*, 246.
(186) Métivier, R.; Leray, I.; Lebeau, B.; Valeur, B. *J. Mater. Chem.* **2005**, *15*, 2965.
(187) Palomares, E.; Vilar, R.; Durrant, J. R. *Chem. Commun.* **2004**, 362.
(188) Coronado, E.; Galán-Mascarós, J. R.; Martí-Gastaldo, C.; Palomares, E.; Durrant, J. R.; Vilar, R.; Gratzel, M.; Nazeeruddin, M. K. *J. Am. Chem. Soc.* **2005**, *127*, 12351.
(189) Dolci, L. S.; Marzocchi, E.; Montalti, M.; Prodi, L.; Monti, D.; Di Natale, C.; D'Amico, A.; Paolesse, R. *Biosensors & Bioelectronics* **2006**, *22*, 399.
(190) Zhang, X.-B.; Guo, C.-C.; Li, Z.-Z.; Shen, G.-L.; Yu, R.-Q. *Anal. Chem.* **2002**, *74*, 821.
(191) Chen, B.; Yu, Y.; Zhou, Z.; Zhong, P. *Chem. Lett.* **2004**, *33*, 1608.
(192) Zhu, C.; Li, L.; Fang, F.; Chen, J.; Wu, Y. *Chem. Lett.* **2005**, *34*, 898.
(193) Rex, M.; Hernandez, F. E.; Campiglia, A. D. *Anal. Chem.* **2006**, *78*, 445.
(194) Huang, C.-C.; Chang, H.-T. *Anal. Chem.* **2006**, *78*, 8332.
(195) Lee, J.-S.; Han, M. S.; Mirkin, C. A. *Angew. Chem., Int. Ed.* **2007**, *46*, 4093.
(196) Swager, T. M. *Acc. Chem. Res.* **1998**, *31*, 201.
(197) Thomas, S. W.; Joly, G. D.; Sawger, T. M. *Chem. Rev.* **2007**, *107*, 1339.
(198) Zhang, Y.; Murphy, C. B.; Jones, W. E. *Macromolecules* **2002**, *35*, 630.
(199) Sasaki, D. Y.; Padilla, B. E. *Chem. Commun.* **1998**, 1581.
(200) He, C.-L.; Ren, F.-L.; Zhang, X.-B.; Han, Z.-X. *Talanta* **2006**, *70*, 364.
(201) Walt, D. R. *Curr. Opin. Chem. Biol.* **2002**, *6*, 689.
(202) Epstein, J. R.; Walt, D. R. *Chem. Soc. Rev.* **2003**, *32*, 203.
(203) Pallavicini, P.; Diaz-Fernandez, Y. A.; Foti, F.; Mangano, C.; Patroni, S. *Chem. Eur. J.* **2007**, *13*, 178.
(204) Murphy, C. J. *Anal. Chem.* **2002**, *74*, 520A.
(205) Walt, D. R. *Nat. Mater.* **2002**, *1*, 17.
(206) Somers, R.; Bawendi, M.; Nocera, D. G. *J. Mater. Chem.* **2007**, *17*, T37.
(207) Han, M. S.; Lytton-Jean, A. K. R.; Oh, B.-K.; Heo, J.; Mirkin, C. A. *Angew. Chem., Int. Ed.* **2006**, *45*, 1807.
(208) Song, K.-C.; Kim, M. H.; Kim, H. J.; Chang, S.-K. *Tetrahedron Lett.* **2007**, *48*, 7464.
(209) Tamayo, A.; Pedras, B.; Lodeiro, C.; Escriche, L.; Casabó, J.; Capelo, J. L.; Covelo, B.; Kivekäs, R.; Silanpää, R. *Inorg. Chem.* **2007**, *46*, 7818.
(210) Wang, H.; Chang, W.-H. *Tetrahedron* **2007**, *63*, 8825.
(211) Wu, F.-Y.; Zhao, Y.-Q.; Ji, Z.-H.; Mu, Y.-M. *J.Fluoresc* **2007**, *17*, 460.
(212) Shiraishi, Y.; Maehara, H.; Ishizumi, K.; Hirai, T. *Org. Lett.* **2007**, *9*, 3125.
(213) Zhang, X.; Shiraishi, Y.; Hirai, T. *Tetrahedron Lett.* **2007**, *48*, 5455.
(214) Soh, J. H.; Swamy, K. M. K.; Kim, S. K.; Kim, S.; Lee, S.-H.; Yoon, J. *Tetrahedron Lett.* **2007**, *48*, 5966.
(215) Yang, H.; Zhou, Z.; Huang, K.; Yu, M.; Li, F.; Yi, T.; Huang, C. *Org. Lett.* **2007**, *9*, 4729.
(216) Othman, A. B.; Lee, J. W.; Wu, J.-S.; Kim, J. S.; Abidi, R.; Thuéry, P.; Strub, J. M.; Dorsselaer, A. V.; Vicens, J. *J. Org. Chem.* **2007**, *72*, 7634.
(217) Yoon, S.; Miller, E. W.; He, Q.; Do, P. H.; Chang, C. J. *Angew. Chem., Int. Ed.* **2007**, *46*, 6658.
(218) Lee, M. H.; Cho, B.-K.; Yoon, J.; Kim, J. S. *Org. Lett.* **2007**, *9*, 4515.
(219) Liu, J.; Lu, Y. *Angew. Chem., Int. Ed.* **2007**, *46*, 7587.
(220) Liu, J.; Brown, A. K.; Meng, X.; Cropek, D. M.; Istok, J. D.; Watson, D. B.; Lu, Y. *Proc. Natl. Acad. Sci. USA* **2007**, *104*, 2056.
(221) Li, H.; Zhang, Y.; Wang, X.; Gao, Z. *Microchim Acta.* **2008**, *160*, 119.
(222) Huang, C.-C.; Yang, Z.; Lee, K.-H.; Chang, H.-T. *Angew. Chem., Int. Ed.* **2007**, *46*, 6824.
(223) Darbha, G. K.; Ray, A.; Ray, P. C. *ACS Nano.* **2007**, *1*, 208.

CR068000Q